

1

G104060

ABSTRACT

HORIZONTAL SLIPFORM CONSTRUCTION WITH LOW SLUMP CONCRETE

By

Frederick T. Hsia

Horizontal slipform construction of concrete structures can be used for highway median barriers, low earth retaining structures, noise attenuation and sound barrier supports, and other highway appurtenances. The fresh concrete structure emerging from the extrusion form has no lateral support and approximates an unconfined plane strain condition. Failure occurs immediately when maximum shear stresses exceed the shear strength. An understanding of the properties of low slump concrete in its fresh state was needed in order to broaden the application of horizontal slipform construction. In this research, the mortar-void mix design method for low slump concrete has been presented with a numerical example. The physical and mechanical properties of the low slump concrete were investigated in its fresh state and the behavior of two emerging slipform constructed highway median barriers have been analyzed by the finite element method (FEM). A simplified analysis technique for low slump concrete structural sections has been developed which appears to be suitable for use by contractors.

Physical properties of concrete components were investigated according to conventional test procedures. Mechanical properties of

this fresh concrete, including yield stress, ultimate strength, elastic modulus and plastic modulus, were determined by unconfined compression tests in the laboratory. Factors influencing mechanical properties were investigated according to variations in mix design and test conditions. Unconfined compression test results show that low slump fresh concrete, with an ultimate strength up to 12.5 psi and vibration period up to 100 sec., is workable and should be acceptable for horizontal slipform construction. The stress-strain curve shape shows a brittle type behavior with an approximate yield stress to ultimate strength ratio close to 0.95. A shear type failure with an angle of 55 to 60 degrees from the horizontal appeared in most laboratory samples and both of the reported field failures.

An experimentally slipform constructed section was analyzed by the FEM, using laboratory test results converted to field mix conditions and a bilinear stress-strain model for the fresh concrete behavior. It was found that, by defining the undrained shear strength as a failure criterion, the FEM result was in reasonably good agreement with the observed field failure behavior. Using this observed agreement a simplified analysis method was developed based on the maximum shear stress from the FEM analysis results and the product of the maximum height and the unit weight of the concrete structure. This method gives good agreement with the FEM and the procedure appears to be suitable for use by contractors who wish to estimate wall stability for a given low slump concrete mix design.

The air content requirement for the low slump concrete mix design appears to be unnecessary for free standing concrete structures

Frederick T. Hsia

which are not subject to severe exposure conditions. A change in this requirement would permit slipform construction of higher wall sections due to improved concrete behavior at greatly reduced cost and construction time.

HORIZONTAL SLIPFORM CONSTRUCTION
WITH LOW SLUMP CONCRETE

By

Frederick T. Hsia

A DISSERTATION

Submitted to
Michigan State University
in partial fulfillment of the requirements
for the degree of

DOCTOR OF PHILOSOPHY

Department of Civil Engineering

1977

DEDICATION

To Min-Gee, Constance and Eric with all my love

ACKNOWLEDGMENTS

The writer would like to express his appreciation to his major professor, Dr. O.B. Andersland, Professor of Civil Engineering, for his encouragement, patience, and academic advice throughout the completion of this doctoral dissertation. Thanks also go to the other members of the writer's doctoral committee: Dr. W.A. Bradley, Professor of Metallurgy, Mechanics, and Material Science; Dr. T.S. Vinson, Associate Professor of Civil Engineering; and Dr. R.S. Carmichael, Assistant Professor of Geology.

Special appreciation goes to Dr. R.R. Goughnour, President of Strahan Manufacture Co. Inc., Florida, for his time and suggestions.

Thanks are also extended to the writer's colleagues in the Research Laboratory of the Michigan Department of State Highways and Transportation for their technical advice.

TABLE OF CONTENTS

| | Page |
|--|------|
| ACKNOWLEDGEMENTS | iii |
| LIST OF TABLES | vi |
| LIST OF FIGURES | vii |
| CHAPTER | |
| I. INTRODUCTION | 1 |
| 1.1 Horizontal Slipform Concrete Construction | 1 |
| 1.2 Objectives of Research | 4 |
| II. LITERATURE REVIEW | 6 |
| 2.1 Slipform Construction | 6 |
| 2.2 Low Slump Concrete | 11 |
| 2.2.1 Basic Composition | 12 |
| 2.2.2 Physical Properties | 18 |
| 2.2.3 Mechanical Properties | 22 |
| 2.2.4 Factors Affecting Mechanical Properties | 32 |
| 2.2.5 Mix Design | 44 |
| 2.3 Failure Criterion for Fresh Concrete | 48 |
| 2.4 Analysis Technique for Fresh Concrete Sections | 53 |
| III. MATERIALS AND MIX DESIGN | 58 |
| 3.1 Concrete Materials | 58 |
| 3.1.1 Cement | 59 |
| 3.1.2 Coarse Aggregate | 59 |
| 3.1.3 Fine Aggregate | 60 |
| 3.2 Mix Design - Mortar Void Method | 61 |
| 3.2.1 Basic Information | 63 |
| 3.2.2 Design Procedure | 69 |
| IV. LABORATORY PROCEDURE | 76 |
| 4.1 Gradation of the Aggregates | 76 |
| 4.2 Physical Properties | 80 |
| 4.3 Unconfined Compression Test | 83 |

| CHAPTER | Page |
|--|------|
| V. FIELD AND LABORATORY EXPERIMENTAL RESULTS | 91 |
| 5.1 Physical Properties | 91 |
| 5.2 Stress-Strain Behavior of the Fresh Concrete | 93 |
| 5.3 Two Field Construction Examples Illustrating Failure | 93 |
| 5.3.1 Straight Wall Experimental Section | 105 |
| 5.3.2 Florida Median Barrier Section | 107 |
| VI. PRESENTATION AND DISCUSSION OF RESULTS | 110 |
| 6.1 Physical Properties | 110 |
| 6.1.1 Specific Gravities and Percent Absorption | 110 |
| 6.1.2 Unit Weight | 111 |
| 6.1.3 Voids Content of the Coarse Aggregates | 112 |
| 6.1.4 Basic Water Content of the Mortar | 115 |
| 6.2 Sample Size and Failure Patterns | 115 |
| 6.3 Strength Characteristics of the Fresh Concrete | 122 |
| 6.3.1 Stress-Strain Behavior | 122 |
| 6.3.2 Mix Properties and Mechanical Behavior | 124 |
| 6.4 Air Content Requirements | 147 |
| 6.5 Stresses in the Experimental Section | 151 |
| 6.5.1 Undrained Shear Strength | 151 |
| 6.5.2 Development of Failure Zones | 153 |
| 6.6 Simplified Analysis for Wall Stability | 160 |
| VII. SUMMARY AND CONCLUSIONS | |
| 7.1 Engineering Properties of Low Slump Fresh Concrete | 166 |
| 7.2 Behavior of a Horizontal Slipformed Concrete Structure | 168 |
| 7.3 Practical Implications of the Investigation | 169 |
| REFERENCES | 171 |
| APPENDICES | |
| A. Unconfined Compression Test Data | 175 |
| B. Basic Water Content Test Data | 209 |
| C. Critical Mortar Content Calculation | 210 |
| D. Typical Work Sheet for Mix Proportion | 214 |
| E. Recommended Guidelines for Application | |
| E.1 Unconfined Compression Test on Low Slump Concrete | 215 |
| E.2 Use of the Simplified Method for Estimate of Section Stability | 216 |

LIST OF TABLES

| Table | | Page |
|----------------|---|------------|
| 2.1 | Range in slump and flow of concrete for various degrees of consistency | 13 |
| 2.2 | The angle of internal friction at various rates of strain (after Ritchie, 1962) | 41 |
| 3.1 | General description of Grade 35S concrete mixtures | 58 |
| 3.2 | Physical requirements for 6A coarse aggregate | 62 |
| 3.3 | Grading requirements for 6A coarse aggregates | 62 |
| 3.4 | Grading requirements for 2NS fine aggregates | 62 |
| 3.5 | v_m and w_m data | 66 |
| 4.1 | Gradation of aggregates | 81 |
| 4.2 | Percentage for each size group of crushed aggregates | 82 |
| 5.1 | Physical properties of fine aggregates | 91 |
| 5.2 | Physical properties of coarse aggregates | 92 |
| 5.3 | Physical properties of cement and mortar | 92 |
| 5.4 | Basic water content by percentage of water weight | 92 |
| 5.5 | Mix design and test conditions | 94 |
| 5.6 | Mechanical properties of the fresh concrete | 96 |
| 6.1 | Comparison of the mix design and field proportions | 151 |
| 6.2 | Stress conditions and stress ratios for the structural shapes | 162 |
| A-1 to A-34 | Unconfined compression test data | 175 208 |
| B-1 | Basic water content test data | 209 |

LIST OF FIGURES

| Figure | | Page |
|--------|---|------|
| 1.1 | Fresh concrete structure emerging from the slipform machine | 3 |
| 1.2 | A slump failure of the fresh concrete structure | 3 |
| 2.1 | Typical Michigan highway median barrier | 8 |
| 2.2 | Georgia median barrier wall for variable roadway height | 8 |
| 2.3 | Fresh concrete being augered into the Aukerman machine | 9 |
| 2.4 | Vibrators for the Aukerman form | 9 |
| 2.5 | Interrelationship of aggregate (A), cement (c), water (w), and gel (G) | 15 |
| 2.6 | Space relationships for paste components at various stages of hydration, (a) fresh paste, (b) reaction one-third complete, (c) reaction two-thirds complete, (d) reaction completed | 15 |
| 2.7 | Typical stress-strain curve for low slump compacted fresh concrete | 26 |
| 2.8 | Cylinder dimensions used for calculation of initial slump in the fresh concrete | 26 |
| 2.9 | Stress-strain curve for low slump concrete including strains due to gravity forces | 29 |
| 2.10 | Vibration and compaction relationship for 1/2 in. slump concrete | 43 |
| 2.11 | Typical curve showing the relationship between water content and mortars and the volume of the mortar (after Bauer, 1949) | 46 |
| 2.12 | Mohr-Coulomb failure criterion | 51 |
| 2.13 | Unconfined compression loading case | 51 |

| Figure | Page |
|--|------|
| 3.1 Relationship between compressive strength and cement-space ratio (after Bauer, 1949) | 65 |
| 3.2 Basic water content curves for various sand-cement ratios (a_m/c_m) | 67 |
| 3.3 Characteristic mortar voids curve | 68 |
| 4.1 Limits of gradation | 78 |
| 4.2 Gradation curves for test samples | 79 |
| 4.3 Mixer and vibrator | 84 |
| 4.4 6 in. × 12 in. mold with 2 in. extension tube on top | 84 |
| 4.5 Air indicator and a metal wire used to scour out the mortar | 88 |
| 4.6 The compression test machine with a failed sample | 88 |
| 5.1 Stress-strain curves for various effective water-cement ratios | 97 |
| 5.2 Stress-strain curves for various periods of hydration | 98 |
| 5.3 Stress-strain curves for various cement contents | 99 |
| 5.4 Stress-strain curves for various mortar contents | 100 |
| 5.5 Stress-strain curves for various concrete temperatures | 101 |
| 5.6 Stress-strain curves for various effective water-cement ratios for crushed aggregate | 102 |
| 5.7 Stress-strain curves for various air contents | 103 |
| 5.8 Stress-strain curves for various strain rates | 104 |
| 5.9 An experimental section slipform constructed by A.C. Aukerman Co. of Jackson, Michigan | 106 |
| 5.10 Shear failure of the experimental section | 106 |
| 5.11 The 68 in. high Florida median barrier | 108 |
| 6.1 Air content and unit weight relationship | 113 |
| 6.2 Void contents of gravel (from Troxell, 1968) | 113 |

| Figure | Page |
|--|------|
| 6.3 Stress and strain in a uniaxial compression test (Lambe, 1951) | 116 |
| 6.4 Failure patterns for low slump concrete in unconfined compression | 118 |
| 6.5 (a) Applied stresses in the triaxial test (b) Stresses acting on an element of the loaded cylinder | 119 |
| 6.6 Two examples showing the dead zones of failed samples | 123 |
| 6.7 Influence of effective water-cement ratio on mechanical properties (round gravel) | 126 |
| 6.8 Influence of period of hydration (t_1) and period after vibration (t_2) on mechanical properties | 127 |
| 6.9 Influence of sand-cement ratio on mechanical properties | 128 |
| 6.10 Influence of cement factor on mechanical properties | 129 |
| 6.11 Influence of mortar content on mechanical properties | 130 |
| 6.12 Influence of effective water-cement ratio on mechanical properties (crushed gravel) | 131 |
| 6.13 Influence of shape of the coarse aggregate on mechanical properties | 132 |
| 6.14 Influence of concrete temperature on mechanical properties | 133 |
| 6.15 Influence of air content on mechanical properties | 134 |
| 6.16 Influence of rate of shear on mechanical properties | 135 |
| 6.17 The honeycombed structure of Sample 31 for an extremely low mortar content | 139 |
| 6.18 Characteristics of mortar content. (a) relationship between mortar content and unit weight of fresh concrete. (b) relationship between mortar content and sand-gravel ratio | 141 |
| 6.19 Vibration effort and ultimate strength relationship | 146 |
| 6.20 Effect of water-cement ratio upon permeability | 149 |

| Figure | | Page |
|--------|--|------|
| 6.21 | The finite element configuration of the experimental section | 154 |
| 6.22 | Deformation of a median barrier of wet mix | 155 |
| 6.23 | Deformation of a failure zone for the experimental slipformed wall section | 157 |
| 6.24 | Maximum shear zones for Florida median barrier section | 158 |
| 6.25 | Relationship between stress ratio and shape factor | 164 |
| 6.26 | Relationship between stress ratio and \bar{y}/h ratio | 164 |

LIST OF SYMBOLS

- a = solid volume of fine aggregate per unit volume of freshly made concrete,
- a_m = solid volume of fine aggregate per unit volume of freshly made mortar,
- A = cross-sectional area,
- b = solid volume of coarse aggregate per unit volume of freshly made concrete,
- b_0 = solid volume of coarse aggregate per unit volume of loose coarse aggregate,
- B = shape factor,
- c = solid volume of cement per unit volume of freshly made concrete; cohesion,
- c_m = solid volume of cement per unit volume of freshly made mortar,
- C_{ijrs} = material constants in the Generalized Hooke's Law,
- d = width, size of aggregate,
- D = maximum particle size,
- e = change in volume of the specimen,
- E_1 = elastic modulus (Young's modulus),
- E_2 = plastic modulus,
- f = coefficient of friction,
- G_a, G_b, G_c = bulk specific gravity of fine aggregate, coarse aggregate and cement,
- h = height,
- H = sample height,

I = moment of inertia,

k = a constant used in the strain rate-strength equation,

$[k]$ = the structure stiffness matrix,

ℓ = length, unsupported length,

m = weight of the mortar

M = mortar content, ratio between the weight of the mortar and the weight of the fresh concrete, volume of mortar per cubic yard of concrete,

M_{cr} = critical mortar content,

P_t = fraction of the total particles finer than size d ,

q = grading ratio (= 0.45),

r = radius of gyration,

$[r]$ = vector of nodal point displacements,

R = radius,

$[R]$ = vector of nodal point forces,

S = specific heat of solid material, strength at a given rate of loading R psi per second, slump, stress ratio,

S_1 = strength at a rate of 1 psi per second,

$[S]$ = stress transformation matrix,

t = period of hydration,

t_1 = period of hydration after vibration

T, T_a, T_c, T_f, T_w = temperature of the fresh concrete, aggregate (surface dry), cement, free moisture, mixing water,

u = percent of air in computing the cement factor,

v = void volume per unit volume of freshly made concrete.
(The volume of voids equals the volume of mixing water plus a small volume of air voids.),

v_m = volume of the voids per unit volume of mortar,

V = volume of concrete,

w = volume of water per unit volume of freshly made concrete,

w_m = volume of the water per unit volume of mortar,

$W_a, W_b, W_c, W_f, W_w, W$ = weight of fine aggregate, coarse aggregate, cement, free moisture on aggregate, water, and fresh concrete,

\bar{y} = center of gravity,

$\gamma, \gamma_a, \gamma_b, \gamma_c, \gamma_w, \gamma_{dl}, \gamma_{dv}$ = unit weight of fresh concrete, fine aggregate, coarse aggregate, cement, water, dry loose coarse aggregate, dry vibrated coarse aggregate,

δ_0 = initial slump due to the weight of the sample,

∇ = del operator,

ϵ = strain on the modified coordinate system,

ϵ_0 = initial strain due to the weight of the sample,

ϵ_1 = strain of a point in the elastic part of the original coordinate system,

ϵ_a = axial strain,

ϵ_l = lateral strain,

ϵ_{rs} = strain tensor,

ϵ_u = strain at ultimate strength,

ϵ_y = strain at yield stress,

θ = angle between the failure plane and the horizontal,

Θ = summation of normal stresses in x, y, and z directions,

ν = Poisson's ratio,

σ = stress on the modified coordinate system,

σ_0 = initial stress due to the weight of the sample,

σ_1 = stress of a point in the elastic part of the original coordinate system,

$\sigma_1, \sigma_2, \sigma_3$ = principal stresses,

σ_u = ultimate strength,

- σ_x = normal stress in x-direction,
- σ_y = yield stress, normal stress in y-direction,
- σ_z = normal stress in z-direction,
- $\sigma_n, \sigma_r, \sigma_\theta$ = normal stress, radial stress, tangential stress,
- $\sigma_{max}, \sigma_{min}$ = maximum and minimum principal stresses,
- σ_{ij} = stress tensor
- $[\sigma]$ = stress matrix,
- τ = shear stress, undrained shear strength,
- τ_{xz} = shear stress in the x-z coordinates,
- τ_{max} = maximum shear stress,
- ϕ = angle of internal friction, stress function,
- ψ = roughness factor.

The Greek Alphabet

| | | | |
|------------|----------------|----------|-------|
| α | Alpha | ν | Nu |
| β | Beta | π | Pi |
| γ | Gamma | ρ | Rho |
| δ | Δ Delta | σ | Sigma |
| ϵ | Epsilon | τ | Tau |
| ξ | Xi | ϕ | Phi |
| η | Eta | χ | Chi |
| θ | Θ Theta | ψ | Psi |
| λ | Lambda | ω | Omega |
| μ | Mu | | |

CHAPTER I

INTRODUCTION

1.1 Horizontal Slipform Concrete Construction

New construction techniques in the past four years include the extensive application of horizontal slipform placement of fresh concrete in special cross-sections such as racing track barriers, retaining structures, noise attenuation and sound barrier supports, bridge railings and highway median barriers, etc. (Lokken, 1974). With the predicted expansion of mass transit systems, horizontal slipform construction should definitely play an important role in the construction of monorails, guideways, and containment structures. Horizontal slipform construction is adaptable to almost any shape with longitudinal dimensions of great extent. Using a newly designed extrusion machine, A.C. Aukerman Co. of Jackson, Michigan has successfully constructed 11 miles of highway median barrier wall up to 80 in. high in Georgia. Drainage-ditch walls on grades as steep as 1:1 have also been slipform placed in Michigan.

Horizontal slipform construction saves both labor and forming material cost. Time is another advantageous factor. With customary ready-mix trucks delivering mix to the extrusion machine, pour production reached 60 cu. yd. an hour, enough concrete to form 3,000 lin. ft. of typical 30 in. high highway median barrier wall per day (Roth, 1974). This production rate compares to in-place form construction

of only about 300 ft. of wall per day.

The ready-mixed concrete is usually delivered to the construction site by truck mixer. It is then poured or augered into the extrusion machine with assistance from vibrators to help compact the fresh concrete while the form is moving forward. The fresh concrete structure emerging from the extrusion form stands with no lateral support as shown in Figure 1.1. The low slump concrete contains a small amount of moisture. As time passes, the fresh concrete quickly gains strength through the hydration process. Therefore, if failure of the structure occurs, it always takes place immediately after extrusion from the form. Both stress failures and excessive deformations are believed due to one or more of the following reasons:

1) Inadequate mix design, hence the fresh concrete fails to offer enough shear strength to maintain the required height or a given shape of structure for self weight loading.

2) Undercompaction of the fresh concrete in the form, especially when the form moves faster than concrete can be effectively extruded.

3) Wet consistency (higher slump) which permits excessive deformations. A failure of this type is shown in Figure 1.2.

It is always a question to both contractors and engineers as to whether, with the available construction materials, a special fresh concrete section will stand immediately after emerging from the extrusion form. In order to answer this question, the basic rheological behavior as well as the strength parameters of compacted fresh concrete have been studied.



Figure 1.1. Fresh concrete structure emerging from the slipform machine.



Figure 1.2. A slump failure of the fresh concrete structure.

1.2 Objectives of Research

Although research on fresh concrete has been directed to areas such as grouting, pumping of concrete, pressure on formwork, the effect of early stripping of formwork on the structural strength of fresh concrete members, and even on vertical slipform construction of high rise buildings, horizontal slipform construction has received little attention. The studies in this project were limited to the stiffness and strength of compacted fresh concrete of low slump (0 to $1\frac{1}{4}$ in.) generally used in horizontal slipform construction.

The general objective of the study was to contribute -- through laboratory work, field observation, and finite element stress-strain analysis -- basic information relative to the compacted fresh concrete behavior, which is needed for developing guidelines and analysis techniques for the mix design of horizontal slipform constructed concrete structures. It is desirable that the extruded fresh concrete structure be structurally stable and be within the acceptable deformation criterion. In order to accomplish this general objective the research program was directed at the rheological and strength behavior of the fresh low slump concrete with the following specific items being investigated:

1) Different mix design methods for low slump concrete were explored. A suitable method was selected and illustrated by a numerical example.

2) Mechanical properties and strength parameters for fresh concrete, including the elastic modulus, plastic modulus, yield stress, ultimate strength and Poisson's ratio, are required for

computation of stresses and strains in the structure under the gravity loading condition in a finite element computer program. Variation of these mechanical properties for different mix designs was studied using the unconfined compression test. Factors affecting the mechanical properties, such as hydration period and water-cement ratio, were also investigated.

3) The various failure criteria for fresh concrete were investigated. A suitable failure criterion for the low slump fresh concrete was established in accordance with the observed experimental test results.

4) A finite element analysis technique was presented and predicted results were compared to the observed field behavior for two horizontal slipformed walls.

5) A simplified analysis technique was developed for use by contractors who wish to determine the suitability of their mix design in the horizontal slipform construction of a given structural cross-section.

CHAPTER II

LITERATURE REVIEW

Information directly oriented to the rheological behavior and shear strength parameters of compacted fresh concrete is very limited. None of the references provide information on low slump concrete. Most of the literature concerns the strength parameters of fresh concrete based on triaxial tests while others relate only to the cement paste as a viscoelastic model. Stresses and strains for fresh concrete structures, calculated by finite element methods, are virtually non-existent. However, it is desirable to provide some background on the composition and hydration process of fresh concrete for this project. The mechanical properties, mix design and failure criteria are also of importance to the understanding of low slump fresh concrete behavior. Horizontal slipform construction has been used as an example for the illustration of analysis technique, hence this Chapter also includes some background on slipform construction.

2.1 Slipform Construction

The emphasis on highway safety has fostered the increased use of median barriers. These barriers help keep vehicles from accidentally entering the opposite lane and the consequences of a head-on collision. Olson, et al. (1970) shows that rigid barriers must resist true forces in the range of 20,000 to 30,000 pounds for speed and impact angles

of 65 mph and 25 degrees, respectively. The concrete median barrier is being used in lieu of other type barriers to reduce maintenance problems including high repair costs, safety of maintenance crews, and disruption of traffic during maintenance operations. The rigid barriers serve the needs of high speed-high volume traffic on a facility with a narrow median.

Contractors today are combining equipment and ingenuity to make horizontal slip-forming an efficient, cost-cutting way to construct concrete median barriers. With conventional forming, about 300 ft per day is the national average while horizontal slipforming boosts daily production to as much as 1,500 ft per day. If a central mix plant were available, 2,000 ft a day might be possible (Lokken, 1971).

A typical cross-section of the median barrier, adopted by the Michigan Department of State Highways and Transportation is shown in Figure 2.1. Although most of the barriers are approximately of this height, higher barriers (Figure 2.2) are used to separate lanes at different grades. A.C. Aukerman Co. of Michigan has slipformed over 11 miles of median barrier on I-85 widening projects in Atlanta, Georgia. The wall heights ranged from 44 to 80 in. on this job (Donnelly, 1973).

Figures 2.3 and 2.4 show the Aukerman extrusion machine which was built to its specifications by Huron Manufacturing Co. It is rubber tire mounted, diesel-powered, and electronically controlled from a string line for line and grade. The slipforms, designed by Aukerman, were built by Steinke-Fenton Sheet Metal Co., Jackson, Michigan. They have telescoping sides that allow them to extrude both

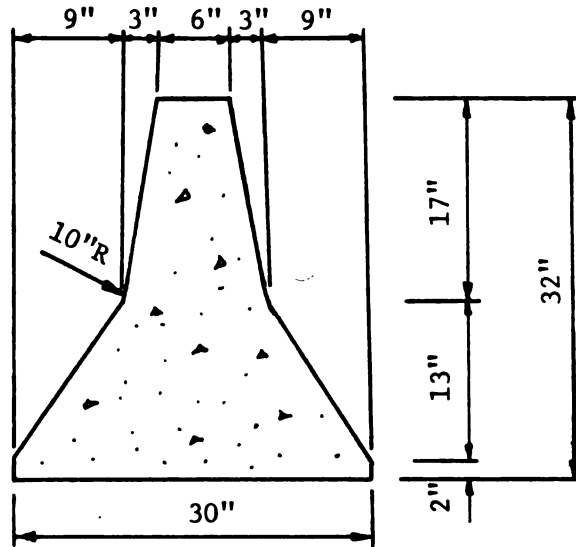


Figure 2.1. Typical Michigan highway median barrier. (FHWA, 1971)

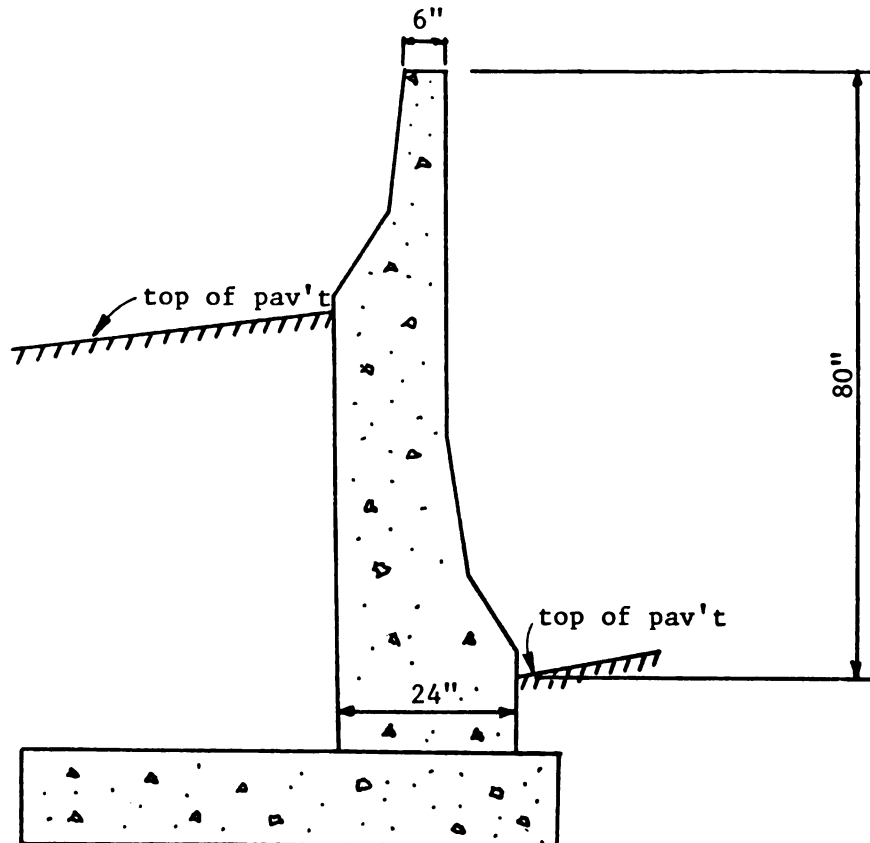


Figure 2.2. Georgia median barrier wall for variable roadway height. (FHWA, 1971)



Figure 2.3. Fresh concrete being augered into the Aukerman form.



Figure 2.4. Vibrators for the Aukerman form.

the standard, symmetrical barrier section and the distorted sections on superelevated roadways. In addition, the forms are designed to accommodate anchor bolts and electrical junction boxes for the roadway lighting system, as well as all barrier reinforcement. The form is 9 ft long, closed at the front and extrudes from the rear end.

Concrete is poured or augered into the form through a hopper at the front of the machine. It is then compacted by six 10,000 rpm, speed-type vibrators that extend 17 in. from the front of the form. Depending on the workability of the concrete, the machine moves forward at speeds ranging from 6 in. to 10 ft per minute. For the maximum speed of 10 ft per minute, the concrete is compacted for a minimum of 8.5 seconds which permits complete compaction. During the vibratory compaction, the fresh concrete is transformed to a liquid state. As the steel form moves forward, the concrete is molded and pressurized by the form to the shape of the structure. The vibration wave is quickly damped by the stiff mass of concrete since the structure formed by the extrusion form does not show any trace of vibration.

When failure occurs, it appears immediately after the concrete has been extruded from the form. The appearance suggests that it is either a slump failure due to the wet consistency of the concrete mix or a shear type failure due to the height of the barrier wall. The latter case occurs when the concrete is of dry consistency. The geometric-cross-section of the wall is another controlling factor. The larger height to width ratios are associated with the lower stability of the structure. Goughnour (1975) indicated that the speed of the extrusion machine or placement rate is inversely proportional to the height-width ratio of the wall.

The concrete used in slipform construction is usually of zero to 1½ in. slump. According to Troxell et al. (1968), it can be considered as a "stiff" or low slump concrete. Some of the characteristics of the stiff concrete are that it can be tamped into a solid dense mass, satisfactory for vibratory compaction, it tends to stand upright and holds together fairly well but crumbles if chuted. Laboratory observations indicate that the stiff concrete usually approximates an elastic behavior up to failure by shear.

2.2 Low Slump Concrete

The property most frequently thought of in relation to fresh concrete is the relative ease with which different concrete mixes can be handled and compacted, such ease being loosely referred to as "workability." The well-known slump test has been used for years as an empirical assessment of workability for purposes of comparison.

The ACI Standard "Recommended Practice for Selecting Proportions for Concrete (ACI 613-54)" presents the details of a method for proportioning concrete having 1 in. to 7 in. slump. The slump test becomes impractical for slumps less than 1 in. Popovics (1962a) has stated that slump is a function of water content:

$$S = C \left(\frac{W_w}{V} \right)^n$$

where C is an integration constant, S is the slump, W_w is the weight of the water, V is the volume of the concrete and n is the instrument constant. Popovics also found that C is a function of the composition of the mixture. For concrete of low water-cement ratio, the water content is very low and the slump becomes very small.

U

W

a

ve

er

a

t

CC

CC

CC

CC

is

of

be

er

2.

tr

tr

Co

Co

W

Co

SE

(C

in

Dr

SE

Usually the concrete used in horizontal slipform construction of a wall of average height (e.g., 3 ft.) is of low water-cement ratio with a slump of less than $1\frac{1}{2}$ in. Hence the slump test is of minimum or no value on projects involving horizontal slipform construction. However, the slump is a commonly used term and in a larger sense, it is a function of the strength of the fresh concrete. For this reason, the terminology "low slump concrete" is often employed with slipform construction.

Troxell et al. (1968) set forth ranges in slump and flow of concrete for various degrees of consistency as given in Table 2.1.

Fresh concrete of "dry" to "stiff" consistency, in Table 2.1, is defined as "low slump" concrete for this research. One distinct characteristic of low slump concrete is that it approximates elastic behavior in a compacted state. Therefore, its mechanical properties are more closely related to the elastic behavior.

2.2.1 Basic Composition

This section describes the composition of fresh concrete and the physical aspect of hydration.

Composition of Fresh Concrete

Fresh concrete is a composite material consisting of cement, water and aggregates in which cement and water form a "cement paste" to serve as a binding medium, while the aggregates, ranging from fine sand (called fine aggregate) to pebbles or fragments of stones (called coarse aggregate), form the filler material. Entrapped air in a suitably proportioned compacted fresh concrete is usually only 1 or 2 percent. Entrained air for particular purposes may run several percent of the volume of the mass.

Table 2.1. Range in slump and flow of concrete for various degrees of consistency (after Troxell et al., 1968).

| Consistency | Slump, in. | Flow, % | Remarks |
|-------------|--------------------------------|---------|--|
| Dry | 0-1 | 0-20 | Crumbles and falls apart unless carefully handled; can be consolidated into rigid mass under vigorous ramming, heavy pressure, or vibration but exhibits voids or honeycomb unless special care is used. |
| Stiff | $\frac{1}{2}$ - $2\frac{1}{2}$ | 15-60 | Pile tends to stand upright; holds together fairly well but crumbles if chuted; with care and effort can be tamped into solid dense mass; satisfactory for vibratory consolidation. |
| Medium | 2- $5\frac{1}{2}$ | 50-100 | Alternative terms are plastic, mushy, quaking; easily molded although some care is required to secure complete consolidation. |
| Wet | 5-8 | 90-120 | Pile flattens readily when dumped; can be poured into place. |
| Sloppy | 7-10 | 110-150 | Grout or mortar tends to run out of pile, leaving coarser material behind. |

Aggregates, usually inert minerals, are considered as ideal elastic solids which obey Hooke's Law while being deformed. The fresh paste is a suspension, not a solution, of cement in water. Chemical reaction, known as hydration, takes place in the paste to produce a substantial part of the hydration product known as "gel." Water in the paste approximates an ideal Newtonian fluid which cannot support a shear stress, and shear deformation will continue as long as any shear stress is applied. When cement particles are present in the water, a non-Newtonian fluid is formed by the paste which has a shear rate dependent viscosity. Once the cement paste mixes with aggregates its mechanical properties approximate that of a Bingham solid or a brittle solid, depending on the water-cement ratio. Fresh concrete used in slipforming approximates a brittle solid because of its initial strength. In concrete technology, a common term, "mortar," is used in defining the mixture of cement paste and fine aggregates. The configuration of all the elements in a fresh concrete can be represented as shown in Figure 2.5. This figure shows aggregates "suspended" (coated by paste) in water, and the existence of continuous passages for water along the fresh concrete body.

Physical Aspects of Hydration

Immediately after cement is mixed with water, the solid cement particles are dispersed in the liquid water forming a suspension. In this suspension the cement particles are separated an average distance of 5 to 10 microns by the combination of gravitational force, buoyant force, Van Der Waal's force (interparticle attraction), and repulsive electrostatic forces derived from ionic charges on the surface of the

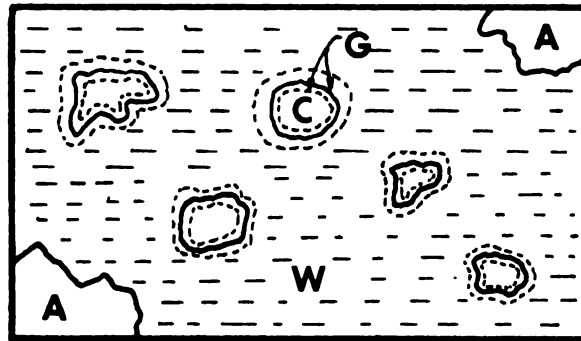


Figure 2.5. Interrelationship of aggregate (A), cement (C), water (W), and gel (G).

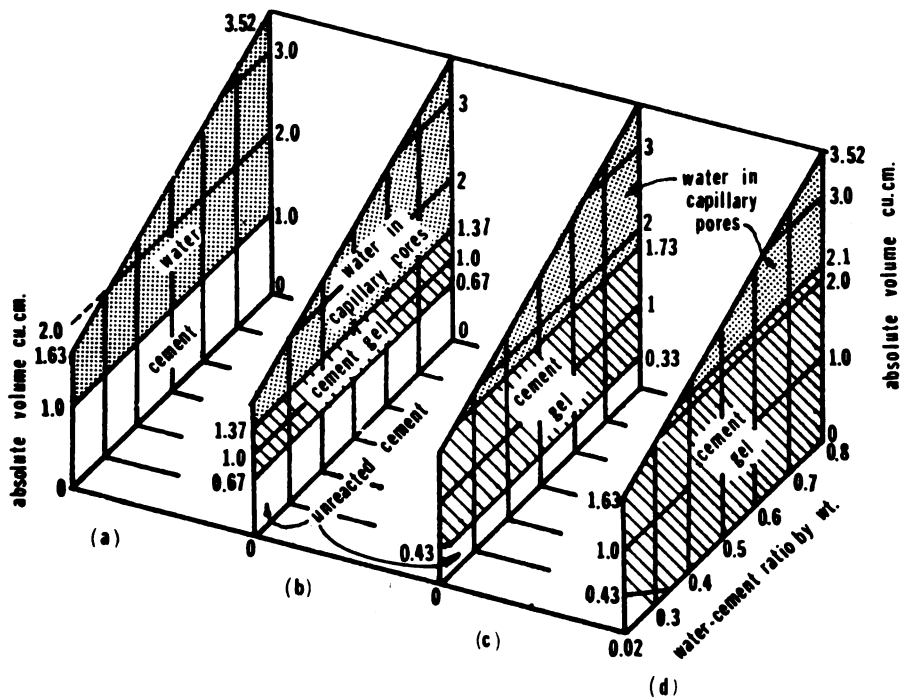


Figure 2.6. Space relationship for paste components at various stages of hydration. (a) fresh paste; (b) reaction one-third complete; (c) reaction two-thirds complete; (d) reaction completed. Assumptions: specific gravity of cement = 3.15.

particles. Due to the initial closeness of the cement particles and the Van Der Waal's forces, the fresh concrete mass tends to consolidate as a single block to produce the phenomenon as "bleeding."

A chemical reaction, known as hydration, takes place when the surfaces of the cement particles react with water. A substantial part of the hydration product is a "gel" which is a two-component dispersion system in which the solid phase is of colloidal dimensions. After the formation of an initial layer of gel, some of the reaction products occupy the space made available by the dissolution of the cement particles. Although the particles of gel are of extremely small size, the arrangement of their constituent molecules is in the form of layered structures somewhat analogous to the structure found in some clay minerals. The major material formed from the cement paste is called tobermorite gel. Hardened cement paste consists of a collection of interwoven filaments of tobermorite gel interspersed with other reaction products. The space between the various particles is called the "gel pore" space. Evidently, water in these small "gel pores" (15 to 20 A), under the influence of the surface forces of the gel particles as mentioned in the above paragraph, does not exhibit the same properties as "free water."

During the early stage of the reaction, products have not completely filled the space that existed between the original cement particles; there are spaces which are considerably larger than gel pores. These spaces are called "capillary pore" space. With pastes of moderate-to-low water-cement ratios the capillary pores tend to be filled with cement gel as hydration proceeds.

Troxell et al. (1968) has reported that if 1 cu cm of cement undergoes complete reaction, it will produce 2.1 to 2.2 cu cm of cement gel which includes both solid particles and gel pores. The additional 1.1 to 1.2 cu cm of space must be made available through the replacement of volumes originally occupied by the mixing water. If not, some of the cement remains unhydrated. Troxell (1968) illustrates this space relationship in the four stages of hydration as shown in Figure 2.6. From Figure 2.6 it is seen that water in the capillary pores, which is the "free water," reduces as hydration proceeds.

Roughly, the amount of water required for complete hydration of cement is half of that used in making average concrete. The excess water over that sufficient for hydration is required for purposes of workability (Troxell et al., 1968).

At the beginning of the mixing, the mixing water fills in between the space of the original cement particles (unhydrated cement particles). It is this initial volume of water which defines the "effective water-cement ratio." If the mixing water is reduced, resulting in a lower effective water-cement ratio, not only is the gel volume decreased, but some of the interparticle attraction and capillary forces are increased; thus the paste exhibits a greater strength.

A fresh concrete can be manipulated for periods of one to perhaps two hours after mixing, then it gradually stiffens. As hydration proceeds, the reaction products take up what was originally free water, gel and other reaction products begin to occupy more space, and therefore the mobility of the paste is decreased. Finally, if

the mass is left undisturbed, an increasing quantity of gel and other hydration products develop sufficiently close contact and bonds of increasing strength, such that the mass develops rigidity. Figure 2.6(d) illustrates this rigidity condition. At some point, the mass can sustain load without flowing, and the paste is said to have "set." Initial set, usually 2 to 4 hours after mixing, is the beginning of noticeable stiffening and final set, 5 to 8 hours after mixing, is regarded as the hardening period of the paste. The scope of this research, as can be readily seen, is confined to the earlier stage of hydration, i.e., within the first hour after mixing.

2.2.2 Physical Properties

Some physical properties of fresh concrete and aggregates are required in order to characterize the quality of the concrete relative to engineering purposes and to describe the factors which influence the strength of the fresh concrete. Those properties important to this research include bulk specific gravity of the fine aggregates and coarse aggregates, unit weight of the fresh concrete and of the coarse aggregate, void percentage of the coarse aggregates, and mortar content per cubic yard of concrete. Properties less important but which serve informative purposes include bulk specific gravity (saturated surface dry), apparent specific gravity, and percent absorption of both fine and coarse aggregates.

Specific Gravity and Percent Absorption

The specific gravity of the aggregate is the ratio of the unit weight of the aggregate to the unit weight of water. Since some aggregates are dense and impermeable while others are porous, the

common term specific gravity generally refers to bulk specific gravity which is the ratio of the weight in air of a given volume of aggregates (including both the permeable and impermeable voids) at the standard temperature to the weight in air of an equal volume of distilled water at the standard temperature. If there is no surface or free moisture on the aggregate but all voids within the particles are filled with water, the bulk specific gravity so determined is called a saturated surface dry condition. The apparent specific gravity is the ratio of the weight in air of a given volume of the impermeable portion of the aggregate (that is, the solid matter including its impermeable pores or voids) at a stated temperature to the weight in air of an equal volume of distilled water at the same temperature.

The percent absorption, a measurement of the total internal moisture content of an aggregate in the saturated surface-dry condition, is determined by finding the weight of a surface-dried sample after it has been soaked for 24 hours and again weighed after being oven-dried; the difference in weights is expressed as a percentage of the dry sample weight. The percent absorption is a measure of the porosity of an aggregate. It is also used as a correction factor in determination of free moisture by the oven-drying method. As long as this quantity is less than 1.5 percent and the water contact period is short (e.g., less than 1 hour), the percent absorption can be neglected in computing the water-cement ratio.

Unit Weight

The unit weight, γ , in pounds per cubic foot of the fresh concrete depends on the proportion and the unit weight of each

constituent in the concrete. Air content, obviously, is another important influencing factor. For the same proportions and constituents, higher air contents always give a lower unit weight to the fresh concrete (Troxell et al., 1968). Unit weight is measured by dividing the sample weight with its volume. Vibrator compaction is generally applied before measurement of the weight and volume, therefore it is actually a compacted unit weight.

Both compacted and loose unit weights of coarse aggregate are determined by standard ASTM methods. These determinations permit computation of the void ratio of the coarse aggregate.

Voids Content of the Coarse Aggregates

Voids content is the volume of voids between the coarse aggregate particles in a given bulk volume of coarse aggregate. It may be computed indirectly using the unit weight of the aggregate and the specific gravity of the particles in line with ASTM Standards. The voids content is used to determine the critical mortar content as required in Section 2.2.4.

Mortar Content Per Cubic Yard of Concrete

Mortar content, as used here, is different from that which appeared in Section 2.2.4. In Section 2.2.4 mortar content is expressed on a weight basis while in this section, mortar content is computed on a volume basis. Equation 2.1 gives M , the volume of mortar per cubic yard of concrete.

$$\begin{aligned}
 M &= \frac{V_m}{V} \times 27 \\
 &= \left(\frac{W_c}{\gamma_c} + \frac{W_w}{\gamma_w} + \frac{W_a}{\gamma_a} \right) \left[\frac{27}{(W/\gamma)} \right] \\
 &= \left(\frac{W_c}{\gamma_c} + \frac{W_w}{\gamma_w} + \frac{W_a}{\gamma_a} \right) \left[\frac{27 \gamma}{W_a + W_b + W_c + W_w} \right] \quad (2.1)
 \end{aligned}$$

The quantities W_c , W_w , W_a , W_b , W , γ_c , γ_w , γ_a , γ_b , and γ are the weights and unit weights of cement, water, fine aggregate, coarse aggregate, and fresh concrete, respectively. M is used in computing the air content as measured by the air indicator. Usually a conversion table is provided with the air content indicator to convert actual readings to true air content by a factor determined by M of the fresh concrete. Values of M for tests related to measurement of air content were only different in insignificant amounts for this project, hence a unique value of 14 cubic feet was used.

Basic Water Content

The water content at which mortar attains its maximum density is defined as the basic water content. Whenever water is mixed in increasing amounts with the dry mortar ingredients, there is at first an increase in volume of the mortar, which is greater than the volume of the water added, then there is a decrease in volume, followed by an increase in volume. Since the volume of the cement and fine aggregate particles remain unchanged as the water is increased, the change in the volume of the mortar portrays the change in volume of the voids.

The amount of water required for workability is always greater than the basic water content. For convenience, the basic water content is assigned a value of 1.0. Relative water content (R.W.C.) is the amount of water expressed as a multiple of the basic water content. Therefore a R.W.C. of 1.05 indicates that the amount of water required is 1.05 times the basic water content of the mortar.

2.2.3 Mechanical Properties

The mechanical properties of a material being characterized are usually subdivided into three major categories: elastic, plastic, and viscoelastic. A suitable mathematical model(s) is then assigned to represent the material behavior and mechanical properties are evaluated by the model. It is recognized that no model portraying an ideal material behavior can fully represent all aspects of the response of fresh concrete. The selection of a model that retains the significant features of the material's response and which are within the bounds of practicality fall into the area of mathematical modeling. The adequacy of a particular model depends on the problem under study and the overall system in which it will be used. Different components of the same problem may require the material to be characterized differently according to which aspect of material response is important in solving that particular component of the problem. Therefore an understanding of the physical phenomena of the fresh concrete is essential in establishing this model.

Homogeneity and Isotropy of the Material

The generalized form of Hooke's Law expresses the stress tensor σ_{ij} in terms of the strain tensor ϵ_{rs} by a linear

relationship as:

$$\sigma_{ij} = C_{ijrs} \epsilon_{rs} \quad (2.2)$$

where C_{ijrs} represents the material constants which relate the nine components of the stress tensor with 81 coefficients. Not all of these coefficients are independent and the number may be reduced to 2 by noting the symmetry of the stress and strain tensors, the existence of the strain energy function and the isotropy of the material. These two coefficients are, E_1 , known as Young's modulus, and ν , known as Poisson's ratio.

It is recognized that the fresh concrete consisting of water, cement, and aggregate particles is far from being homogeneous and that the elastic properties of a single particle may vary greatly in different directions. However, the vibratory compaction effort during the slipform construction distributes the aggregates and the cement particles randomly and the elastic properties of the larger mass of compacted fresh concrete represent averages for paste and individual particles. So long as the geometrical dimensions defining the form of the fresh concrete body are large in comparison with the dimensions of a single particle, the assumption of homogeneity can be used with accuracy, and if the particles are orientated at random, the material can be treated as isotropic. Experience shows that solutions of the theory of elasticity, based on the assumptions of homogeneity and isotropy, can be applied to hardened concrete structures with great accuracy. The shape of the stress-strain curve and the failure pattern of the compacted fresh concrete samples in an unconfined

compression test are similar when compared to those for the hardened concrete. It is assumed that the isotropic and homogeneous characteristics are also applied to the compacted fresh concrete with reasonable accuracy.

Unconfined Compression Test on Fresh Concrete

Uzomaka (1971) conducted his unconsolidated-undrained triaxial tests on fresh concrete within a time limit from the end of mixing to the end of each test of approximately 3 hours. Owing to the complexity of the triaxial test, other researchers' tests were assumed to require the same amount of time. Although sugar was added to retard the hydration, no exact quantitative study has appeared in the literature to describe its influence on the strength parameters as a function of hydration time for fresh concrete. As a matter of fact, Ashworth (1965) reported that sugar can only serve as a water-reducing, set-retarding admixture similar in character to many commercial retarders. Slipform construction is usually finished within an hour after the end of mixing whereas running a triaxial test requires a much longer time. Also, the slipform constructed structure is in a plane-strain state, therefore the two horizontal principal stresses are different in magnitude. The confining pressure in a triaxial test is restricted to an all around pressure which does not simulate field conditions in slipform construction.

Triaxial tests, together with the Mohr-Coulomb failure criterion, were developed to help solve soil mechanics problems which often involve semi-infinite elastic half space boundary conditions. Horizontal slipform constructed structures involve different boundary

conditions since concrete is extruded from a confined condition in the construction machine to a laterally unconfined condition. Should failure occur, it is an immediate one with no time available for consolidation or change in water content. As long as the fresh concrete structure can stand by itself, it more or less bears some resemblance to a cohesive soil. Therefore, a strain-controlled undrained, unconfined compression test appears to best serve the needs of this project.

Unconfined compression tests have their shortcomings such as underestimating strength due to the lack of confining pressure and sampling disturbance, etc. However, a confining pressure appears to have little influence on slipform constructed fresh concrete structures which can expand freely in the lateral direction and sampling disturbance is not applicable for this case. The choice of test method for any particular engineering problem will depend upon a number of factors, especially the availability of equipment and economics. The unconfined compression test seems, at the present time, to fit this particular problem better than any other test method.

Direct shear tests have been considered for determining the strength parameters of some inner elements of the structure. However, disadvantages for this test method, such as non-uniform stress and strain and a predetermined shear surface, which is not necessarily the weakest one, eliminated it from consideration.

A typical stress-strain curve for low slump compacted fresh concrete and the unconfined compression test is shown in Figure 2.7. Mechanical properties obtainable from the stress-strain curve are defined as follows:

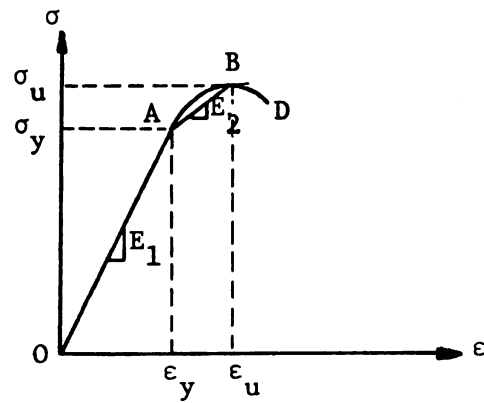


Figure 2.7. Typical stress-strain curve for low slump compacted fresh concrete.

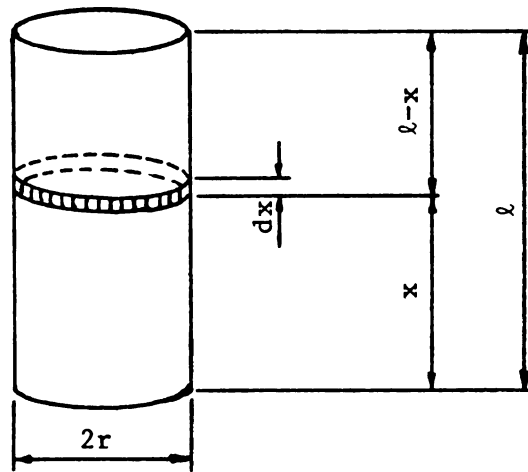


Figure 2.8. Cylinder dimensions used for calculation of initial slump in the fresh concrete.

σ_u = ultimate strength,

σ_y = yield stress,

ϵ_u = axial strain at ultimate strength,

ϵ_y = axial strain at yield stress,

E_1 = elastic or Young's modulus, and

E_2 = plastic modulus, straight line connecting (σ_y, ϵ_y)
and (σ_u, ϵ_u) .

Initial Slump

The slump test gives only a relative measure of workability and it does not determine any fundamental engineering properties. Still the "initial slump" of a test sample is a useful engineering property. The initial slump represents subsidence of the test sample due to gravity forces when the cylinder or cone is removed. This initial slump and the accompanying initial stresses developed in a sample are derived mathematically in the following paragraph.

Let γ equal the unit weight of the low slump concrete shown in Figure 2.8. Then the weight of the sample, W , above level x becomes

$$W = \gamma \pi r^2 (\ell - x) \quad (2.3)$$

The stress on the plane dx equals

$$\sigma = W/\text{Area} = \gamma(\ell - x) \quad (2.4a)$$

Assuming elastic behavior, Hooke's Law gives the deformation $d\delta$ in the element dx as

$$d\delta = \frac{\sigma dx}{E_1} \quad (2.4b)$$

where E_1 is the Young's modulus.

Combining Equations (2.4a) and (2.4b), and taking the integration limits at 0 and l gives

$$\delta = \int_0^l \frac{\gamma(l-x)dx}{E_1} = \frac{\gamma l^2}{2E_1} + C$$

Using the boundary conditions $\delta = 0$ when $l = 0$, the integration constant C equals zero. The following initial conditions are therefore established.

$$\delta_0 = \frac{\gamma l^2}{2E_1} \quad (2.5)$$

$$\epsilon_0 = \frac{\gamma l}{2E_1} \quad (2.6)$$

$$\sigma_0 = \frac{\gamma l}{2} \quad (2.7)$$

where δ_0 , ϵ_0 , and σ_0 are initial slump, initial strain, and initial stress due to the weight of the sample. Figure 2.9 illustrates the superposition of ϵ_0 and σ_0 into the stress-strain curve from an unconfined compression test.

In Figure 2.9, point P on the elastic part of the stress-strain curve was obtained from the unconfined compression test. It has coordinates σ_1 and ϵ_1 in the original coordinate system from which E_1 may be computed. With the value of E_1 and other known properties, ϵ_0 and σ_0 values are obtained from Equations (2.6) and (2.7). These two values are then superimposed as shown in Figure 2.9

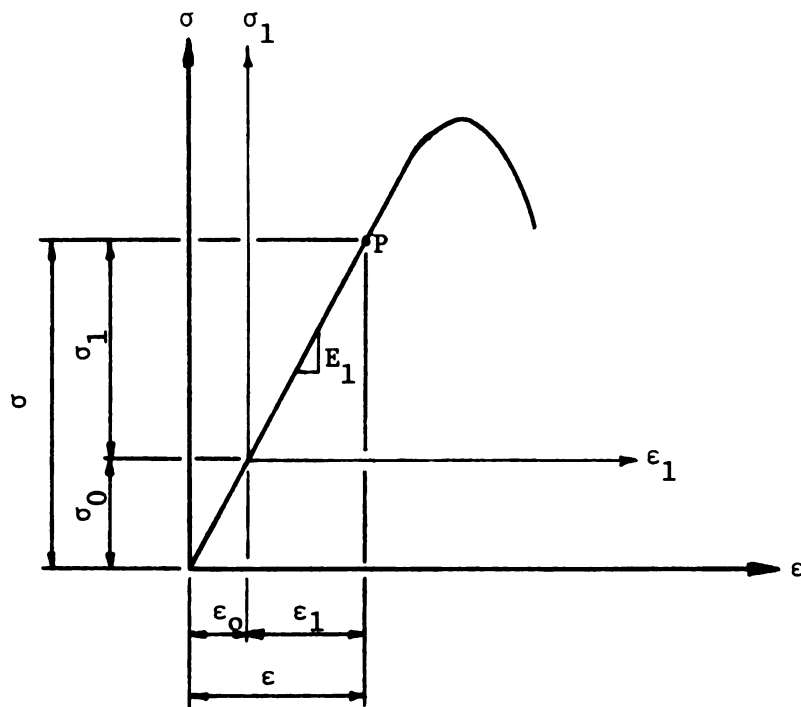
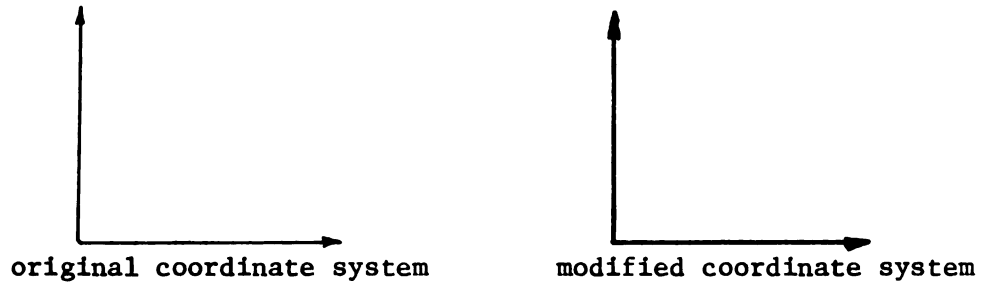


Figure 2.9. Stress-strain curve for low slump concrete including strains due to gravity forces

to form the modified coordinate system. It is obvious from this figure that any point on the modified stress-strain curve has coordinates $\sigma = \sigma_0 + \sigma_1$ and $\epsilon = \epsilon_0 + \epsilon_1$. The values of the new coordinates σ and ϵ determine the stress-strain curve representative of low slump concrete as it leaves the extrusion machine.

Poisson's Ratio

Poisson's ratio is an elastic constant which is difficult to evaluate for most materials. For an ideal, isotropic, cylindrical specimen of material subjected to a uniaxial stress rate, Poisson's ratio becomes

$$\nu = \frac{\epsilon_l}{\epsilon_a} \quad (2.8)$$

where ϵ_l and ϵ_a are the lateral and axial strains, respectively. Dehlen (1969) has theoretically shown that, if perfectly frictionless caps and bases are used in the triaxial test, the errors associated with uneven lateral strain of the specimen should be less than 10 percent. Therefore, Equation (2.8) can only be used to calculate Poisson's ratio provided that end friction is eliminated. Values of ν increase gradually with increasing temperatures and increasing axial compressive stresses. Generally speaking, ν depends on the type of material, the relative density and the stress state (Nair, 1973).

From physical considerations, ν for an elastic isotropic material should be between -1 and 0.5, although experience does not exhibit any material with negative values of ν (Malvern, 1969). Also, experimentally determined values of ν are in some cases

greater than 0.5. These large values of ν may at least partially be caused by the nonuniform stress and deformation conditions that exist in the specimens and also by materials not behaving as ideal elastic solids. Dilatancy effects can produce a value of ν greater than 1/2. From the theory of elasticity volume change of the sample under shear stress can be related to Poisson's ratio as

$$e = \frac{1 - 2\nu}{E} \theta \quad (2.9)$$

where e = change in volume of the specimen and

$$\theta = \sigma_x + \sigma_y + \sigma_z \cdot$$

Equation (2.9) shows that for an incompressible material, such as a fully saturated soil, the Poisson's ratio is equal to 0.5.

The volume change can be evaluated by measuring the deformation profile of the specimen directly or by filling the triaxial cell with a fluid and measuring its change in volume. Since both methods are limited by experimental problems, values for Poisson's ratio are often estimated for an engineering analysis or design problem.

Hardened concrete has ν values within the range of 0.15 to 0.3; a completely saturated fresh concrete specimen under incompressible conditions should have a ν value close to 0.5. For practical purposes, and recognizing that several percent of air may exist in the fresh concrete, ν has been assumed equal to 0.4 for problems involving the slipform construction with fresh concrete.

2.2.4 Factors Effecting Mechanical Properties

Uzomaka (1971) and Ritchie (1968) have included water-cement ratio, aggregate-cement ratio, angularity of aggregate, grading of aggregates and type of cement as the five most important factors influencing the strength of fresh concrete. Due to limitations in their test methods, they have ignored another important factor -- the variation of the period of hydration.

After a careful review of the literature, it was concluded in this study that there are at least fourteen parameters that affect the strength of the compacted fresh concrete. Some of them have very negligible effects while others either cannot be controlled in the field or are difficult to be simulated in the laboratory test; standardization eliminated some of these factors. The fourteen parameters are listed below and only the first eleven factors are discussed individually in the following subsections.

1. Effective water-cement ratio (W_w/W_c)
2. Period of hydration (t_1)
3. Period after vibration (t_2)
4. Cement content (W_c/m)
5. Mortar content (M)
6. Particle shape
7. Concrete temperature (T)
8. Aggregate gradation
9. Air content
10. Rate of strain
11. Vibration effort

12. Cement characteristic
13. Concrete volume
14. Water reducing admixture

Letters in the parentheses following some of the items are designated to represent that particular parameter. Some parameters are usually expressed on a volumetric basis in mix design. However, laboratory tests are always much smaller in scale as compared to actual construction, hence volumetric expressions were converted into weight bases for the best control and convenience in this study.

Effective Water-Cement Ratio (W_w/W_c)

The effective water-cement ratio, W_w/W_c , is measured as the ratio between the weight of water, W_w , and the weight of cement, W_c , in the mix design. Fresh concrete consists essentially of cement-water paste which is the "active" ingredient, and "inert" mineral aggregates. Workability of the mass is provided by the lubricating effect of the paste. The more diluted the paste, the greater the spacing between cement particles, and thus the weaker will be the ultimate paste structure at any stage of hydration. Since absorbed water in the aggregate does not contribute to the chemical reaction (hydration), only water added to the mix is counted in evaluating the value of W_w/W_c .

Period of Hydration (t_1)

The process of hydration makes the fresh concrete become stiffer as time elapses. This is because the strength of a paste develops in large part from the bonds formed between the very small

particles that compose the cement gel. Generally, the greater the number of such particles and the denser the gel structure, the stronger will be the gel mass. As shown by Figure 2.6, the longer the period of hydration the more cement gel will be produced resulting in a stronger structure. To look at it another way, hydration reduces the water-cement ratio by reducing the amount of "free water" which results in a stronger structure. Theoretically, the effective water-cement ratio at various stages of hydration can be calculated provided the hydration rate is known. Seki, et al. (1969) published an article concerning the relationship between compressive strength of concrete and the effective water-cement ratio calculated from the hydration rate of cement. However, refined work still is needed in this area to provide accurate measurements for a range of mixes. For practical purposes, the period of hydration is used as a parameter in this research project. The period of hydration t_1 is defined as the period between the start of the mixing and the beginning of the unconfined compression test.

Period After Vibration (t_2)

When water is first mixed with other ingredients, a tiny part of it is absorbed by the dry aggregates while a large part of it contributes to the hydration action. There is also a large part which contributes only to workability since the mixing action in a mixer is usually not as rigorous as that produced by a vibrator. Between the period of the start of mixing and when the vibrator is inserted for action, some strength develops in the fresh concrete due to hydration. However, the stiffened concrete can always be brought back to

its original workability if more water is added. In the field, this period, based on experience, is limited to 60 minutes. Vibration always gives a better mixing action for concrete of dry consistency. For practical engineering purposes, it therefore is desirable to establish another strength evaluation parameter as the "period after vibration" t_2 , which is defined as the period between the start of vibration and the beginning of the unconfined compression test. It is believed that the structure of the fresh concrete is much more unstable before vibration as compared to that when the vibration has been completed.

Cement Content (W_c/m)

For a given effective water-cement ratio, the cement content in the mortar is expressed as:

$$\frac{W_c}{m} = \frac{W_c}{W_c + W_w + W_a} = \frac{1}{1 + \frac{W_w}{W_c} + \frac{W_a}{W_c}} \quad (2.10)$$

In this equation, m is the weight of the mortar. It is apparent that as long as water-cement ratio remains unchanged, cement content is a function of W_a/W_c .

In a certain sense, fresh concrete can be viewed as a combination of paste and aggregates. Since mineral aggregates are much stronger than the paste, the strength of the fresh concrete is somewhat limited by the amount of paste. Over a reasonable range, cement and sand may be interchanged by equal solid volumes, resulting in changes in both cement content and water-cement ratio without affecting

total water content or slump (U.S. Bureau of Reclamation, 1963). If the water-cement ratio is kept unchanged, an increase in strength is accomplished by decreasing the cement content (or by increasing the W_a/W_c ratio). It should be pointed out here that this decrease in cement content actually is accompanied by a reduction of water content in the concrete since water-cement ratio was said to be constant at all times. If water content is to be held constant, then higher strength can be achieved by increasing cement content since the water-cement ratio is actually decreased. Ritchie (1968) reported this phenomenon in the triaxial testing of fresh concrete and Powers (1968) showed the same findings in plastometer tests of fresh concrete. Troxell et al. (1968) made a similar statement, "if water-cement ratio is to be held constant, an increase in slump is accomplished by increasing the amount of paste (or more conveniently, by decreasing the amount of aggregate) resulting in a richer and therefore a more expensive mix." However, the cement content can only be decreased to certain limits in order to produce fresh concrete with a maximum strength. A further reduction in cement content will decrease the cohesive force such that there is insufficient paste to bind all the aggregates together. Therefore, a lean mix definitely can be justified for economic reasons, but beyond a certain limit, it can either decrease the strength or reduce the workability of the mix, for the other function of the paste is to provide lubrication.

For practical purposes, the cement content can be converted into a "cement factor" as commonly used in concrete technology. The "cement factor" for a concrete mix is the cement content expressed in

terms of sacks of cement per cubic yard of concrete. Equation (2.11) expresses this quantity in the mix design on a weight basis

$$\begin{aligned}
 CF &= \frac{\text{sack of cement}}{\text{cu yd. of concrete}} \\
 &= \frac{(W_c/94) (1 - u\%)}{(V/27) (1 - 2\%)} \\
 &= \frac{27\gamma W_c (1 - u\%)}{94 W (1 - 2\%)} \quad (2.11)
 \end{aligned}$$

In this equation V is the volume of the concrete in cubic feet, W is the weight of concrete in pounds, γ is the concrete unit weight in pounds per cubic foot, and W_c is the weight of the cement which is assumed to be 94 pounds per sack. Since non-air-entrained cement was used in this project, the air content of the mix was estimated to be close to 2 percent. u percent is the air content desired when air-entraining agents are added.

Mortar Content (M)

Mortar content M is defined as the ratio between the weight of the mortar and the weight of the concrete while keeping the water-cement ratio and the cement content W_c/m (or W_a/W_c) unchanged. Mortar content is evaluated by the following equation.

$$M = \frac{m}{W} = \frac{W_a + W_c + W_w}{W} \quad (2.12)$$

In a fresh concrete structure, the mortar is always weaker than the coarse aggregate. A decrease in mortar content will increase the strength of the concrete and decrease the workability of the fresh concrete since one of the functions of the mortar is to provide lubrication of the fresh, plastic mass.

The strength increase characteristic due to decrease in mortar content has a limitation. Beyond that limit, a further decrease in mortar content will lead to insufficiency of mortar to fill the voids between the coarse aggregates; hence a honeycomb structure which exhibits less strength will be produced. Theoretically, this limit rests on the condition that the volume of mortar just fills the volume of voids between the coarse aggregates, and the mortar content so determined is defined as the critical mortar content, M_{cr} . The calculation of the critical mortar content is shown in Appendix C. However, this perfect condition can hardly be achieved without leaving a honeycomb structure since additional mortar above the critical mortar content is always required to give the necessary workability for compaction.

If W_b is the weight of the coarse aggregate, Equation (2.12) can further be refined:

$$\begin{aligned}
 M &= \frac{W_a + W_c + W_w}{W} = \frac{W_a + W_c + W_w}{W_a + W_b + W_c + W_w} \\
 &= \frac{1}{1 + \frac{W_b}{W_a + W_c + W_w}} = \frac{1}{1 + \frac{1}{\frac{W_a}{W_b} \left(1 + \frac{W_c}{W_a} + \frac{W_c}{W_a} \frac{W_w}{W_c}\right)}} \quad (2.13)
 \end{aligned}$$

The W_c/W_a ratio and W_w/W_c ratio are constants in evaluating the influence of the mortar content on the strength. It is readily seen from Equation (2.13) that mortar content actually is a function of W_a/W_b ratio. The larger the W_a/W_b ratio, the larger the mortar content and hence the weaker the fresh concrete.

Physically, this is also conceivable since the coarse aggregates are more intact and therefore stronger than the fine aggregate.

Particle Shape

The shape of coarse aggregate governs the resistance of the individual particles to movement within the mix. The more angular the coarse aggregate, the better interlocking it exhibits under shear stress, and therefore the higher strength it preserves. Generally speaking, in a comparable mix coarse aggregates of crushed stone require a higher water-cement ratio than natural gravels do in achieving the required slump. Shape of the coarse aggregate determines the angularity and specific surface area. Since not enough variety of crushed stone was available to determine this interrelationship with respect to strength of the concrete, a different coding system was selected for making comparisons. Effective water-cement ratio, the most important parameter, was selected for this purpose. Water-cement ratios similar to those used in mix designs for natural gravels were also used in mix designs for crushed gravels. The two sets of results on unconfined compression tests were then compared to demonstrate the influence of the shape of the coarse aggregates.

Concrete Temperature (T)

Temperature greatly influences hydration rate, therefore the gain in strength of concrete is directly proportional to its temperature. Although the temperature of the concrete is difficult to control in the laboratory, an estimate of the temperature of the concrete can be made (U.S. Bureau of Reclamation, 1963) as follows:

$$T = \frac{S(T_a W_a + T_c W_c) + T_f W_f + T_w W_w}{S(W_a + W_c) + W_f + W_w} \quad (2.14)$$

where the symbols are identified in the following tabulation.

| Material | Weight | Temperature |
|--------------------------------|--------|-------------|
| Aggregates (surface dry basis) | W_a | T_a |
| Cement | W_c | T_c |
| Free moisture on aggregates | W_f | T_f |
| Mixing water (added) | W_w | T_w |

S = specific heat of the solid materials

Aggregate Gradation

The relative compaction of fresh concrete depends greatly upon the gradation of all the aggregates. Smaller amounts of paste are required to fill the space and surround the aggregate particles completely for a well-graded mixture than for a harsh or poorly graded one. Also, it should be noted, that there are an infinite number of gradings which will produce a given fineness modulus, therefore fine modulus cannot be used as an evaluation criterion.

This factor is evaluated by grain size distribution curves on the gradation chart. Higher strength is demonstrated by a higher percentage of coarse aggregates in the gradation chart. The W_a/W_b ratio is related to the gradation.

Air Content

Air content is a function of water-cement ratio, stirring time, stirring speed and volume of batch, and the amount of air-entraining agent added (Powers, 1968). Within a reasonable range of the mix

design variables and standard mixing procedures, only the last item actually affects the air content. Vibration of normal amounts does not materially affect the amount of entrained air. One study revealed that 3 minutes of vibration reduced the percentage of air by 1 to 3 units over a range of consistencies (Troxell et al., 1968). The general effects of air entrainment are to increase workability, decrease density (unit weight), decrease strength, reduce bleeding and segregation, and increase durability. The air content is measured by the air indicator and is expressed quantitatively by the percent of air entrained in the total volume of concrete.

Rate of Strain

For strain-controlled tests on soils a rate of strain of approximately $\frac{1}{2}$ to 2 percent per minute is frequently employed. Lambe (1965) and Casagrande (1951) reported an increase in strength as the rate of strain was increased in undrained tests of cohesive soils. For triaxial testing of fresh concrete, Ritchie (1962) reported its influence as summarized in Table 2.2. The same phenomenon has been reported in testing hardened concrete (Troxell et al., 1968).

Table 2.2. The angle of internal friction at various rates of strain (after Ritchie, 1962).

| Mix (cement/ aggregate) | Rate of Axial Strain | | |
|-------------------------------|---------------------------|---------------------------|---------------------------|
| | A | B | C |
| | 2.1 percent per minute | 4.3 percent per minute | 8.5 percent per minute |
| 1 : 3 | 12° | 10° | 2° |
| 1 : 6 | 32° | 33° | 40° |

It appears that rate of strain has little or no effect on the angle of internal friction over the speed range A to B, but that for high rates of loading there is a marked change.

Vibration Effort

Concrete used in horizontal slipform construction is very stiff, usually of zero to one inch slump. Low slump concretes have poor workability when compaction is attempted by hand rodding. When vibration is used these concretes are considered to have excellent workability characteristics. The efficiency of any vibrator depends upon its frequency and speed. Tests have shown that for complete compaction a concrete of $\frac{1}{2}$ inch slump required 90 seconds vibration at 4,000 rpm, 45 seconds at 5,000 rpm, and 25 seconds at 6,000 rpm (Troxell et al., 1968). These vibration effects can be plotted (Figure 2.10) to demonstrate complete and incomplete compaction efforts.

The primary function of vibration in concrete is to produce compressive waves in the mortar and give the mortar a temporary fluidity. In this way it creates relative motion of mortar with respect to the denser particles (coarse aggregates) "suspended" in it. In a flocculent structure of concentrated cement particles such motion tends to open up each constriction in interparticle space and thus to increase the minimum distance between particles. Since interparticle attraction diminishes rapidly with the increase in interparticle distance, the effect of vibration is to weaken interparticle attraction and to allow the whole concrete mixture to become mobile under any external force. The structure matrix of the fresh concrete after complete compaction can be described as follows. The only material in direct contact with

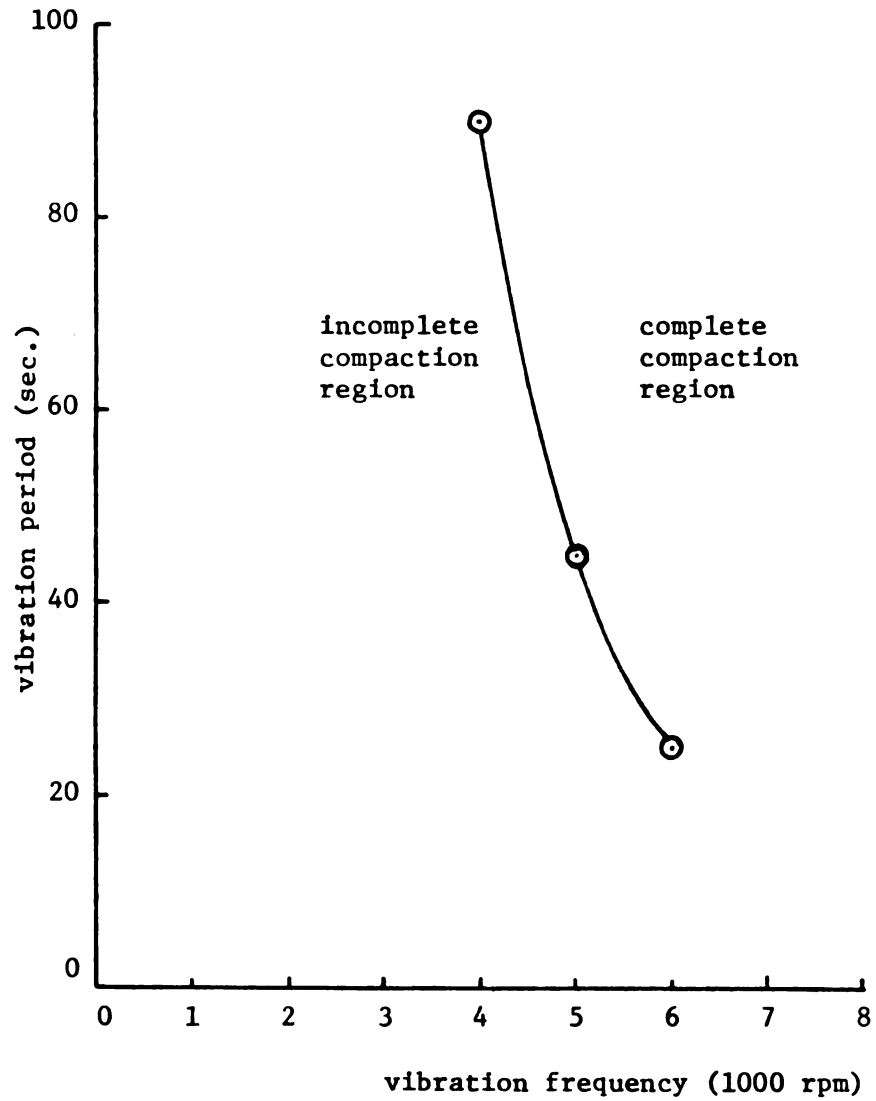


Figure 2.10. Vibration and compaction relationship for 1/2 in. slump concrete. (Troxell, et al., 1968)

the aggregate is the cement paste. Even at the bottom surface, the paste matrix enveloped each aggregate grain, leaving no external evidence that the specimen contained aggregates. Figure 2.5 shows the configuration of all the elements in fresh concrete after complete compaction.

Undercompaction reduces the strength of low slump fresh concrete. Even with the best equipped vibrating system, undercompaction may be introduced if the extrusion machine proceeds too rapidly.

2.2.5 Mix Design

Mix design is used to produce economical concrete of satisfactory workability while fresh, and of satisfactory quality after hardening. The method of expressing the proportion for mix design is to give amounts of cement, fine aggregates, coarse aggregates, and water either by weight or by volume for the batch. Likewise, the content of entrained air or an admixture is expressed separately.

With given materials, the following four variable factors are considered in specifying a concrete mix (Troxell et al., 1968):

- (1) Water-cement ratio -- expresses the dilution of paste.
- (2) Cement content or cement-aggregate ratio -- varies directly with amount of paste of given dilution.
- (3) Gradation of the aggregate -- in practical proportioning the aggregate gradation is controlled by varying the amounts of fine and coarse aggregate, usually as a percentage of sand (fine aggregate) in the total aggregate.
- (4) Consistency -- related to the practical requirement of placement and hence is not subject to manipulation in

proportioning as the other three variables; it is usually expressed in terms of slump or of ball penetration.

Although various mix design methods and theories have been documented in the literature, only two of them are considered of importance relative to low slump concrete; the "mortar-voids" method and the ACI method for no-slump concrete.

Mortar-Voids Method: This method was established by Talbot and Richart (1922). Three important concepts were introduced in this method:

- (1) The volume of voids is the sum of the volumes of water and entrapped air.
- (2) The strength of concrete is equal to the strength of the mortar in it.
- (3) Whenever water is mixed in increasing amounts with the dry mortar material, there is at first an increase in volume of the mortar because of capillary forces at contacts between particles of cement and sand, then there is a decrease in volume as the capillary forces disappear while the voids are filled with water. Additional water causes the volume of the mixture to increase by the amount of the added water. This phenomenon can best be represented in Figure 2.11.

In Figure 2.11, the water content at which the voids are just filled with water and the volume is a minimum, is called the basic water content, to which other relative water contents are referred.

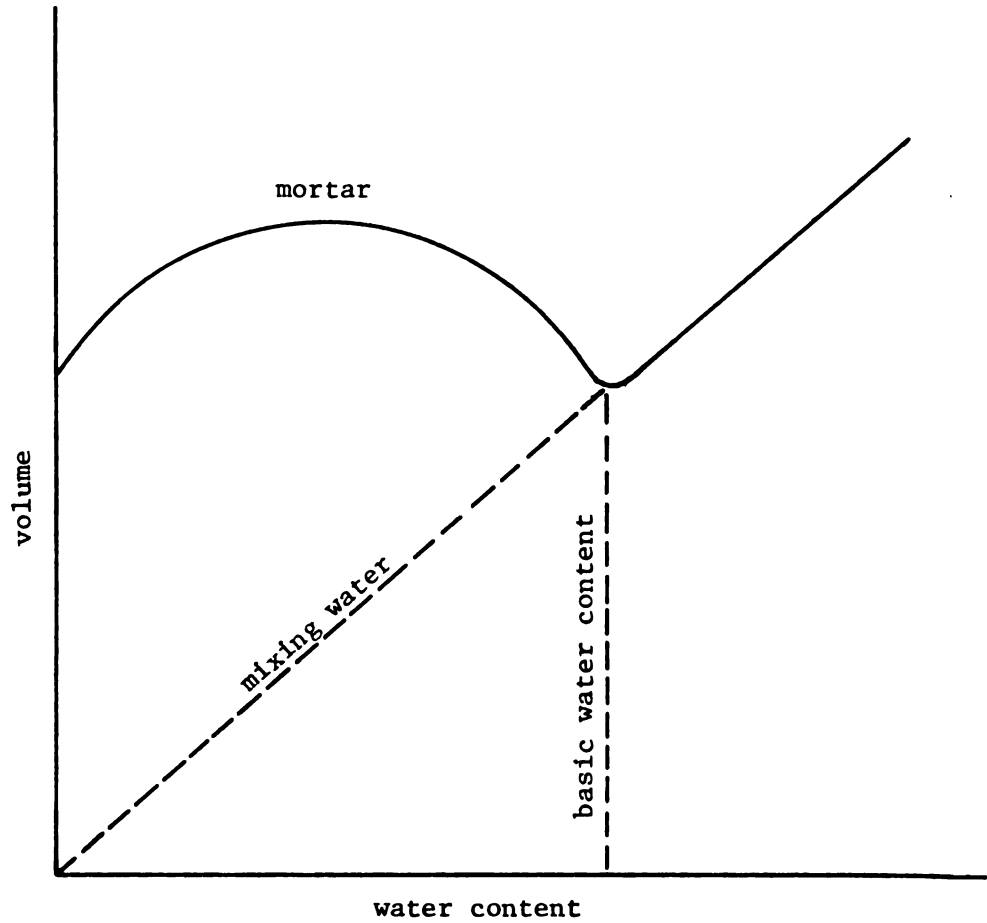


Figure 2.11. Typical curve showing the relationship between water content of mortar and the volume of the mortar. (after Bauer, 1949)

The amount of water required for workability is always greater than the basic water content.

This method includes a four-step procedure to accomplish the mix design. They are outlined as follows:

(1) Establish the relationship between the strength of the mortar and the void-cement ratio over a range for the particular materials and water content. These relationships are determined by laboratory testing.

(2) With the desired strength and the relative water content known from previous experience, the volume of voids, water, cement and sand per unit volume of mortar are computed according to the relationship established in Step (1).

(3) Through test and computation, determine the solid volume of the coarse aggregate.

(4) The solid volume of each component in a unit volume is computed, and the quantities of all materials are converted into terms of those used in batching at the job.

This method is rather complicated and has not been widely used, but its theory is considered basic and it can be applied consistently even to rather harsh mixes (Troxell et al., 1968). It has been put to use by the Illinois and Michigan Highway organizations.

ACI Method for No-Slump Concrete: Conventional ACI methods of mix design apply only to concrete having a slump of 1 inch or more. For slumps less than 1 inch the slump test becomes impractical. In 1965, ACI published a method to design no-slump concrete (ACI, 1965) which covers concrete mixtures with slump up to 1 inch.

In this method, tables for consistency requirements, relative water content, water-cement ratio and compressive strength are provided for the mix design. As long as the slump test is not practical, three other types of equipment to measure consistency have been introduced, the Vebe apparatus, the compacting-factor apparatus, and the Thaulow drop table. Details for these methods are given in the Proceedings of the Journal of the American Concrete Institute (Vol. 62, No. 1, January 1965).

2.3 Failure Criterion for Fresh Concrete

One of the most important problems in engineering mechanics is the formulation of a limiting criterion that will indicate the development of discontinuities within the material body being analyzed. In this capacity, the criterion is said to reflect the failure of the material or the limits of its strength. The boundary loading capable of inducing failure is that able to overcome equilibrium. The philosophy of failure associated with the above description is said to be one of limiting equilibrium. For a plane strain case with dimensions of extensive length, equilibrium equations prior to the initial development of a discontinuity can be expressed as

$$\frac{\partial \sigma_x}{\partial x} + \frac{\partial \tau_{xz}}{\partial z} = 0 \quad (2.15a)$$

$$\frac{\partial \tau_{xz}}{\partial x} + \frac{\partial \sigma_z}{\partial z} - \gamma = 0 \quad (2.15b)$$

Equation (2.15) indicates that three unknown stresses exist with only two equations available to solve the problem. Equilibrium

conditions alone are not sufficient to provide a stress field within the material body. Another expression which can provide a measure of the circumstances governing the motion of a part of the material is required to fill this gap. This specific expression is a yield or failure criterion which is capable of furnishing a relationship valid for both simple laboratory tests and complex stress states in the field. For use in engineering problems, it is most practical to express the failure criterion as a relationship between the principal stresses when the material is in a state of limiting equilibrium.

Three most widely used failure (or yield) criteria are von Mises yield criterion, the Tresca criterion, and the Mohr-Coulomb failure criterion. The first two criteria serve adequately with experimental results on metals and the last one is well accepted in soil mechanics.

The Tresca criterion states that yielding will occur when the maximum shear stress reaches a critical constant value which is equal to one half the yield stress in a uniaxial test. Inasmuch as the maximum shear stress always equals one-half of the difference between maximum and the minimum principal stresses, the Tresca criterion then asserts that yielding will occur when any one of the following six conditions is reached.

$$\begin{aligned}\sigma_1 - \sigma_2 &= \pm \sigma_y \\ \sigma_2 - \sigma_3 &= \pm \sigma_y \\ \sigma_3 - \sigma_1 &= \pm \sigma_y\end{aligned}\tag{2.16}$$

where σ_1 , σ_2 , and σ_3 are principal stresses and σ_y is the yield stress in a uniaxial test.

The von Mises criterion specifies yield for

$$1/2[(\sigma_1 - \sigma_2)^2 + (\sigma_2 - \sigma_3)^2 + (\sigma_3 - \sigma_1)^2] = \sigma_y^2 \quad (2.17)$$

The von Mises criterion usually fits (but not always) the experimental data better than the Tresca (Mendelson, 1968). Also, unlike the Tresca criterion, the von Mises yield condition is seen to include dependence on the intermediate principal stress.

Mohr-Coulomb's failure criterion can best be represented by Figure 2.12. In this figure τ and σ_n are shear and normal stresses on a given plane, respectively, while σ_1 and σ_3 are the major and minor principal stresses, respectively. Both the angle of internal friction, ϕ , and the cohesion, c , can be evaluated in a series of triaxial tests. Failure occurs when the shear stress reaches the failure envelopes represented by the two straight lines inclined at an angle ϕ with the abscissa. The equation associated with failure in this figure can be expressed as

$$\sigma_1 - \sigma_3 = 2 c \cos \phi + (\sigma_1 + \sigma_3) \sin \phi \quad (2.18)$$

In the case of unconfined compression tests used to determine the undrained shear strength, τ , of fresh concrete, σ_3 goes to zero and a reasonable approximation is that ϕ becomes zero. Then Equation 2.18 reduces to

$$c = \tau = \frac{\sigma_u}{2} \quad (2.19)$$

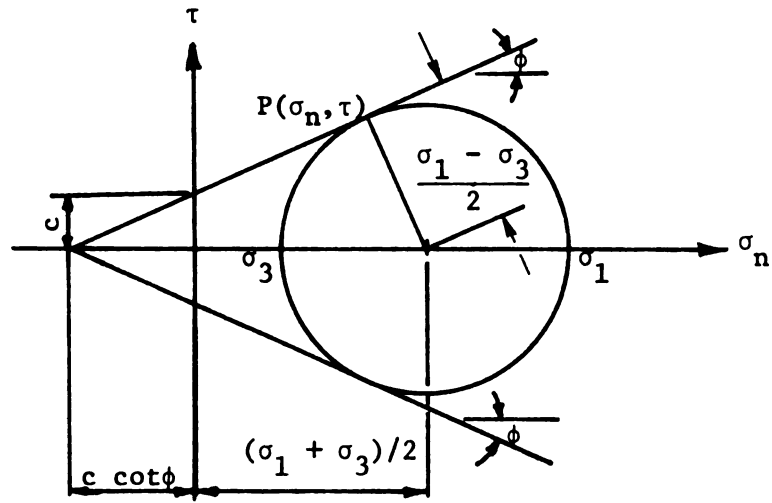


Figure 2.12. Mohr-Coulomb failure criterion.

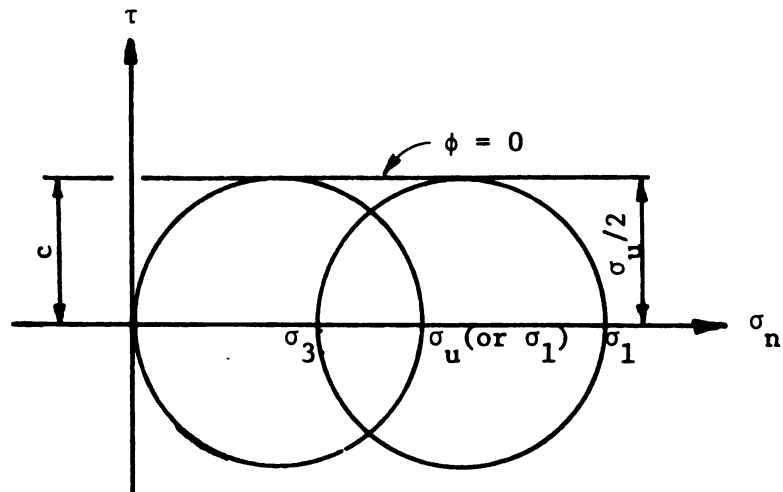


Figure 2.13. Unconfined compression loading case.

where σ_u equals the ultimate strength and is equivalent to σ_1 in the unconfined compression test. Equation (2.19) indicates that the undrained shear strength of the fresh concrete is one-half of the ultimate strength. The unconfined compression loading case is shown in Figure 2.13.

The Mohr-Coulomb failure criterion with ϕ equal to zero permits the maximum shear strength of the fresh concrete to be expressed as:

$$\tau_{\max} = \frac{\sigma_{\max} - \sigma_{\min}}{2} \quad (2.20)$$

where σ_{\max} and σ_{\min} are the maximum and minimum principal stresses. They can be evaluated within a cross-section by either a theoretical analysis or by a finite element computer program. Equation (2.20) may be rewritten in the form

$$\sigma_{\max} - \sigma_{\min} = \sigma_u = 2 \tau_{\max} \quad (2.21)$$

Comparing Equation (2.21) with Equation (2.16) it is noted that for the special case with $\phi = 0$, the Mohr-Coulomb criterion and the Tresca criterion coincide with the only difference being that the Tresca criterion uses yield stresses while the Mohr-Coulomb criterion uses ultimate strength as the limit.

Both Tresca and von Mises criterion have the disadvantage that they predict the same strength in tension and compression, which is impossible for fresh concrete. On the other hand, the Mohr-Coulomb failure criterion, with $\phi = 0$, gives a simple and clear concept which appears to be reasonably acceptable for describing the

strength of fresh concrete. It will be shown in a later chapter that this criterion appears to be acceptable when strength and stress comparisons are made using the finite element stress analysis and observed field failure examples.

Moreover, failure in horizontal slipform construction occurs shortly (less than a minute) after the structure emerges from the extrusion machine, hence little or no drainage can take place during this interval. This undrained condition satisfies the $\phi = 0$ concept commonly used in soil mechanics (Lambe and Whitman, 1969; Bishop and Henkel, 1962).

2.4 Analysis Techniques for Fresh Concrete Sections

In the previous section, failure was defined as the condition when the maximum shear stress reaches or exceeds the undrained shear strength of the material. It is understood that when the fresh concrete structure is under gravity loading conditions, some portions of the mass may reach failure condition before the rest of the structure does. When failure develops in those portions, they cannot carry any more load. The next increment of load, which the failed portions are unable to carry, will be redistributed among the unfailed portions. Very quickly, a progressive failure develops until the entire structure collapses. This phenomenon is common to many kinds of engineering problems.

The processes of crack initiation and growth differ among various materials (Majidzadeh et al., 1973). Generally speaking, the destructive action damages the structural integrity by several distress mechanisms developed within the mass and which propagate

either independently or by interaction to produce disintegration, distortion and/or failure. The mechanism of the crack growth can be explained in terms of the energy balance at the tip of the discontinuity. The work of the external force (or body force in the case of slipform construction) at the crack tip is divided into stored elastic energy, surface energy required to form cracks, and deformation energy required for irreversible changes in the material body as plastic or viscous flow occurs.

The study of fracture mechanics is complicated and is beyond the scope of this project. The analysis technique associated with a fresh concrete structure is confined to the development of failure zones where the maximum shear stress values exceed the undrained shear strength of the fresh concrete.

In the theory of elasticity, the condition of compatibility has been written in a form by incorporating the equations of equilibrium (Timoshenko and Goodier, 1970) as

$$\nabla^4 \phi = 0 \quad (2.22)$$

where ∇ is the del operator and ϕ is the stress function. Thus, the solution of a two-dimensional problem, when the weight of the body is the only body force, reduces to finding a solution of Equation (2.22).

However, sections of irregular shapes are difficult to solve by the ordinary theory of elasticity method due to the difficulty of assuming an appropriate stress function. In view of this fact, the finite element method is used for the analysis. The basic concept

of the finite element method (Zienkiewicz, 1971) is an idealization of an actual elastic continuum as an assemblage of discrete elements interconnected at their nodal points. For the analysis of two dimensional stress fields, triangular and rectangular plate elements are normally used. To maintain compatibility between the edges of adjacent elements, it is assumed that deformations (within each element) vary linearly in the x and z directions. With this assumption, stiffness of the complete structure is obtained by superposing the appropriate stiffness coefficients of the individual elements connected to each nodal point. Evaluation of nodal point displacements and element stresses may be expressed in the following matrix forms.

$$[R] = [K] [r] \quad (2.23)$$

$$[\sigma] = [S] [r] \quad (2.24)$$

where $[r]$ = vector of all nodal point displacements in the complete assemblage

$[R]$ = the vector of the corresponding nodal force

$[K]$ = the structure stiffness matrix

$[\sigma]$ = stresses in all of the elements

$[S]$ = stress transformation matrix which takes account of the assumed linear patterns in the elements, and their given material properties.

It is seen from Equations (2.23) that nodal point displacements are evaluated from given nodal forces, and from Equation (2.24) that stresses in all of the elements are obtained from nodal displacements.

Concerning the finite element plane-strain analysis procedure, in general, it may be noted that: (1) compatibility is satisfied everywhere in the system; (2) equilibrium is satisfied within each element; and (3) equilibrium of stresses is not satisfied along the element boundaries, in general, but the nodal forces are in equilibrium.

The finite element program used in the Analysis, "FEASTS", was originally developed by Wilson and modified by Christian and Goughnour (1966). This computer program can be used to determine the deformations and stresses within certain types of stress bodies. The program will analyze problem situations in any of the following categories: axially symmetric, plane stress and plane strain. Elastic, non-linear material properties are considered by a successive approximation technique.

Plane-strain conditions were assumed in calculation of the stress fields developed by the gravitational body force of the slip-form constructed concrete structure. The stress-strain relationship or modulus of elasticity was assumed to be homogeneous throughout the body. For the problems, the material must have a linear stress-strain relationship, while a bi-linear relationship is applied to the elastoplastic problems.

This program is by no means the best program to analyze a fresh concrete structure. However, before more knowledge pertaining to the characteristic of the fresh concrete can be achieved, this program was considered adequate for interpretation of the stress-deformation behavior of a fresh concrete structure. An advantage of

this program is that if the non-linear effects are small, such as for low-slump fresh concrete, the procedure is guaranteed to converge.

CHAPTER III
MATERIALS AND MIX DESIGN

The materials used in this research follows closely those specified in the Michigan Department of State Highways and Transportation (MDSHT) 1976 "Standard Specifications for Highway Construction." Details on the materials are given in Section 3.1. For low-slump concrete, the mix design is different from that of ordinary concrete. With the materials used in this research project, the mortar-void method of mix design is described in detail.

3.1 Concrete Materials

The concrete used in this research is specified as Grade 35S in the Michigan Highway Department's specification. This grade is used for median barrier construction. A general description of this mixture is given in Table 3.1.

Table 3.1. General description of Grade 35S concrete mixture

| cement content | | coarse aggregate | fine aggregate | maximum slump (in.) | modulus of rupture, design, min. (psi) | | | compressive strength, 28 days, min. (psi) |
|------------------|---------------------|------------------|----------------|---------------------|--|------------|------------|---|
| pounds per cu yd | sacks (94 lb) cu yd | | | | at 7 days | at 14 days | at 28 days | |
| | | | | | | | | |

The detailed description of the cement, coarse aggregate, fine aggregates, and air-entraining agent is given in the following sections.

3.1.1 Cement

General Portland Cement Type I, used in this project, conformed to ASTM Standards, Designation C 150. This cement was manufactured by General Portland Inc.'s Paulding, Ohio plant. Although air-entrained Type IA portland cement is normally used for barrier construction, there is a trend to the use of non-air-entrained cement on current projects as understood from many contractors. The required air content may be obtained by adding air-entraining agents at the batching plant. Most of the samples prepared for this project did not contain air-entraining agents because air content was not an easily controlled property. For those samples which required a variation in air content, Darex was added during sample preparation.

3.1.2 Coarse Aggregates

Coarse aggregates were obtained from two sources, which included round gravel from the Standard Ready-Mix Inc.'s Lansing pit and crushed gravel from Michigan Aggregate Co.'s Bundy Hill pit. These are Michigan Series 6 Class A aggregates. Their physical requirements, given in the Highway Department's Standard Specification, are listed in Table 3.2.

Gradation requirements are shown in Table 3.3. Crushed gravel used in some of the samples was defined as those particles which have at least one fractured face. The percentage of crushed material was determined by dividing the weight of the fractured

particles by the weight of that portion of the coarse aggregates from which they were selected.

Dilute hydrochloric acid was used on the individual aggregate particles and microscopic inspection was also conducted on aggregate samples used on this project. It was observed that both limestone and metamorphic rocks of sandstone origin were present in the batch of aggregates. Therefore it was concluded, based on particle size and composition, that the coarse aggregate can be classified as "sand and gravel." Troxell et al. (1968) defined "sand and gravel" as a mixture of several kinds of rock materials, hence the overall specific gravity will depend upon the relative proportions of each type.

3.1.3 Fine Aggregates

Fine aggregates used on this project include Michigan designation 2NS natural sand. These natural sands, obtained from Michigan Aggregate Co.'s Bundy Hill pit, are the fine granular material resulting from the natural disintegration of rock. It consists of clean, hard, durable, uncoated particles of sand, free from clay lumps, and soft or flaky material. According to the Michigan Highway Department's specification, these sands shall be free from organic impurities to the extent that when subjected to the organic impurities test, the sand shall not produce a color darker than Plate 3 (light brown). When subjected to the Mortar Tensile Strength test, mortar specimens containing the fine aggregate shall develop a tensile strength of at least 100 percent of the strength developed in the same time by a mortar prepared in the same manner with the same cement and Ottawa sand. When the fine aggregate is subjected to the soundness test,

the weighted percentage loss shall not be more than 16 percent. The gradation requirement is shown in Table 3.4.

3.2 Mix Design-Mortar Void Method

With the materials specified in Section 3.1, it was necessary to follow a proper mix design procedure to produce the low slump concrete. Two methods are available for mix design of low slump concrete -- the ACI no-slump method and the mortar void method. The ACI no-slump method was not used on this project for the reason that it required special equipment to measure consistency and the water requirement must be experimentally adjusted. Available equipment permitted use of the mortar void method.

The mortar void method also required some experimentally determined factors in its application. Since this method has been adopted by MDSHT, all the information pertaining to experience or experiment was well documented. Therefore, the mortar-void method was selected for proportioning low-slump concrete on this project.

For convenience the design procedure uses the nomenclature adopted by Talbot and Richart (1922) which has been widely followed.

It is summarized below:

a = solid volume of fine aggregate per unit volume of freshly made concrete.

a_m = solid volume of fine aggregate per unit volume of freshly made mortar.

b = solid volume of coarse aggregate per unit volume of freshly made concrete.

b_0 = solid volume of coarse aggregate per unit volume of loose coarse aggregate.

c = solid volume of cement per unit volume of freshly made concrete.

Table 3.2. Physical requirements for 6A coarse aggregates.

| | |
|---|---------------------|
| wear - Los Angeles abrasion | 40 percent maximum |
| soundness | 12 percent maximum |
| soft particles | 2.5 percent maximum |
| sum of soft particles, chert and hard absorbent particles | 9 percent maximum |
| thin or elongated particles | 15 percent maximum |

Table 3.3. Grading requirements for 6A coarse aggregates.

| sieve analysis (ASTM C-136) - total percent passing | | | |
|---|---------|-------|-----------------|
| 1 1/2-in. | 1/2-in. | No. 4 | loss-by-washing |
| 100 | 30-60 | 0-8 | 1.0 maximum |

Table 3.4. Grading requirements for 2NS fine aggregates

| sieve analysis (ASTM C-136) - total percent passing | | | | | | | |
|---|--------|-------|--------|--------|--------|---------|-----------------|
| 3/8-in. | No. 4 | No. 8 | No. 16 | No. 30 | No. 50 | No. 100 | loss-by-washing |
| 100 | 95-100 | 65-95 | 35-75 | 20-55 | 10-30 | 0-10 | 0-3 |

c_m = solid volume of cement per unit volume of freshly made mortar.

v = void volume per unit volume of freshly made concrete.
The volume of voids equals the volume of mixing water plus a small volume of air voids.

v_m = volume of the voids per unit volume of mortar.

w = volume of water per unit volume of freshly made concrete.

w_m = volume of the water per unit volume of mortar.

From the above definitions it follows that:

$$a + b + c + v = 1 \quad (3.1)$$

3.2.1 Basic Information

Certain basic information must be known before the mortar-void mix design method can be applied. This information comes either from laboratory test results or from field construction experience and includes the percent water absorption by the aggregates, dry loose unit weight of the coarse aggregates, the specific gravities of the ingredients, and the cement content. These items are described below:

Cement Content. Concrete may be thought of as a combination of a cement paste and aggregate. Cement paste and fine aggregates form the mortar in the concrete. It is observed that when properly cured concrete is ruptured, the break is through or across the particles of coarse aggregate and not around them indicating that the coarse aggregate is weaker than the surrounding mortar. Therefore, the strength of the hardened concrete is governed by the strength of the mortar filling the spaces between the particles of coarse aggregate provided that all other factors relating to the concrete mixture remain constant and that the volume of coarse aggregate is not

extremely high. Talbot and Richart define the expression, $\frac{c}{v + c}$, as the cement-space ratio which represents the volume of the cement in a unit volume of freshly made cement paste. Their research results indicated that there is a relationship between compressive strength and cement-space ratio, the larger values of cement-space ratio giving the greater hardened concrete strengths (Bauer, 1949). The Talbot-Richart tests also indicated that there was an appreciable difference in strength for the same cement-space ratio when the consistency of the concrete varied. A summary of their test results is shown in Figure 3.1. In this figure R.W.C. represents relative water content which is explained in the next subsection. It is apparent that Figure 3.1 gives strengths which are much too low for today's high quality Type I cement.

The MDSHT has conducted an investigation of the relationship between cement content and compressive strength of the hardened concrete. According to the MDSHT specification, a minimum compressive strength of 3,000 psi is required for slipform construction of concrete median barriers. This strength calls for a cement content of 6 sacks per cubic yard of concrete (Shehan, 1970). This figure will be used in the mix design for this project.

Relative Water Content. In Section 2.2.2 relative water content (R.W.C.) was defined as a multiple of the basic water content to provide the workability of the concrete in its fresh state. The R.W.C. was determined by actual field experience (Shehan, 1970). For the low-slump concrete used for slipform construction of median barriers, MDSHT recommends a R.W.C. = 1.05. MDSHT engineers

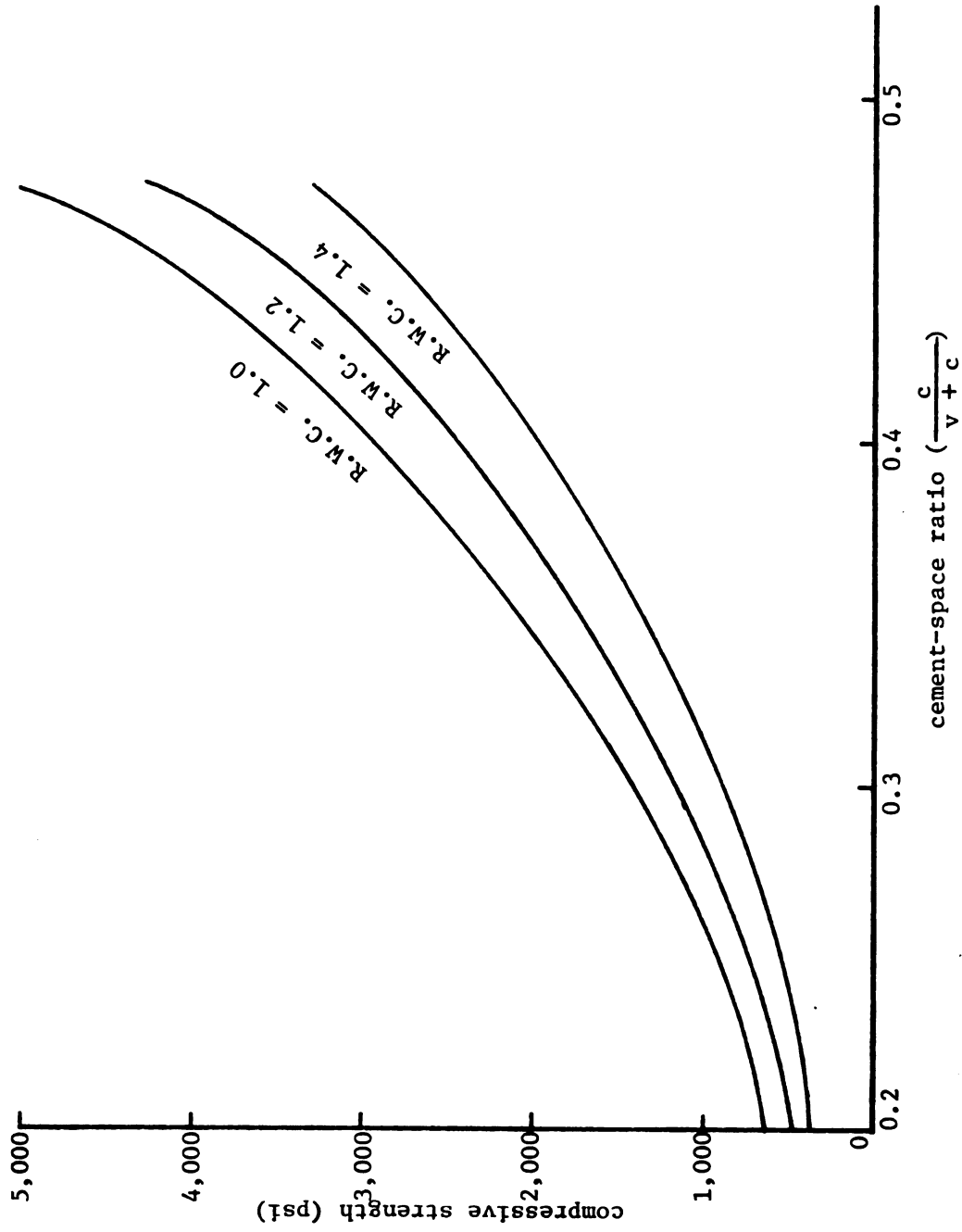


Figure 3.1. Relationship between compressive strength and cement space ratio. (from Bauer, 1949)

indicated that a R.W.C. of 1.0 could possibly be used for slipform construction of high walls.

Characteristic Mortar Voids Curves. Three typical basic water content curves derived for the materials used on this project are shown in Figure 3.2. The basic water contents for each sand-cement ratio (a_m/c_m) were noted and are given in Table 3.5. After selection of the R.W.C. = 1.05, it was recorded in the same table and each basic water content was multiplied by the R.W.C. factor. These results are also recorded in Table 3.5. The corresponding values of v_m for each of the calculated w_m was determined by the use of Figure 3.2 and is also recorded in Table 3.5. These values of v_m and w_m for the R.W.C. = 1.05 are plotted as a function of a_m/c_m in Figure 3.3. These two curves will be referred to as the characteristic mortar voids curves for that particular R.W.C., in this case 1.05.

Table 3.5. v_m and w_m data.

| a_m/c_m | w_m at R.W.C. = 1.0 | w_m at R.W.C. = 1.05 | v_m at R.W.C. = 1.05 |
|-----------|-----------------------|------------------------|------------------------|
| 2 | 0.265 | 0.278 | 0.288 |
| 3 | 0.247 | 0.259 | 0.269 |
| 4 | 0.229 | 0.240 | 0.258 |

The Workability Factor b/b_0 . This factor was employed to determine the amount of coarse aggregate to be used in the concrete mix in order that there would be a definite excess of mortar over

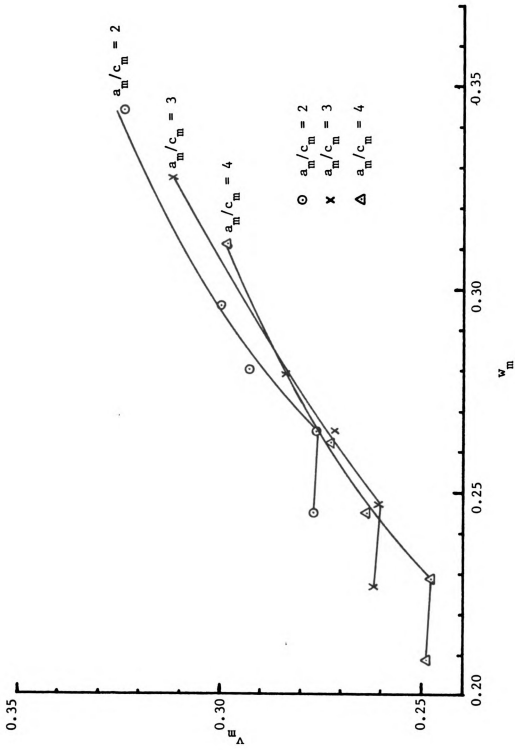


Figure 3.2. Basic water content curves for various sand-cement ratios (a_m/c_m).

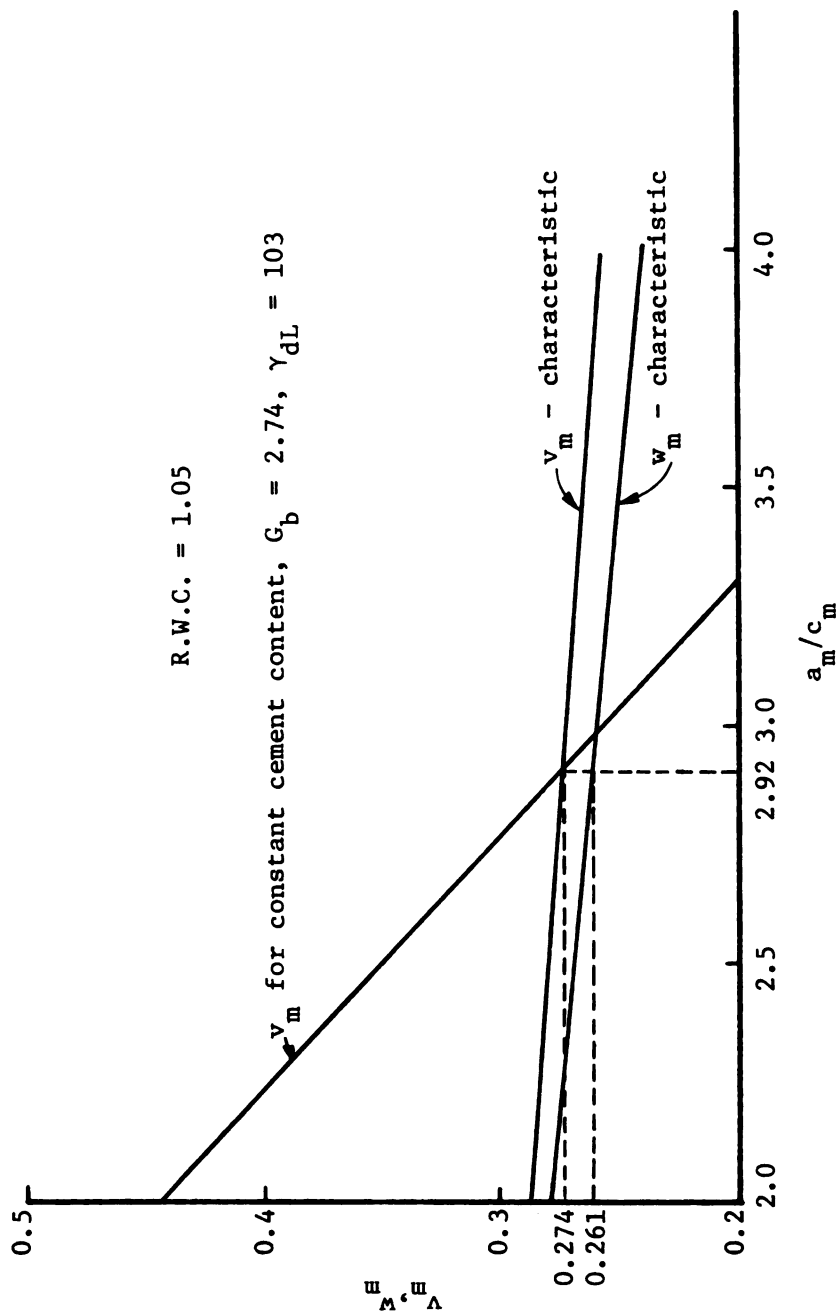


Figure 3.3. Characteristic mortar voids curves.

that required to fill the spaces or voids between the particles of coarse aggregate. If the volume of the mortar used in making a given volume of concrete were exactly equal to the volume of the voids in the coarse aggregate, then the b/b_0 ratio would be exactly equal to 1.0. Since it is not possible to do this (see Chapter VII discussion), it is desirable to find out how close to 1.0 the mix design may come and still insure satisfactory finishing qualities.

Talbot and Richart (1922) suggested values of b/b_0 of from 0.65 to 0.75. Maximum values of b will equal about 0.4 and 0.45 for crushed stone and gravels, respectively. MDSHT recommends a b/b_0 value of 0.7 to be used for slipform construction of median barriers.

3.2.2 Design Procedure

With the above basic information available, the design procedure will be outlined step by step in every detail. The reasons for following this procedure include:

- 1) To illustrate a suitable mix design method for low slump concrete.
- 2) To employ the results of the mix design as a guide for establishing the range of proportions used in the unconfined compression test.

First, the design procedure requires values for the physical properties of the cement and aggregates and basic information relative to the mortar-voids relationships, relative water content, and workability factor. These items are listed below:

$$G_a = \text{specific gravity of fine aggregate (oven dry)} = 2.68$$

G_b = specific gravity of coarse aggregate (oven dry) = 2.74

G_c = specific gravity of cement = 3.12

Absorption of fine aggregate = 1.28 percent

Absorption of coarse aggregate = 1.32 percent

γ_{dl} = dry loose unit weight of coarse aggregate = 103 pcf

Cement content = 6 sacks per cu yd of concrete

b/b_0 = workability factor = 0.7

R.W.C. = relative water content = 1.05

Step 1

Compute the solid volume of coarse aggregate per unit volume of dry loose coarse aggregate, b_0 :

$$b_0 = \frac{\gamma_{dl}}{G_b \gamma_w} \quad \text{where } \gamma_w \text{ is the unit weight of water, and}$$

$$b_0 = \frac{103}{2.74 \times 62.4} = 0.6024 \text{ cu ft.}$$

Compute the solid volume of coarse aggregate per unit volume of concrete, b :

$$b = 0.7 b_0 = (0.7) (0.6024) = 0.4217 \text{ cu ft/cu ft of concrete.}$$

Compute the volume of mortar per unit volume of concrete. According to Equation (3.1), this quantity is determined by subtracting the value of b from 1.0:

$$1 - b = 1 - 0.4217 = 0.5783 \text{ cu ft/cu ft of concrete .}$$

Step 2

Compute the solid volume of cement per unit volume of concrete, c , using 1 cu yd = 27 cu ft and 1 sack of cement = 94 lb, hence

$$c = \frac{\frac{(6)(94)}{27}}{27} = \frac{(6)(94)}{(27)(3.12)(62.4)} = 0.10729 \text{ cu ft/cu ft of concrete.}$$

The actual quantity of cement in the concrete is the same as that present in the mortar. However, the quantity of cement per unit volume of concrete differs from the cement per unit volume of mortar. Since the volume of mortar per unit volume of concrete equals $(1 - b)$ and the solid volume of cement per unit volume of concrete is known, the solid volume of cement per unit of mortar, c_m , is given by the expression

$$c_m = \frac{c}{1 - b} = \frac{0.10729}{0.5783} = 0.18553 \text{ cu ft/cu ft of mortar.}$$

Step 3

Since mortar contains the three constituents, a_m , c_m , and v_m , step 2 leaves only v_m and a_m to be determined. By definition the whole is equal to the sum of its parts. Therefore, one unit volume of mortar equals

$$a_m + c_m + v_m = 1 \quad (3.2)$$

By transfer of terms and multiplying a_m by $\frac{c_m}{c_m}$, v_m is solved as:

$$v_m = (1 - c_m) - c_m \cdot \frac{a_m}{c_m} \quad (3.3)$$

This equation shows that v_m and a_m/c_m are dependent and independent variables in a linear relationship. Therefore, if two sand-cement ratios, a_m/c_m , are substituted in the equation, then two values of v_m can be calculated to define the line which will include

all of the v_m values which satisfy the equation. Therefore,

$$\text{for } a_m/c_m = 2, v_m = (1 - 0.18553) - (0.18553)(2) = 0.443$$

$$\text{for } a_m/c_m = 3, v_m = (1 - 0.18553) - (0.18553)(3) = 0.258$$

These values, when plotted on Figure 3.3, determine the straight line. The coordinates of the point of intersection of this line and the characteristic v_m line, plotted previously, give the values of v_m and a_m/c_m for the cement and fine aggregate to be used for the concrete mix proportion requirements.

Step 4

From the curve intersection (Figure 3.3) read v_m equal to 0.274 and a_m/c_m equal to 2.92. By reading vertically below the point of intersection on the characteristic w_m line obtain the value of w_m equal to 0.261 corresponding to the value of a_m/c_m equal to 2.92.

The value of the sand-cement ratio in the mortar is the same as the sand-cement ratio in the concrete, thus:

$$a_m/c_m = a/c \quad (3.4)$$

The values of a , v , and w can now be estimated as:

$$a = \frac{a_m}{c_m} \cdot c = (2.92)(0.10729) = 0.313 \text{ cu ft/ unit volume of concrete,}$$

$$v = v_m (1 - b) = (0.274)(0.5783) = 0.158 \text{ cu ft/unit volume of concrete,}$$

$$w = w_m (1 - b) = (0.261)(0.5783) = 0.151 \text{ cu ft/unit volume of concrete.}$$

Step 5

Present day mix design always requires entrained air. The MDSHT specifies an air content of 6.5 percent with a tolerance of plus or minus 1.5 percent for all exposed concrete. In order to compensate for the increased volume of concrete caused by the entrained air, an appropriate adjustment is made in the volume of voids, v . This means that the volume of air voids per unit volume of concrete will be 0.065 cu ft. At the same time the solid volume of fine aggregate, a , must be decreased by a volume equal to the increase in the volume of voids, v . Therefore,

$$w + \text{air} = 0.151 + 0.065 = 0.216 = \text{adjusted } v,$$

$$0.216 - v = 0.216 - 0.158 = 0.058 = \text{volume to be deducted from } a,$$

and

$$a - 0.058 = 0.313 - 0.058 = 0.255 = \text{adjusted } a.$$

The total volume of ingredients per unit volume of concrete, Equation (3.1), should be checked with reasonable accuracy.

$$\begin{array}{r} a = 0.255 \\ b = 0.4217 \\ c = 0.1073 \\ v = \underline{0.216} \\ \hline 1.0000 \end{array}$$

Step 6

The solid volumes of all the ingredients per unit volume of concrete are now converted to weights by multiplying the solid volume per unit volume of concrete by the unit weight of the ingredient and then divided by the number of sacks of cement per unit volume of concrete. This gives the weight of each ingredient per sack of cement

as follows:

$$W_a = \frac{27a G_a \gamma_w}{6} = \frac{(27) (0.255) (2.68) (62.4)}{6} = 192 \text{ lb}$$

$$W_b = \frac{27b G_b \gamma_w}{6} = \frac{(27) (0.4217) (2.74) (62.4)}{6} = 324 \text{ lb}$$

$$W_c = \frac{27c G_c \gamma_w}{6} = \frac{(27)(0.1073) (3.12) (62.4)}{6} = 94 \text{ lb}$$

$$W_w = \frac{27 w \gamma_w}{6} = \frac{(27) (0.151) (62.4)}{6} = 42.4 \text{ lb}$$

Step 7

The free water on aggregates in excess of their absorption must be considered as part of the mixing water. The fine aggregate used in the laboratory was oven-dried and coarse aggregates were air dried (moisture content approximately 0.15 percent). However, a survey of Michigan highway median barrier construction jobs indicates that field water contents average about 4.6 and 1.5 percent for fine aggregates and coarse aggregates, respectively. Using the absorption for fine aggregate as 1.28 percent, the amount of free water remaining equals (4.6 - 1.28) or 3.32 percent. Therefore, the mixing water contributed by the sand equals $(192 \text{ lb} \times \frac{3.32}{100})$ or 6.37 lb. Using the absorption of coarse aggregate as 1.32 percent, the free water remaining equals (1.5 - 1.32 percent) or 0.18 percent and the amount of mixing water in the coarse aggregate equals $(324 \text{ lb} \times \frac{0.18}{100})$ or 0.58 lb. The quantity of mixing water to be added now equals $[42.4 - (6.37 + 0.58)]$ or 35.5 lb.

At this stage, final adjustments in the mix have been completed and the weights for each ingredient per sack of cement are

$$W_a = 192 \text{ lb} ,$$

$$W_b = 324 \text{ lb} ,$$

$$W_c = 94 \text{ lb} ,$$

$$W_w = 35.5 \text{ lb} .$$

The mix design characteristics are given by the following proportions:

$$W_w/W_c = 0.378, \quad W_a/W_c = 2.04, \quad W_a/W_b = 0.59 ,$$

$$M = \frac{W_a + W_c + W_w}{W_a + W_b + W_c + W_w} = 0.5$$

With minor adjustments for computational convenience, this mix design was assigned as the "standard mix design" used for Sample No. 5 in Chapter V.

CHAPTER IV
LABORATORY PROCEDURES

Physical and mechanical properties of fresh concrete are normally determined in the laboratory. Aggregate gradation influences the mechanical properties of the fresh concrete, hence it becomes necessary to specify gradation limits. Methods and equipment for measurement of these engineering characteristics are described below. Reference is made to standard test procedures where possible.

Laboratory tests consist of three major groups; sieving and proportioning of the aggregates to certain gradations, evaluation of the physical properties of the cement, aggregates, mortar, the fresh concrete, and the unconfined compression test on the fresh concrete.

4.1 Gradation of the Aggregates

For quality control purposes, the gradation of the fine aggregates and that of the coarse aggregates must be closely controlled for all the tests. Using selected weights for each aggregate, the gradation for the fine and coarse aggregates were combined into one combined gradation.

It is well recognized that an ideal grading curve (Popovics, 1962b) can be closely approximated by a parabola expressed as

$$P_t = \left(\frac{d}{D}\right)^q \quad (4.1)$$

where P_t is the fraction of the total particles finer than size d , and D is the maximum particle size. The grading ratio, q , is experimentally determined.

Generally speaking, an ideal gradation gives the minimum mineral voids, or maximum aggregate density. It is based on this criterion that the grading ratio is normally determined. Andreasen and Anderson (1929) found the value of q equal to 0.5 for their aggregates. Nijboer (1948) made a series of tests on compacted bituminous concrete mixtures and found that the maximum aggregate density occurred for a gradation having a q value of 0.45. Both Andreasen and Nijboer stated that grading ratio is independent of the maximum size D .

Since a q value of 0.45 was recommended by the Bureau of Public Roads (1962) and has been adopted by many highway departments, a grading chart with the abscissa scale raised to the 0.45 power was used on this project. Figure 4.1 shows one of these grading charts prepared by the MDSHT. In this figure, curves A, C, E, and G are the upper and lower limits of the coarse and fine aggregates, respectively, as defined by the MDSHT Specification (1976) for median barrier concrete mix design. Curve B for the coarse aggregates and curve F for the fine aggregates were selected for all the tests in this research. These curves, selected for convenience, are the most representative gradations for the materials used in this report. For different W_a/W_b ratios, curve B and curve F were then combined into different gradation curves as shown in Figure 4.2. These gradation curves were used to illustrate the influence of aggregate gradation on the mechanical properties to be discussed in Section 6.3.2.



SOIL GRAIN SIZE DISTRIBUTION

| | | | | | | | | | | |
|---|------|------|-------|------|------|-------|-------|-------|-------|--------|
| AMERICAN ASSOCIATION OF STATE HIGHWAY AND TRANSPORTATION OFFICIALS CLASSIFICATION | | | | | | | | | | |
| Clay | 0.75 | 0.60 | 0.425 | 0.25 | 0.15 | 0.075 | 0.075 | 0.075 | 0.075 | Gravel |
| UNITED STATES DEPARTMENT OF AGRICULTURE CLASSIFICATION | | | | | | | | | | |
| Clay | 0.75 | 0.60 | 0.425 | 0.25 | 0.15 | 0.075 | 0.075 | 0.075 | 0.075 | Gravel |
| UNITED STATES FEDERAL HIGHWAY ADMINISTRATION CLASSIFICATION | | | | | | | | | | |
| Clay | 0.75 | 0.60 | 0.425 | 0.25 | 0.15 | 0.075 | 0.075 | 0.075 | 0.075 | Gravel |

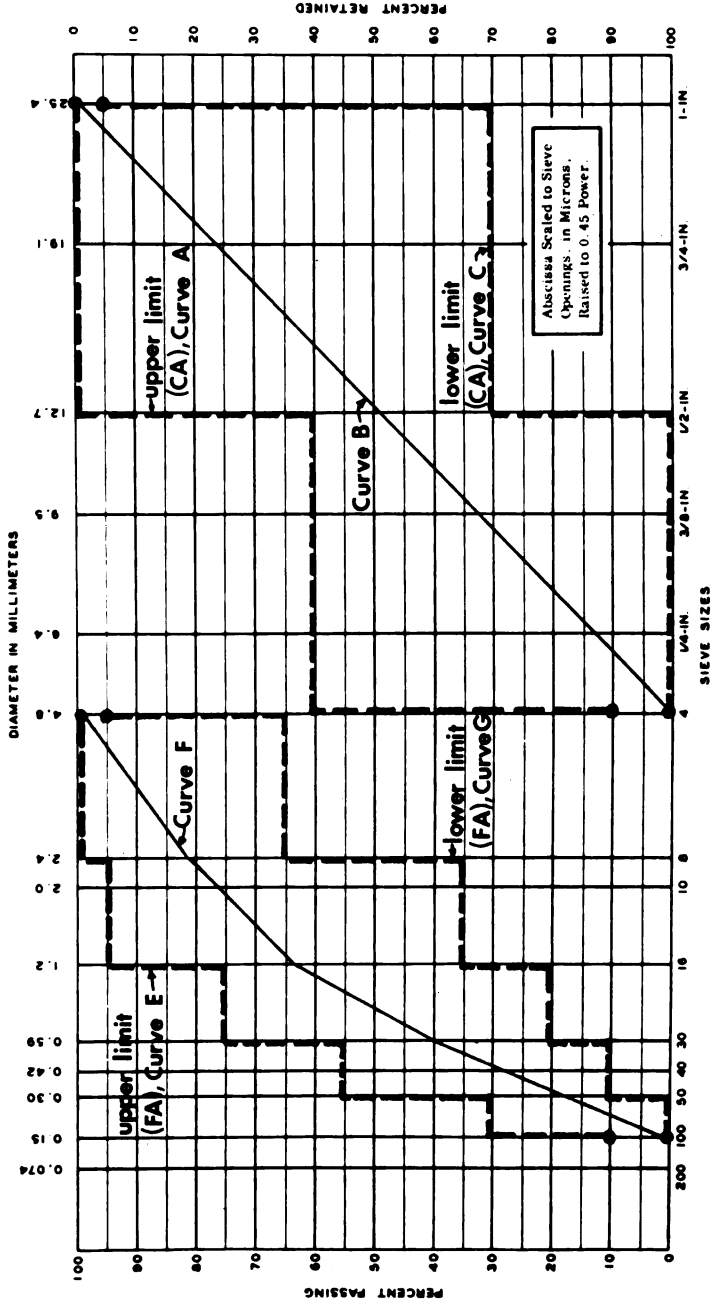


Figure 4.1. Limits for aggregate gradations.



SOIL GRAIN SIZE DISTRIBUTION

| | | | | | |
|---|------|------------------|-------------|--------|--|
| AMERICAN ASSOCIATION OF STATE HIGHWAY AND TRANSPORTATION OFFICIALS CLASSIFICATION | | | | | |
| Clay | Fill | Fine Sand | Coarse Sand | Gravel | |
| UNITED STATES DEPARTMENT OF AGRICULTURE CLASSIFICATION | | | | | |
| Clay | Fill | Fine Sand | Coarse Sand | Gravel | |
| UNITED STATES FEDERAL HIGHWAY ADMINISTRATION CLASSIFICATION | | | | | |
| Clay | Fill | Fine Sand | Coarse Sand | Gravel | |
| | | Very Coarse Sand | | | |

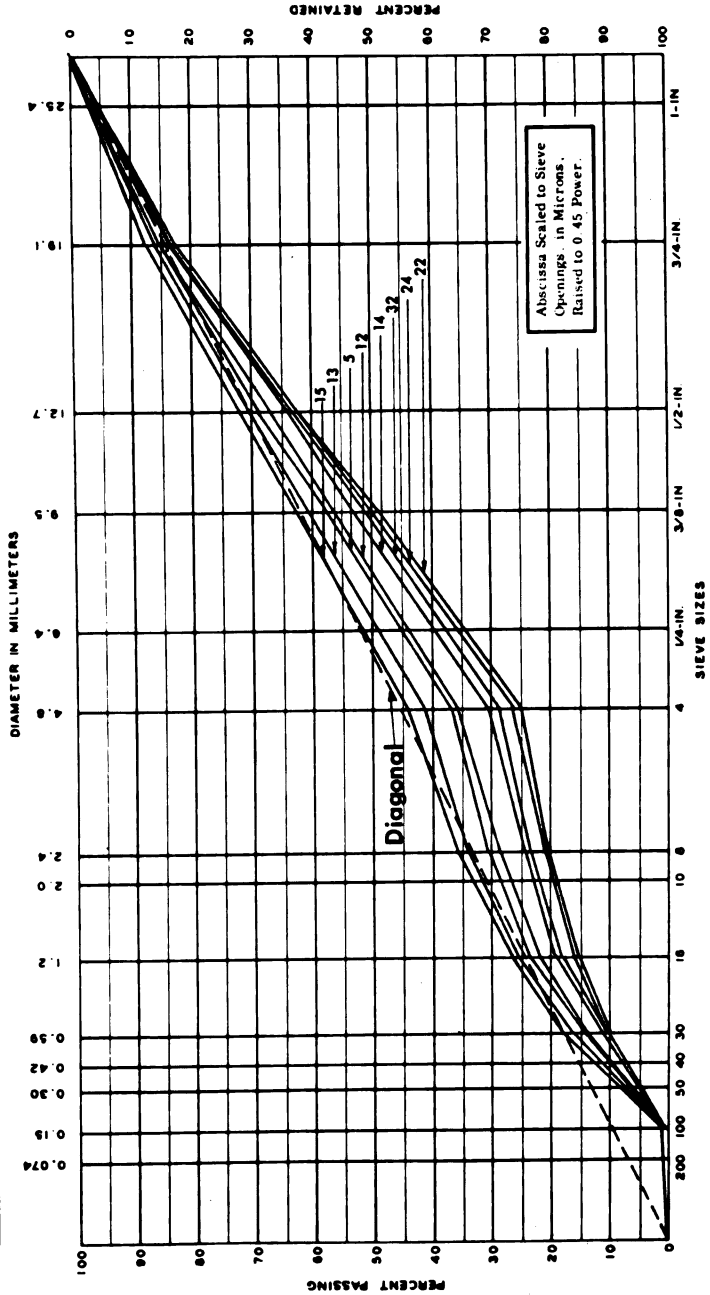


Figure 4.2. Gradation curves for test samples

The fineness modulus is the cumulative percent retained for specified sieve sizes divided by 100. Since one fineness modulus can describe numerous gradations, its value is somewhat limited as an evaluation factor. However, a sieve analysis corresponding to Figures 4.1 and 4.2 are included in Tables 3.3, 3.4, and 4.1.

Crushed stone was also used in some of the tests and the percentage of crushed aggregates in each size group is shown in Table 4.2.

The 1/2-in. or larger crushed aggregate particles were hand-picked while the other sizes are the representative percentage in the group.

4.2 Physical Properties

Physical properties of the cement, aggregates, mortar, and fresh concrete are included under the following items:

(1) Bulk specific gravity, bulk specific gravity (saturated surface dry), apparent specific gravity and percent absorption for fine aggregates -- ASTM C 128-73.

(2) Bulk specific gravity, bulk specific gravity (saturated surface dry), apparent specific gravity and percent absorption for coarse aggregates -- ASTM C 127-73.

(3) Specific gravity of cement -- ASTM C 188-72.

(4) Unit weight of the fresh concrete.

(5) Unit weight (both compacted and dry loose) of the coarse aggregates -- ASTM C 29-71.

(6) Voids content of the coarse aggregates -- ASTM C 30-37.

Table 4.1. Gradation of aggregates.

| standard seive size | percent retained | | | | | |
|---------------------------|------------------|--------------|--------------|--------------|--------------|--------------|
| | Curve B | Curve F | Sample 5 | Sample 12 | Sample 13 | Sample 14 |
| 3/4-in. | 23 | | 14.5 | 14.8 | 13.3 | 16.1 |
| 1/2-in. | 51 | | 32.1 | 32.9 | 29.5 | 35.6 |
| 3/8-in. | 68 | | 42.8 | 43.9 | 39.3 | 47.5 |
| No. 4 | 100 | | 63.0 | 64.5 | 57.9 | 69.9 |
| No. 8 | | 18 | 69.6 | 70.9 | 65.4 | 75.3 |
| No. 16 | | 36 | 76.3 | 77.3 | 74.7 | 80.7 |
| No. 30 | | 60 | 85.2 | 85.8 | 83.1 | 88.0 |
| No. 100 | | 99 | 99.6 | 99.6 | 99.5 | 99.7 |
| percent retained | | | | | | |
| standard seive size | percent retained | | | | | |
| | Sample 15 | Sample 22 | Sample 24 | Sample 31 | Sample 32 | Sample 33 |
| 3/4-in. | 12.7 | 17.0 | 17.0 | 18.6 | 16.6 | 18.0 |
| 1/2-in. | 28.2 | 38.0 | 37.5 | 41.3 | 36.7 | 39.0 |
| 3/8-in. | 37.7 | 51.0 | 50.0 | 55.0 | 49.0 | 52.0 |
| No. 4 | 55.4 | 75.0 | 73.7 | 81.0 | 72.0 | 76.4 |
| No. 8 | 63.4 | 79.0 | 78.4 | 84.0 | 77.0 | 81.0 |
| No. 16 | 71.4 | 84.0 | 83.0 | 88.0 | 82.0 | 85.0 |
| No. 30 | 82.1 | 90.0 | 89.5 | 82.4 | 89.0 | 90.5 |
| No. 100 | 99.6 | 99.8 | 99.7 | 99.8 | 99.7 | 99.8 |

Table 4.2. Percentage for each size group of crushed aggregates.

| Size Group | Percentage (by weight) |
|-------------------|---------------------------|
| 1-in. - 3/4-in. | 100 |
| 3/4-in. - 1/2-in. | 100 |
| 1/2-in. - 3/8-in. | 31 |
| 3/8-in. - No. 4 | 21 |

(7) Mortar content per cubic yard of concrete.

(8) Basic water content.

Procedures for testing are either self-evident by the definition given in Section 2.2.2 or are described in the ASTM Standards under the number designation listed. An exception is the basic water content for which a detailed description using the mortar voids test is presented below.

Mortar Voids Test. For the first series of tests representing an a_m/c_m of 2, weigh the quantities of surface dry sand and cement into the mixing pan and mix thoroughly in the dry condition. Add the required water and mix for one minute. This mortar is then placed in a stainless steel cylinder 3 in. high by 3.25 in. in diameter (volume 404 c.c. measured by water displacement) in four equal layers, tamping each layer with a metal rod which has a round and flat end 1 in. in diameter. Thirty-two strokes are used for each layer. The cylinder is then struck-off with a trowel and weighed. The mortar is then removed from the cylinder, placed back

into the pan and the test is repeated as before using more water to give an additional one percent of water content. The basic water content is selected when the weight of the mortar in the mold is the greatest. Having determined the basic water content, it is necessary to check it by making a new mixture using the same quantities of sand, cement and water. The weight of the mortar in the mold must agree with the original test within 1 gram. After this check, the same mix is again used adding an additional 2 percent of water above that determined for the basic water content and the weight of the mortar determined as in the previous test. After this, an additional 5 percent of water above that determined for the basic water content is added to the mortar and the weight of the mortar in the mold is determined.

This series of tests provides data for mortar having an $a_m/c_m = 2$, and it is then necessary to repeat the series of tests with $a_m/c_m = 3$ and 4 to complete the mortar voids test.

4.3 Unconfined Compression Test

Unconfined compression tests were run on 34 samples for different mix designs and test conditions. Figure 4.6 shows the Wykeham Farrance Compression Test Machine. All tests were constant rate of strain tests with strain rates of 2.5 percent per minute. Exceptions are Samples 27 and 34 in which slower strain rates were applied to check the influence of strain rate on the strength. The load transducer used on this job is a Dynisco TCFT5-1M model which has a maximum capacity of 1,000 lb. All fine aggregates were oven-dried and coarse aggregates air-dried.



Figure 4.3. Mixer and vibrator.



Figure 4.4. 6 in. x 12 in. mold with a 2 in. extension tube on top.

Mixing. Hand mixing is not accepted for low slump concrete according to ASTM standards. Small drum mixers are also not well adapted to laboratory use, because proper mixing action is difficult to obtain and because too large a percentage of the mortar in a small batch sticks to the drum and to the blades. Uzomaka (1971) used a Hobart mixer. The disadvantage of a Hobart mixer is that the blades are fixed in place relative to the mixing bowl, therefore large size coarse aggregates may be jammed between the rotating blade and the bowl to cause damage to the blade. In view of the above difficulties, a Kol brand commercial mixer modeled M-58-1M (Figure 4.3) was used. This mixer is operated by a 1/4 HP, 1,725 rpm, 115 V motor and has a capacity to mix a 50 lb batch. The benefit of this mixer is that it has a loose blade which can be manually adjusted to scrub the mortar adhering to the bottom and the wall of the pail during the mixing action.

The cylindrical sample used for the test has a 6 in. diameter and a 12 in. height. The approximate sample weight equals 30 lb. For every test, approximately 35 lb. of concrete was mixed. The mortar adhering to the pail which could not be scrubbed off was estimated at only 0.5 percent of the total weight of the mortar. Therefore no "buttering" or "over-mortaring" adjustment as recommended by ASTM standards, was necessary.

Prior to starting rotation of the mixer, the pail and the loose blade were damped by a wet cloth. Coarse aggregates, some of the mixing water and the solution of the air-entrained admixture, as required in some of the tests, were then added. The mixer was

started and a few revolutions permitted before adding the fine aggregate and the cement. After restarting the mixer the remaining water was poured in. The mixing lasted for 3 minutes for non-air-entrained concrete and 4 minutes for air-entrained concrete. The machine mixed concrete was then deposited in a clean, damp mixing pan and remixed by trowel for 30 seconds to 1 minute to ensure a uniform mix.

Vibration. To improve workability of the concrete, internal vibration was applied either in one layer or in two layers in a split cylinder mold with a 2 in. extension tube attached to the top of the mold (Figure 4.4). The lining used for the mold included one layer of polyethylene plastic and one layer of paper towel between the plastic and the mold. The vibrator (Figure 4.3) used was a 1-3/8 in. diameter Viber brand made by Viber Co. in Burbank, California. The duration of vibration required depends upon the workability of the concrete. Usually sufficient vibration has been applied as soon as the surface of the concrete has become relatively smooth or when mortar just begins to flush to the surface adjacent to the vibrator. Care was taken to avoid resting the vibrator on the bottom or sides of the mold. The withdrawing of the vibrator was slow enough to ensure that no air pocket was left in the sample.

After the completion of the vibration, the extension tube was removed and the excess concrete was struck off the top surface of the mold. A float was then used to smooth and level the surface.

The mold was not removed until the sample was ready for testing on the compression machine. The sample was weighed just prior to the compression test as a check on the unit weight of the concrete.

Air Content. The air content of the fresh concrete was measured by a model CT-158 air indicator sold by Soil Test, Inc., as is shown in Figure 4.5. Usually, air content is measured by the pressure method in which fresh concrete is placed in the air meter bowl, compacted, and struck-off. A known air pressure is then applied and the change in volume is computed based on Boyle's law. For concrete of dry consistency, adequate compaction to drive out all the entrapped air is hard to achieve, hence the accuracy of the pressure method is open to question. Therefore, the air indicator provides a more accurate measurement of air content in the cement mortar.

After the compression test, air content was measured for three places in a sample -- from the top portion, the middle failure surface and the bottom portion of the sample. The mortar was first compacted by a rod in the cup, followed by filling with isopropyl alcohol to a line on the glass stem. The mortar was agitated in the alcohol by rolling the indicator from vertical to horizontal several times. However, mortar of dry consistency was difficult to mix with the alcohol in this way. Therefore, a metal wire was inserted from the opening to scour out or to loosen the mortar from the glass. Figure 4.5 illustrates use of the wire. The three successive measurements by the indicator were found to be very consistent. Usually less than 8 percent difference was observed. The average measurement value was then converted into the actual air content by a conversion table furnished by the manufacturer. In the conversion table, the mortar content per cubic yard of concrete is required.

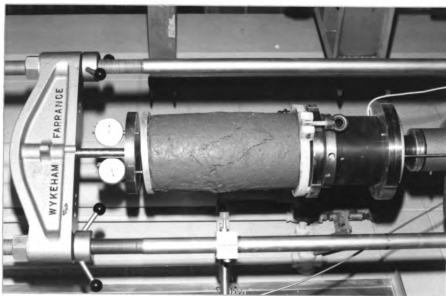


Figure 4.6. The compression test machine and a failed sample.



Figure 4.5. Air indicator and a metal wire used to scour out the mortar.

Temperature. In some of the tests, the temperature of the concrete was either lowered or raised by changing the temperature of the mix components. The purpose of changing the temperature was to evaluate the influence of concrete temperature on the mechanical properties.

The temperature of the concrete was measured, after the vibration of the concrete in the mold, by drilling a hole and inserting the thermometer into the sample. Three readings were taken from the three different holes.

The Compression Test. A sample with the mold was placed on the base plate of the compression machine. The two-piece mold was removed just prior to the start of the test. Since this dry consistency concrete was vibratory compacted into a stiff mass, it will retain its cylindrical shape without any mold or membrane support. A slight uneven slump was observed after the mold was removed. To allow for this condition, an aluminum loading cap with a steel ball (Figure 4.6) was placed on the top of the sample for load transfer to the machine. The strength of the fresh concrete at various rates of strain was investigated in this research and a strain rate of 2.5 percent per minute was selected as a basis for comparison.

Since low slump concrete always produces a fracture type failure at low strains in contrast to large deformations exhibited in some compression tests on clay soils, the test was stopped when the ultimate strength was reached. The angle of rupture was measured after the test and recorded for all shear type failures.

The maximum load observed for the stronger samples was only 500 lb, hence no deformation correction was needed for the loading system.

CHAPTER V
FIELD AND LABORATORY EXPERIMENTAL RESULTS

The experimental results for this project are presented under three headings: physical properties, stress-strain behavior of the fresh concrete and field failure example. Each section may include laboratory test data and/or finite element analysis results.

5.1 Physical Properties

Physical properties of the material are subdivided into four different groups: fine aggregate, coarse aggregate, cement, and mortar. Each group includes a table summarizing its physical properties (Tables 5.1 through 5.4). Figure 3.2 includes the basic water content curves for the mortar with various sand-cement ratios. The data used to plot these curves are tabulated in Table B-1 of Appendix B. Unit weights of the fresh concrete are listed in Table 5.6 of Section 5.2 for each sample.

Table 5.1. Physical properties of fine aggregates.

| | |
|---|------|
| Bulk specific gravity, G_a | 2.68 |
| Bulk specific gravity (saturated surface dry) | 2.71 |
| Percent absorption | 1.28 |

Table 5.2. Physical Properties of Coarse Aggregates

| | |
|---|------------|
| Bulk Specific Gravity, G_b | 2.64 |
| Bulk Specific Gravity (saturated surface dry) | 2.67 |
| Apparent Specific Gravity | 2.74 |
| Percent Absorption | 1.32 |
| Unit Weight (dry rod), γ_b | 111.60 pcf |
| Unit Weight (loose), $\gamma_{d\ell}$ | 103.00 pcf |
| Unit Weight (dry vibrated), γ_{dv} | 114.60 pcf |
| Voids Content at γ_b | 32.30% |
| Voids Content at $\gamma_{d\ell}$ | 37.70% |
| Voids Content at γ_{dv} | 30.40% |

Table 5.3. Physical Properties of Cement and Mortar

| | |
|------------------------------------|---------------------------|
| Type of Cement | Type I Portland Cement |
| Specific Gravity, G_c | 3.12 |
| Volume of Mortar/cu yd of concrete | 14.04 cu ft |

Table 5.4. Basic Water Content by Percentage of Water Weight

| | |
|-----------|---|
| a_m/c_m | Percentage of Water in Total Mortar by Weight |
| 2 | 13 |
| 3 | 12 |
| 4 | 11 |

5.2 Stress-Strain Behavior of the Fresh Concrete

Stress-strain behavior of the fresh concrete has been measured using unconfined compression tests in the laboratory. Altogether 34 tests were run for different mix designs or test conditions. A summary of the test conditions and mix designs is given in Table 5.5. Appendix D is a typical example of the work sheet used for the mix proportion.

Stress-strain behavior in unconfined compression tests is summarized in Figures 5.1 through 5.8. Laboratory data are given in Appendix A-1 through A-34. The stress-strain curves were plotted on modified coordinate systems as illustrated in Section 2.2.3. However, laboratory data in Appendix A shows both the original test data and the modified data. Numbers at the end of each curve indicate the sample number. Stress-strain curves are characterized into different categories according to the different factors affecting mechanical properties as described in Section 2.2.4. The stress-strain curve for Sample No. 5 is included in each category for the reason that this is a standard sample.

Table 5.6 gives a summary of the mechanical properties of the material as measured from the stress-strain curves illustrated in Figures 5.1 through 5.8. Unit weights of samples, γ , are also included in this Table.

5.3 Two Field Construction Examples Illustrating Failure

Shear failures for two field construction examples are described below to provide information for the analysis in the next chapter. In addition, mix designs and other pertinent information

Table 5.5. Mix Design and Test Conditions

| Sample Number | W_w/W_c | W_a/W_c | M | T (°F) | t_1 (min.) | t_2 (min.) | Crushed (c) or Round (R) Gravel | Air Content, percent | CF (sacks/cu yd) | Rate of Shear (percent per min.) |
|---------------|-----------|-----------|-------|--------|--------------|--------------|--|----------------------|------------------|----------------------------------|
| 1 | 0.38 | 2.350 | 0.48 | 71 | 32 | 20 | R | 2.35 | 5.7 | 2.5 |
| 2 | 0.38 | 2.450 | 0.475 | 70 | 32 | 20 | R | 2.35 | 5.5 | 2.5 |
| 3 | 0.40 | 1.934 | 0.5 | 71 | 32 | 20 | R | 2.35 | | 2.5 |
| 4 | 0.43 | 1.934 | 0.5 | 73 | 32 | 20 | R | 2.35 | | 2.5 |
| 5 | 0.38 | 1.934 | 0.5 | 73 | 32 | 20 | R | 2.35 | 6.7 | 2.5 |
| 6 | 0.38 | 1.934 | 0.5 | 72 | 47.5 | 35.5 | R | 2.35 | | 2.5 |
| 7 | 0.38 | 1.934 | 0.5 | 72 | 24.3 | 12.3 | R | 2.35 | | 2.5 |
| 8 | 0.38 | 1.934 | 0.5 | 71 | 40 | 28 | R | 2.35 | | 2.5 |
| 9 | 0.38 | 2.200 | 0.49 | 73 | 32 | 20 | R | 2.35 | 6.1 | 2.5 |
| 10 | 0.38 | 1.750 | 0.51 | 73 | 32 | 20 | R | 2.35 | 7.3 | 2.5 |
| 11 | 0.38 | 1.600 | 0.52 | 73 | 32 | 20 | R | 2.35 | 7.8 | 2.5 |
| 12 | 0.38 | 1.934 | 0.485 | 73 | 32 | 20 | R | 2.35 | | 2.5 |
| 13 | 0.38 | 1.934 | 0.555 | 73 | 32 | 20 | R | 2.35 | | 2.5 |
| 14 | 0.38 | 1.934 | 0.430 | 72 | 32 | 20 | R | 2.35 | | 2.5 |
| 15 | 0.38 | 1.934 | 0.580 | 73 | 32 | 20 | R | 2.35 | | 2.5 |
| 16 | 0.38 | 1.934 | 0.5 | 58 | 32 | 20 | R | 2.35 | | 2.5 |
| 17 | 0.38 | 1.934 | 0.5 | 86 | 32 | 20 | R | 2.35 | | 2.5 |
| 18 | 0.38 | 2.550 | 0.472 | 71 | 32 | 20 | R | 2.35 | 5.3 | 2.5 |
| 19 | 0.38 | 1.934 | 0.5 | 73 | 32 | 20 | C | 2.35 | | 2.5 |
| 20 | 0.40 | 1.934 | 0.5 | 73 | 32 | 20 | C | 2.35 | | 2.5 |
| 21 | 0.355 | 1.934 | 0.5 | 73 | 32 | 20 | C | 2.35 | | 2.5 |
| 22 | 0.38 | 1.934 | 0.366 | 70 | 32 | 20 | R | 2.35 | | 2.5 |
| 23 | 0.43 | 1.934 | 0.5 | 73 | 32 | 20 | C | 2.35 | | 2.5 |
| 24 | 0.38 | 1.934 | 0.38 | 70 | 32 | 20 | R | 2.35 | | 2.5 |
| 25 | 0.355 | 1.934 | 0.5 | 71 | 32 | 20 | R | 2.35 | | 2.5 |

to be continued

Table 5.5. (Continued)

| Sample Number | W_w/W_c | W_a/W_c | M | T (°F) | t_1 (min.) | t_2 (min.) | Crushed (c) or Round (R) Gravel | Air Content, percent | CF (sacks/cu yd) | Rate of Shear (percent per min.) |
|---------------|-----------|-----------|-------|--------|--------------|--------------|---------------------------------|----------------------|------------------|----------------------------------|
| 26 | 0.362 | 1.934 | 0.5 | 70 | 32 | 20 | R | 3.255 | | 2.5 |
| 27 | 0.355 | 1.934 | 0.5 | 70 | 32 | 20 | R | 2.35 | | 0.25 |
| 28 | 0.362 | 1.934 | 0.5 | 70 | 32 | 20 | R | 2.883 | | 2.5 |
| 29 | 0.362 | 1.934 | 0.5 | 70 | 32 | 20 | R | 3.906 | | 2.5 |
| 30 | 0.362 | 1.934 | 0.5 | 71 | 32 | 20 | R | 2.604 | | 2.5 |
| 31 | 0.38 | 1.934 | 0.288 | 71 | 32 | 20 | R | 2.35 | | 2.5 |
| 32 | 0.38 | 1.934 | 0.399 | 72 | 32 | 20 | R | 2.1 | | 2.5 |
| 33 | 0.38 | 1.934 | 0.346 | 70 | 32 | 20 | R | 2.35 | | 2.5 |
| 34 | 0.355 | 1.934 | 0.5 | 71 | 32 | 20 | R | 2.35 | | 0.833 |

Table 5.6. Mechanical Properties of the Fresh Concrete

| Sample Number | Ultimate Strength σ_u (psi) | Yield Stress σ_y (psi) | Elastic Modulus E_1 (psi) | Plastic Modulus E_2 (psi) | σ_y/σ_u (percent) | Unit Weight γ (pcf) |
|---------------|--|-------------------------------------|-----------------------------------|-----------------------------------|----------------------------------|----------------------------------|
| 1 | 14.37 | 13.66 | 1500 | 425 | 95.1 | 154.4 |
| 2 | 15.77 | 14.91 | 1569 | 688 | 94.5 | 155.3 |
| 3 | 5.24 | 4.66 | 341 | 126 | 88.9 | 155.3 |
| 4 | 3.62 | 3.15 | 246 | 102 | 87.0 | 154.4 |
| 5 | 7.57 | 7.03 | 516 | 193 | 93.9 | 154.1 |
| 6 | 9.98 | 9.44 | 761 | 263 | 94.6 | 154.2 |
| 7 | 7.35 | 6.79 | 466 | 169 | 92.4 | 155.3 |
| 8 | 8.28 | 7.84 | 549 | 231 | 94.7 | 155.3 |
| 9 | 10.04 | 9.34 | 1128 | 603 | 93.0 | 155.0 |
| 10 | 6.88 | 6.54 | 400 | 163 | 95.1 | 155.4 |
| 11 | 6.65 | 5.96 | 372 | 119 | 89.6 | 153.8 |
| 12 | 8.07 | 7.34 | 545 | 292 | 91.0 | 153.1 |
| 13 | 7.50 | 7.17 | 398 | 157 | 95.6 | 151.6 |
| 14 | 10.62 | 9.53 | 1542 | 652 | 89.7 | 154.7 |
| 15 | 7.20 | 6.73 | 344 | 168 | 93.5 | 151.2 |
| 16 | 6.99 | 6.66 | 446 | 200 | 95.3 | 153.7 |
| 17 | 10.51 | 9.64 | 873 | 302 | 91.7 | 154.4 |
| 18 | 17.85 | 16.54 | 2026 | 1190 | 92.7 | 153.7 |
| 19 | 9.81 | 9.16 | 690 | 309 | 93.4 | 155.3 |
| 20 | 6.70 | 6.38 | 438 | 252 | 95.2 | 154.7 |
| 21 | 12.17 | 11.51 | 1317 | 528 | 94.6 | 156.9 |
| 22 | 17.76 | 15.25 | 2827 | 1201 | 85.9 | 157.3 |
| 23 | 4.65 | 4.25 | 329 | 119 | 91.4 | 154.4 |
| 24 | 15.27 | 14.64 | 2473 | 1145 | 95.9 | 156.7 |
| 25 | 11.69 | 10.84 | 1373 | 408 | 92.7 | 156.5 |
| 26 | 6.06 | 5.53 | 340 | 129 | 91.3 | 151.2 |
| 27 | 10.80 | 9.94 | 1002 | 518 | 92.0 | 155.0 |
| 28 | 7.18 | 6.38 | 702 | 320 | 88.9 | 153.0 |
| 29 | 5.73 | 4.96 | 371 | 163 | 86.6 | 148.3 |
| 30 | 9.15 | 8.13 | 912 | 349 | 88.9 | 154.3 |
| 31 | 7.68 | 7.06 | 2250 | 496 | 91.9 | 140.4 |
| 32 | 13.13 | 12.41 | 1675 | 851 | 94.5 | 155.6 |
| 33 | 12.08 | 9.54 | 1802 | 677 | 79.0 | 151.8 |
| 34 | 11.43 | 10.45 | 1019 | 452 | 91.4 | 155.2 |

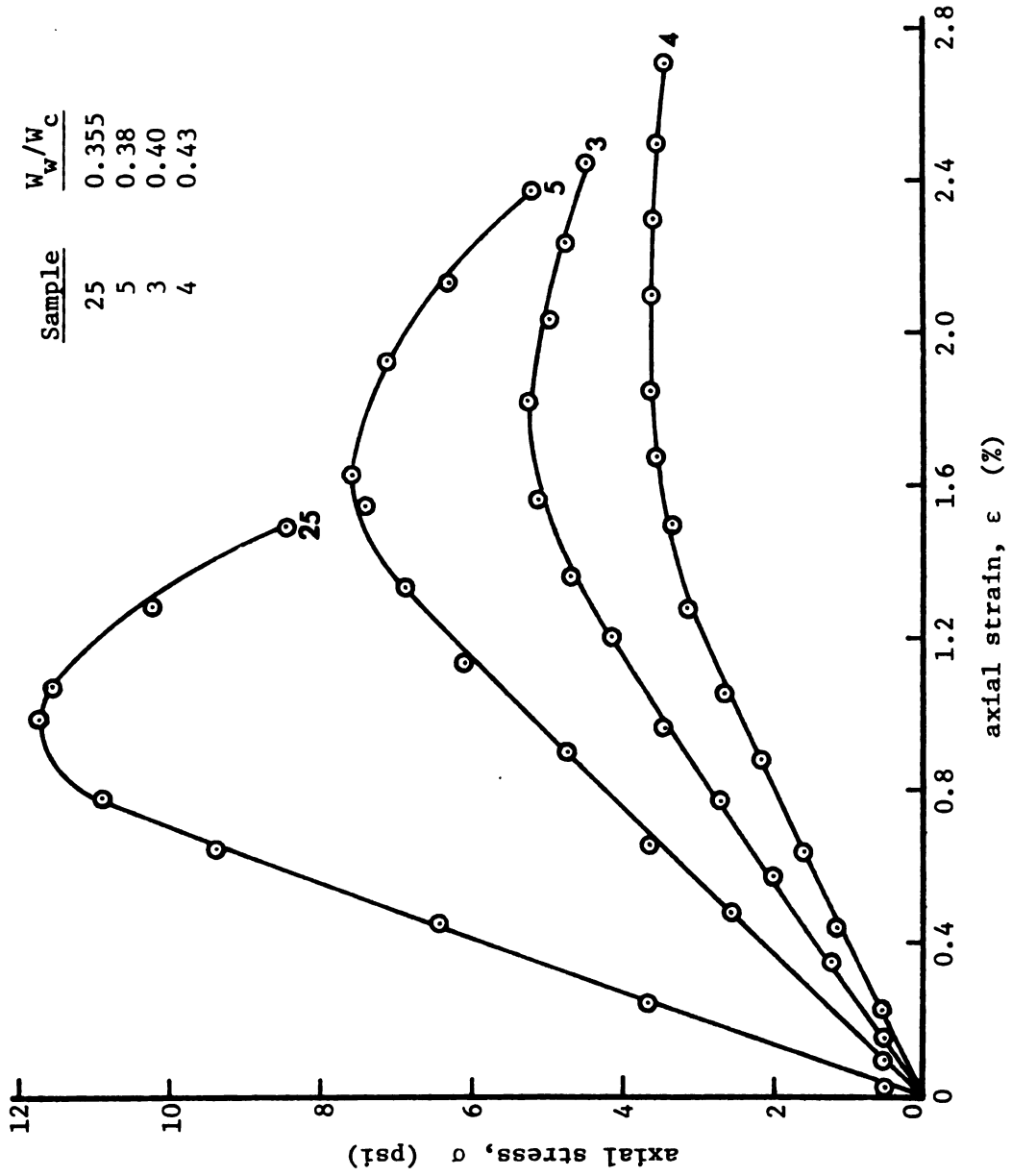


Figure 5.1. Stress-strain curves for various effective water-cement ratios.

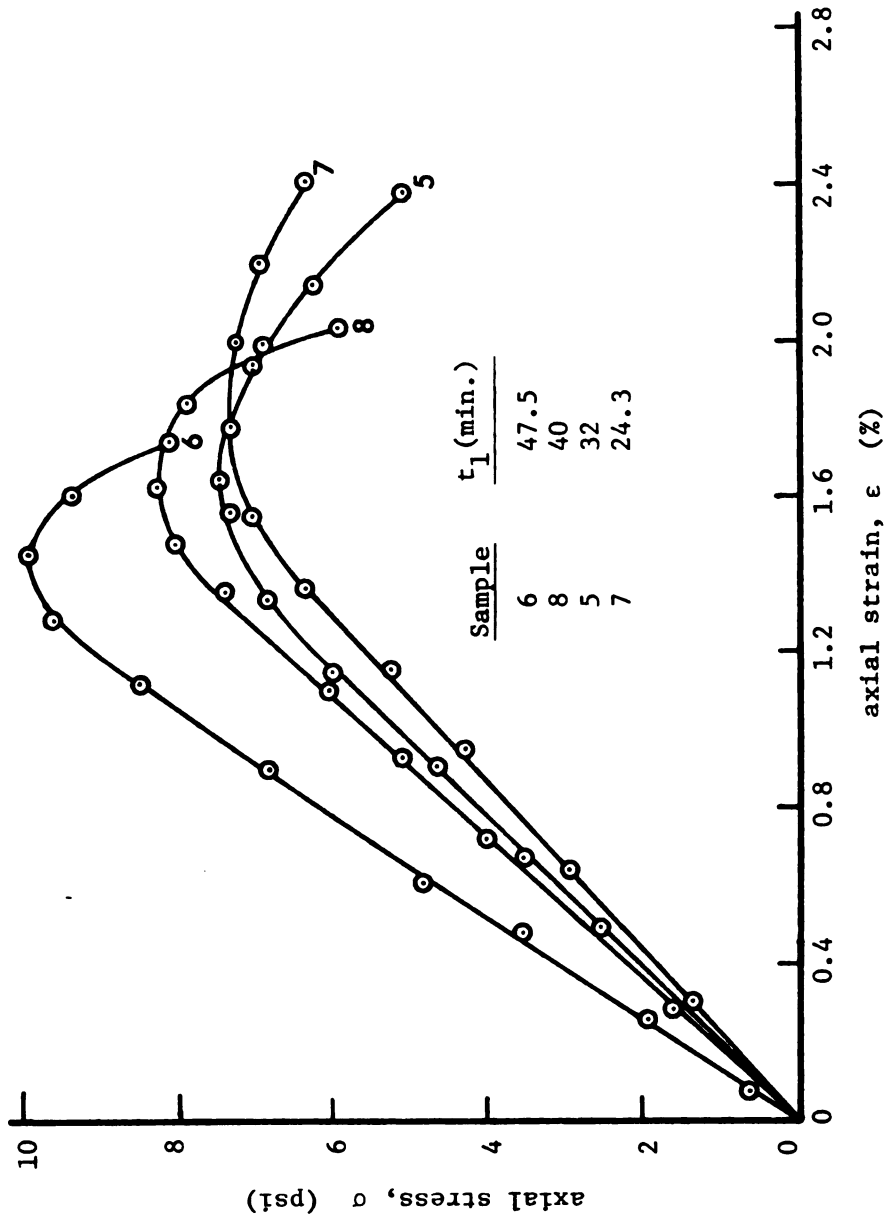


Figure 5.2. Stress-strain curves for various periods of hydration.

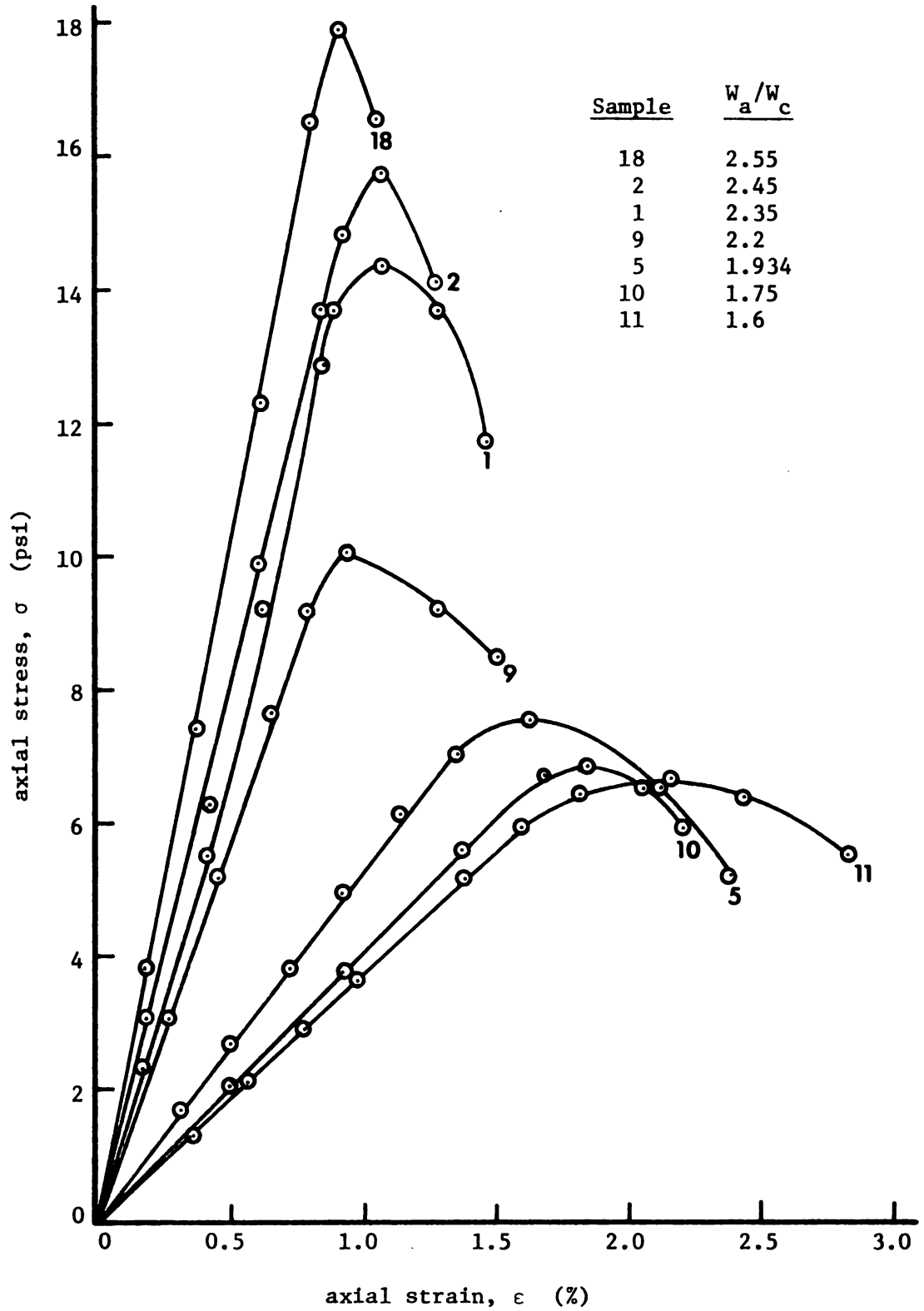


Figure 5.3. Stress-strain curves for various cement contents.

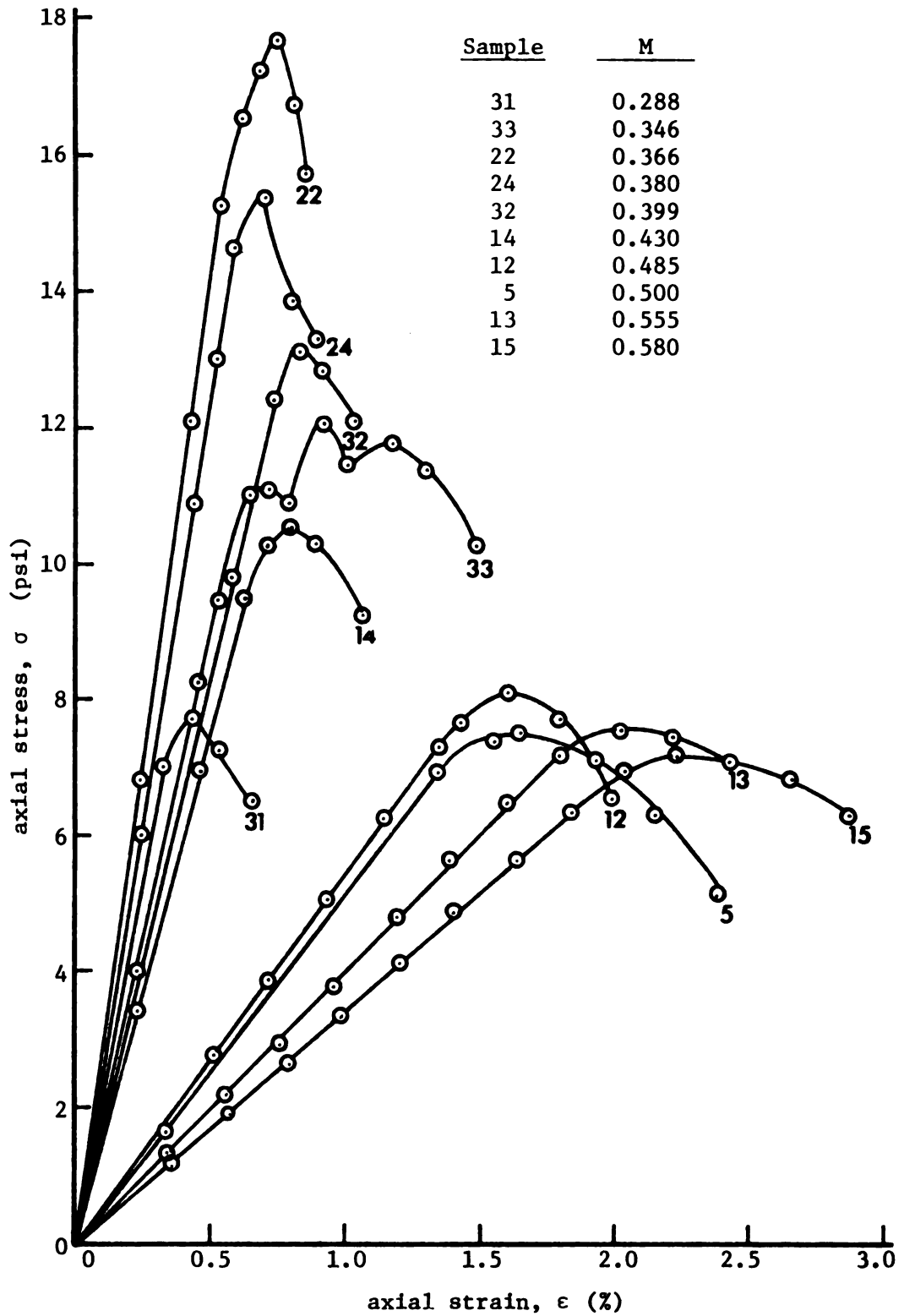


Figure 5.4. Stress-strain curves for various mortar contents.

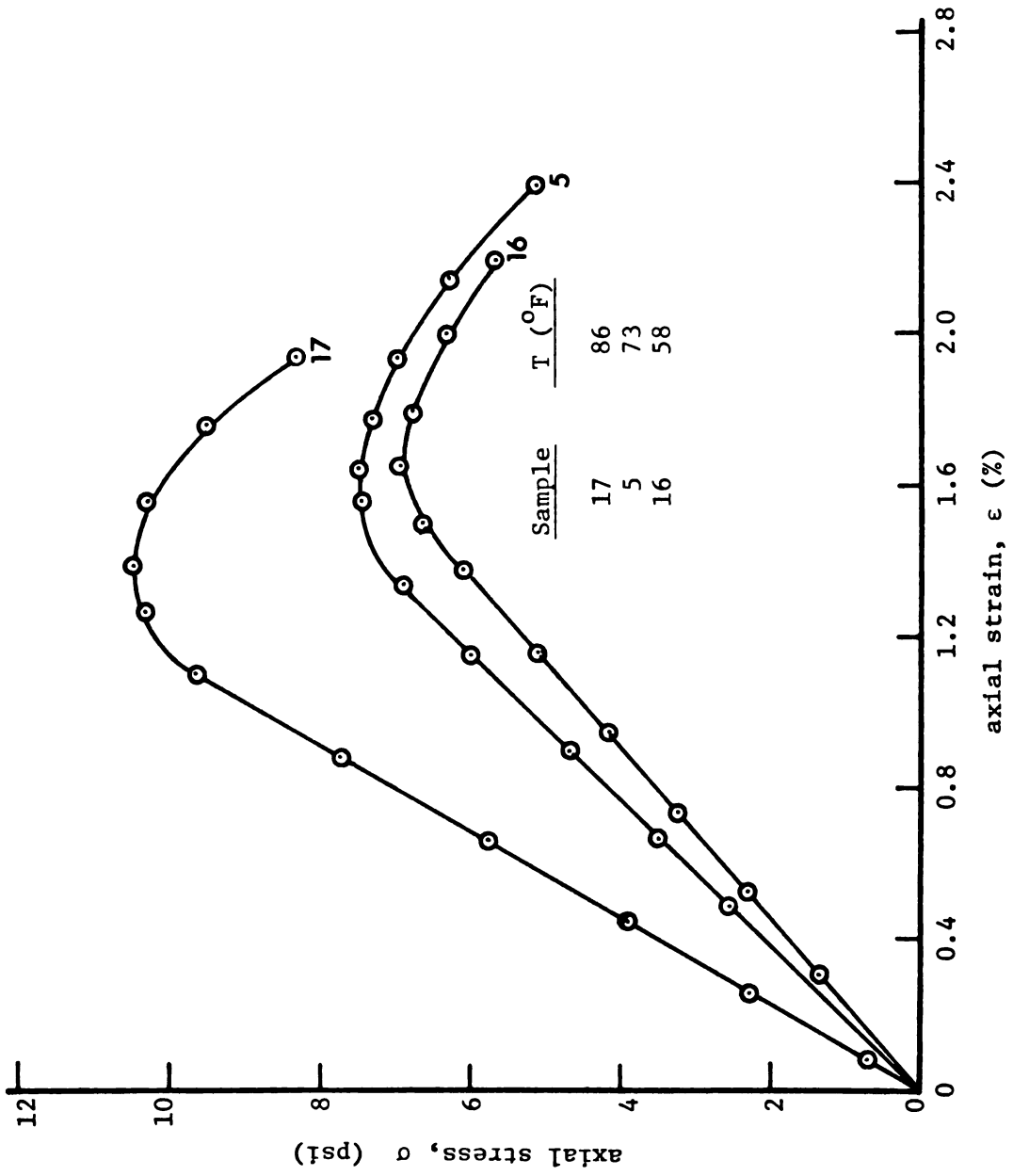


Figure 5.5. Stress-strain curves for various concrete temperatures.

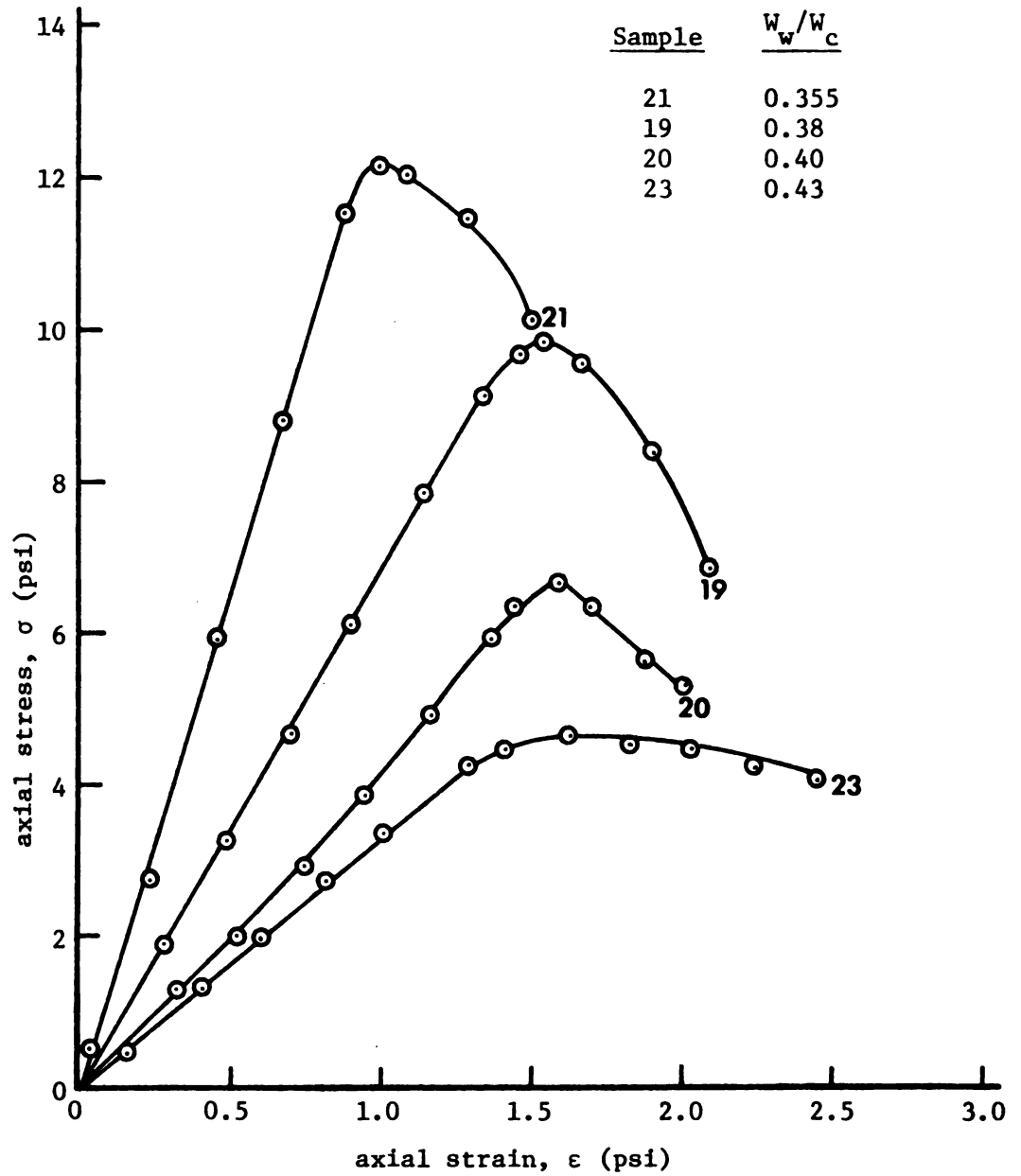


Figure 5.6. Stress-strain curves for various effective water-cement ratios for crushed aggregates.

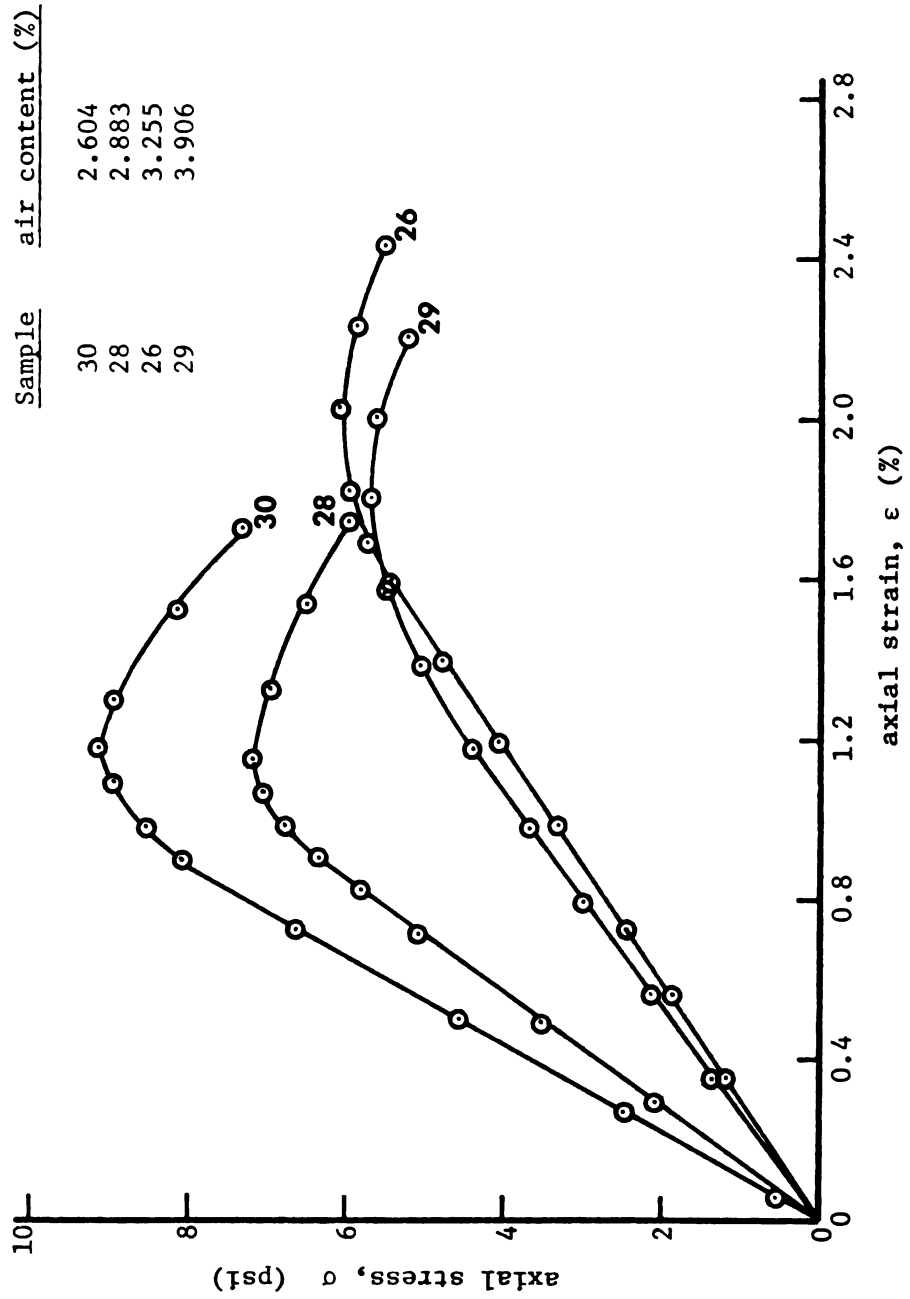


Figure 5.7. Stress-strain curves for various air contents.

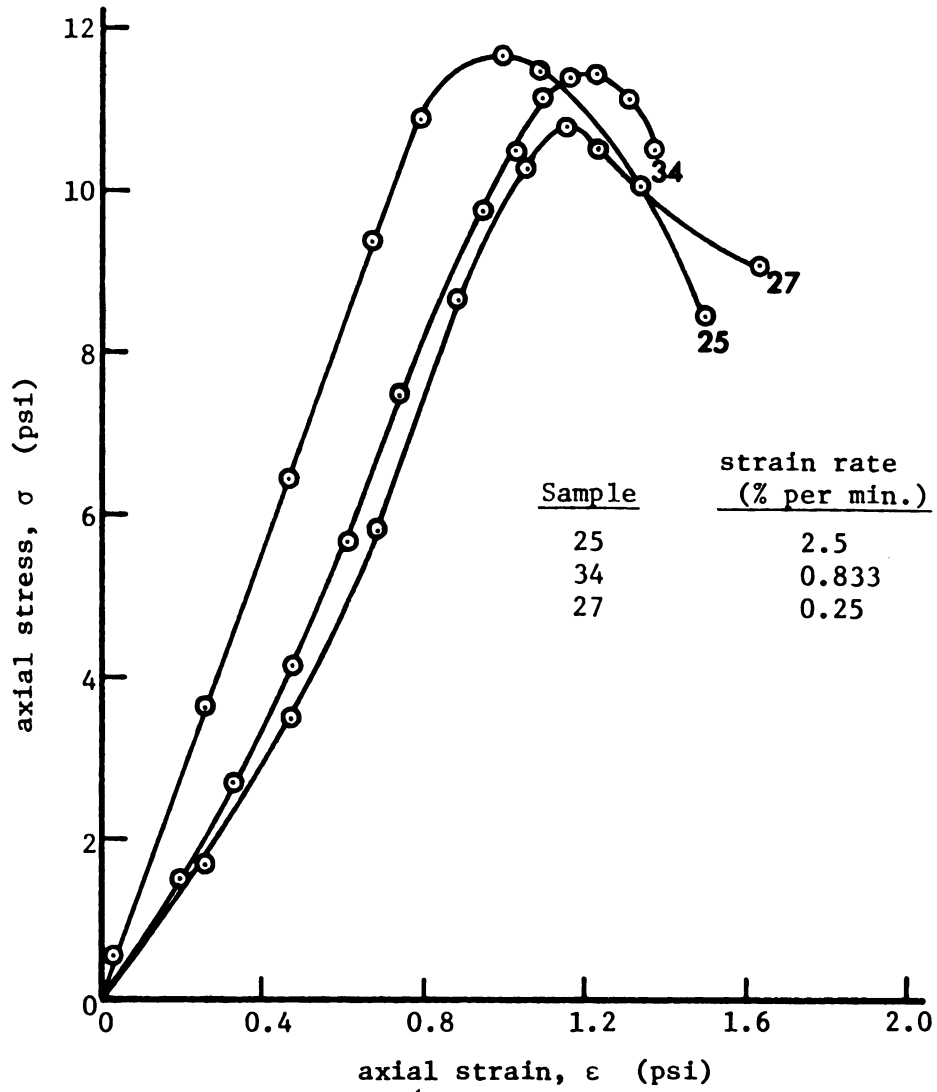


Figure 5.8. Stress-strain curves for various strain rates.

are also included for these field examples.

5.3.1 Straight Wall Experimental Section

In 1971, the experimental section shown in Figure 5.9 was slip-form constructed by A.C. Aukerman Co. of Jackson, Michigan. This section has a relatively thin rectangular shape 58 in. high and 12 in. wide. The mix design for the fresh concrete used in this section is summarized below.

Portland Cement - 564 lb
 Water - 25.3 gal + (includes surface moisture of the aggregates)
 Fine Aggregate - 1,130 lb (Michigan 2NS sand)
 Coarse Aggregate - 1,950 lb (Michigan 6A gravel)
 Air content - 4 percent +
 Slump - less than 1/4 in.
 Hydration Period - 25 minutes ±

Using the notations developed in Section 2.2.4, this mix design can also be proportioned, as needed for analytical purposes in Chapter VI, in the following manner.

$$W_w/W_c = 0.374$$

$$W_a/W_c = 2.0$$

$$M = \frac{W_a + W_c + W_w}{W} = 0.494$$

With the above proportions, the concrete was delivered by Willbee Concrete Co. of Jackson, Michigan to the construction site by the truck mixer. Concrete in the extrusion form was vibrated by six electrical vibrators at 10,000 rpm.

This straight wall experimental section failed immediately after the structure was extruded from the extrusion form while the concrete was still in its fresh state. The failure showed a distinct

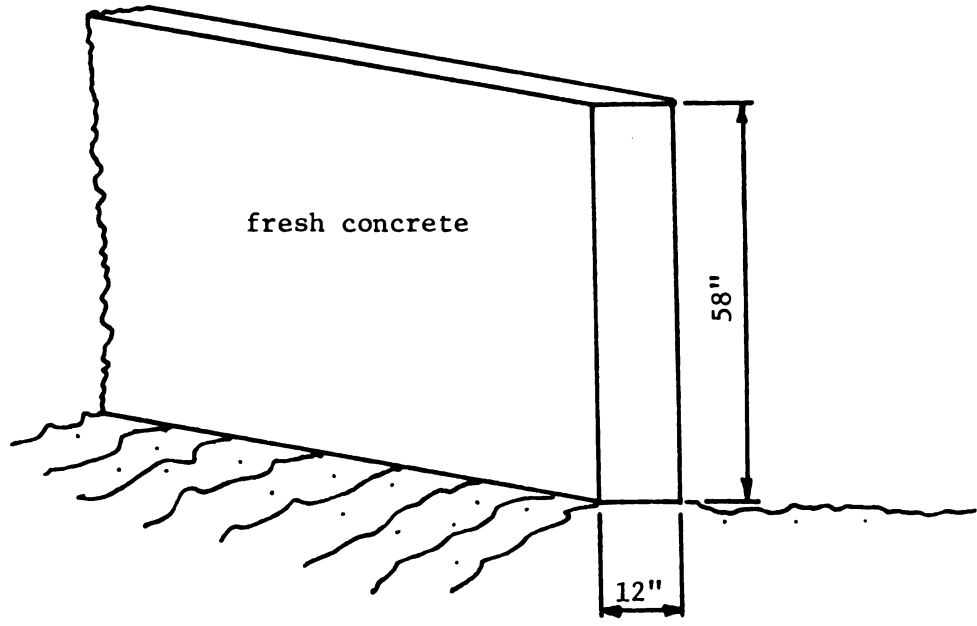


Figure 5.9. An experimental section slipform constructed by A. C. Aukerman Co. of Jackson, Michigan.

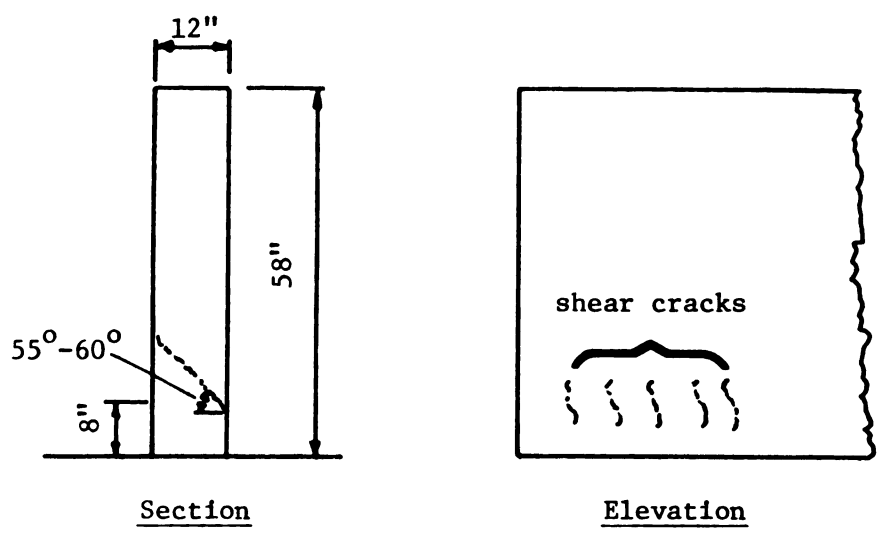


Figure 5.10. Shear failure of the experimental section.

shear failure very similar to the laboratory failed sample shown in Figure 6.4(a). Goughnour (1976) observed the construction of this test section and sketched the failure pattern as shown in Figure 5.10. This figure shows that the shear crack occurred at approximately 8 in. above the ground and that the angle of failure was between 55 to 60 degrees. For this stiff mix no noticeable deformation was observed for the successful section. However, the concrete did have a small slump, less than 1/4 in.

5.3.2 Florida Median Barrier Section

In 1974, A.C. Aukerman Co. constructed median barriers for the Florida Highway Department. Some parts of the barrier wall, apart from the ordinary 2 ft-8 in. high section, were 68 in. high as shown in Figure 5.11. The extraordinary height was needed because of two different roadway elevations. Actually, this condition exists to a greater degree when for construction reasons two adjacent roadways cannot be built to the same level; for example, approaches to bridges at different levels and ramps at diverging roadways. The difference in elevation between roadways can be considerable. In these situations, the barriers facing both roadways can be slipform constructed into a single wall, with the barrier faces at different elevations to fit the transverse profile (Figure 2.2). The slipform machine used for this kind of construction was equipped so that the two side forms were operated from separate and independent electronic vertical controls to more readily accommodate elevation differences.

The mix design used for construction of the Florida barrier section is listed below:

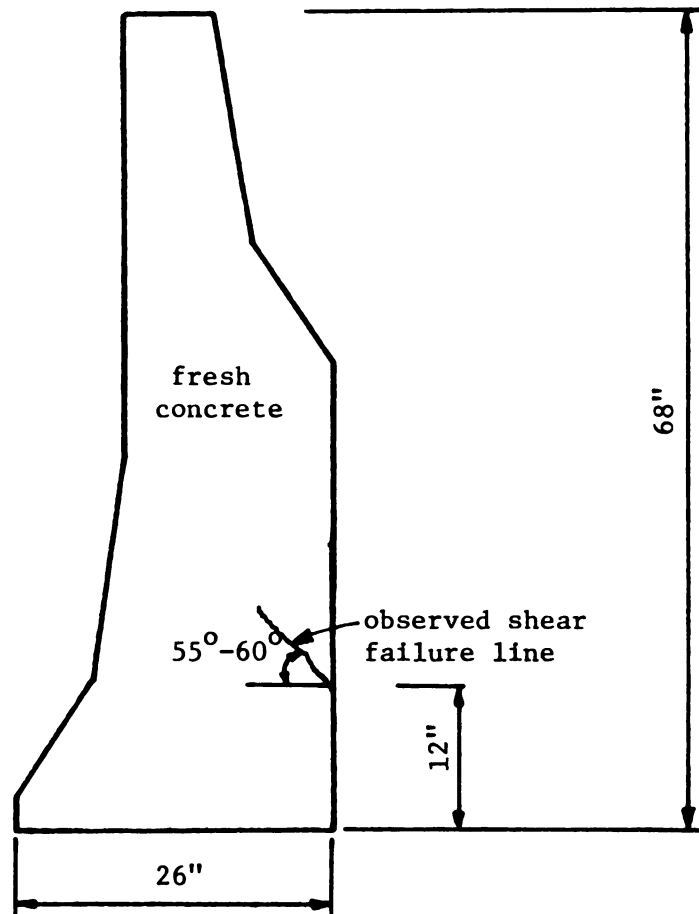


Figure 5.11. The 68 in. high Florida median barrier.

Type I portland cement - 564 lb (Universal Atlas)
Air Content - 3 to 6 percent
Water - 31.9 gal
Coarse Aggregate - 1,625 lb (lime rock $G_b = 2.45$)
Fine Aggregate - 1,240 lb (lime rock screenings, $G_a = 2.53$)
Slump - 0 to 3 in.
Unit Weight (wet) - 136 pcf

The aggregates used in the Florida construction differ from those used for this project, hence, the undrained shear strength of the Florida mix cannot be estimated. However, stresses due to gravity loads may still be evaluated by the finite element method, which appears in the next chapter.

Similar to the straight wall experimental section, the Florida barrier wall failed immediately after the structure was extruded from the extrusion form and it showed a distinct shear failure with the crack occurring approximately 12 in. above the base line. The angle of failure was again 55 to 60 degrees (Goughnour, 1976). Figure 5.11 shows a sketch of the shear failure.

CHAPTER VI INTERPRETATION AND DISCUSSION OF RESULTS

The interpretation and discussion of project results covers field, laboratory, and analysis for the low slump concrete in slip-form construction. It is presented in six sections: physical properties, sample size and failure patterns, strength characteristics of the fresh concrete, air content requirements, stresses in the experimental section, and simplified analysis for wall stability.

6.1 Physical Properties

The physical properties of each ingredient for the fresh concrete will be discussed under four headings: specific gravities and percent absorption, unit weight, void content of the coarse aggregates, and basic water contents of the mortar. All data are summarized in Tables 5.1 through 5.6 and Figure 3.2.

6.1.1 Specific Gravities and Percent Absorption

The specific gravity of the cement was 3.12. This is very typical for the non-air-entrained Type I General Portland cement for which the range of specific gravities can be 3.12 to 3.16.

The bulk specific gravity of the fine aggregate was 2.68 and that for saturated surface dry condition 2.71. These values are very typical, based on information from the MDSHT engineers, for the 2NS sand. The saturated surface-dry sample has a higher value of

bulk specific gravity because its voids within the particles are filled with water.

The bulk specific gravity of the coarse aggregate was 2.64 which falls into the range of that for sand and gravel as given by Troxell et al. (1968) (2.5 to 2.8 with 2.65 average). Bulk specific gravity for the saturated surface-dry condition was 2.67 which is also reasonable. The apparent specific gravity was 2.74. This value is higher because only the impermeable portion of the material is accounted for in the calculation.

The absorption capacity of the fine aggregate was 1.28 percent and that for the coarse aggregate 1.32 percent. Both are typical as compared to the published figures by Troxell et al. (1968), in that the approximate absorption capacity of average concrete sand is 0 to 2 percent and that for average gravel 1/2 to 1 percent. The slightly higher value for the coarse aggregate is believed due to the presence of a small amount of sandstone which is much more porous and have an absorption capacity of 2 to 7 percent as given by Troxell et al. (1968).

6.1.2 Unit Weight

The unit weight of the fresh concrete and that of the coarse aggregate are discussed separately.

Coarse Aggregates. The unit weight of the coarse aggregate was influenced by the specific gravity of the particles, the gradation, shape and surface texture of the particles, the moisture condition of the aggregate, and the compactness of the mass. Table 5.2 gives the unit weight for the dry rodded condition as 111.6 pcf.

This is comparable to the upper limit (Troxell et al., 1968) for the size range of No. 4 to 1-1/2 in. gravel (104 to 112 pcf). It is believed that this high value was due to the gradation, shown as a straight line by curve B in Figure 4.1, which corresponds to a well graded sample. The dry loose unit weight of 103 pcf coincides with the upper limit of the range (95 to 103 pcf) given by Troxell et al. (1968). The dry vibrated unit weight of 114.6 pcf is considered reasonable because the vibrator gives a higher degree of compaction as compared to that produced by rodding compaction.

Fresh Concrete. Unit weights of fresh concrete samples are listed in Table 5.6. Except for Samples 31 and 33, which were poorly compacted honey-combed samples, the unit weight has a range of 148.3 pcf to 157.3 pcf. This range is comparable to that ordinarily used in building and highway construction which has a range of 148 to 152 pcf. The slightly higher unit weight in this project is because no air-entraining agent was added while for ordinary construction a 3 to 8 percent air content is very common. However, Samples 26, 28, 29, and 30 did have an air-entraining agent added resulting in differences in air content. Figure 6.1 shows the variation of unit weight with air content for these samples.

6.1.3 Void Content of the Coarse Aggregate

The voids content of the coarse aggregate for the dry rodded condition equaled 32.3 percent as shown in Table 5.2. An indication of the range in voids content of ordinary gravels has been summarized by Walker (1930). In Walker's experiment the gravel was segregated into three size groups -- 1-1/2 in. to 3/4 in., 3/8 in. to 3/4 in.,

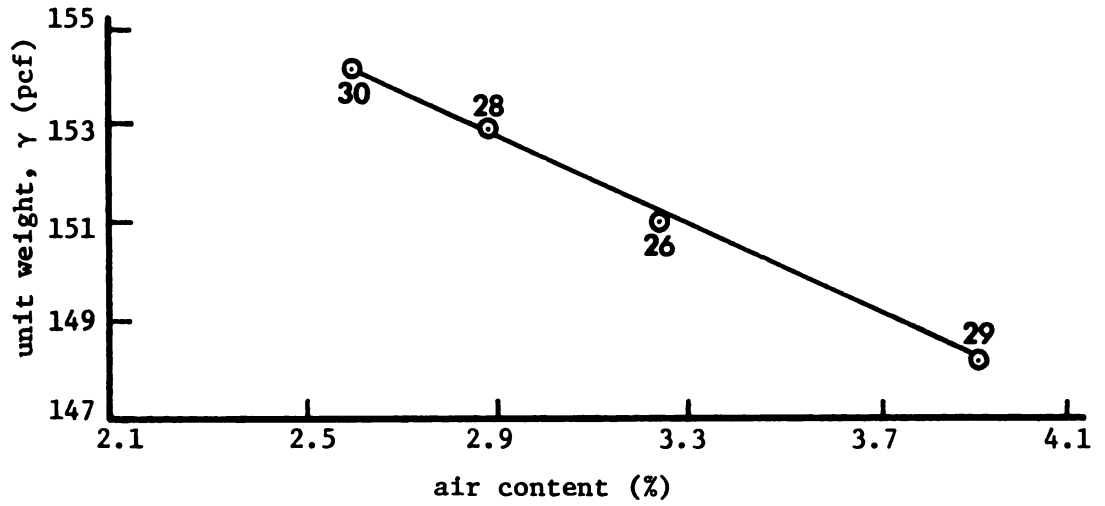


Figure 6.1. Air content and unit weight relationship.

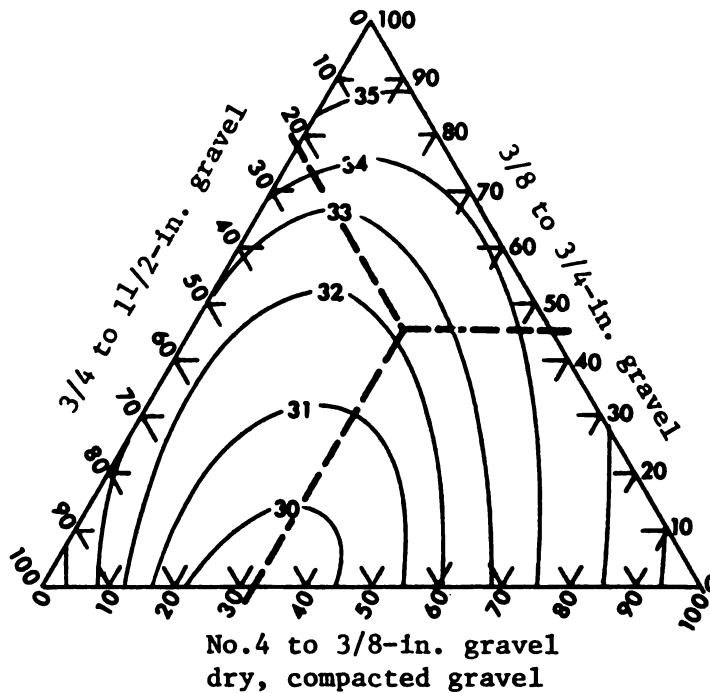


Figure 6.2. Void contents of gravel. (from Troxell, et al., 1968)

and 3/8 in. to No. 4 -- and then recombined. The results were plotted in the form of contours of equal void content on a trilinear diagram as shown in Figure 6.2. A point on a trilinear diagram shows the percentage of each size group of the three-component system. The percentage of each size range increases from 0 to 100 from the base line to the opposite apex.

The gradation for the coarse aggregate used was curve B of Figure 4.1, in which 23 percent comes from 3/4 in. to 1-1/2 in., 45 percent from 3/8 in. to 3/4 in., and 32 percent from No. 4 to 3/8 in. These data are shown on Figure 6.2 with the point falling almost on the 32.3 percent voids contour.

For the dry loose state, the voids content, in general, was about 3 to 4 percent greater than that for the dry rodded compact state (Troxell et al., 1968). Table 5.2 shows a void content at a dry loose state equal to 37.7 percent which is 5.4 percent higher than the dry rod compacted state. Table 5.2 also shows that the void content for a vibrator compacted state equals 30.4 percent. Both values fall in the expected range.

Troxell et al. (1968) also stated that for aggregates of normal range in specific gravity (2.55 to 2.65) a unit weight of 100 pcf corresponds to a void content of about 37 to 39 percent, and an increase in unit weight of 5 pcf corresponds to a decrease in voids of about 3 percent. As referred to in Table 5.2, it is seen that all void contents at the dry rodded compact state, dry loose state, and vibratory compacted state are in reasonable agreement with this approximate estimation.

6.1.4 Basic Water Content of the Mortar

Basic water contents for mortar composed of Type I Portland cement and 2NS sand are listed in Table 5.4. It is seen from this table that the basic water content decreases with increasing sand-cement ratio of the mortar, a_m/c_m . This phenomenon is reasonable since cement particles are much smaller than sand particles, therefore a higher percentage of cement would provide more surface films and hence a higher basic water content.

6.2 Sample Size and Failure Pattern

The unconfined compression test is used for testing those materials which can stand alone with no lateral confining pressure. In compressing a sample between the plane surfaces of the testing machine it is usually assumed that the compressive force is uniformly distributed over the cross-section. The actual stress distribution on the sample ends is much more complicated even when the surfaces are in perfect contact. Friction on the surfaces of contact between the specimen and the loading head of the machine reduces the lateral expansion which accompanies compression at these surfaces and the material at this point is in a more favorable condition, thus creating "dead zones." Since shear stresses develop between the plates and the sample, the principal stresses are rotated resulting in a stress distribution different from the assumed stress condition. Figure 6.3 shows the results for uniaxial compression.

For a deformation Δh of the cylinder, the strain along the axis of the cylinder is $\Delta h/S$, whereas along the edge, the strain is

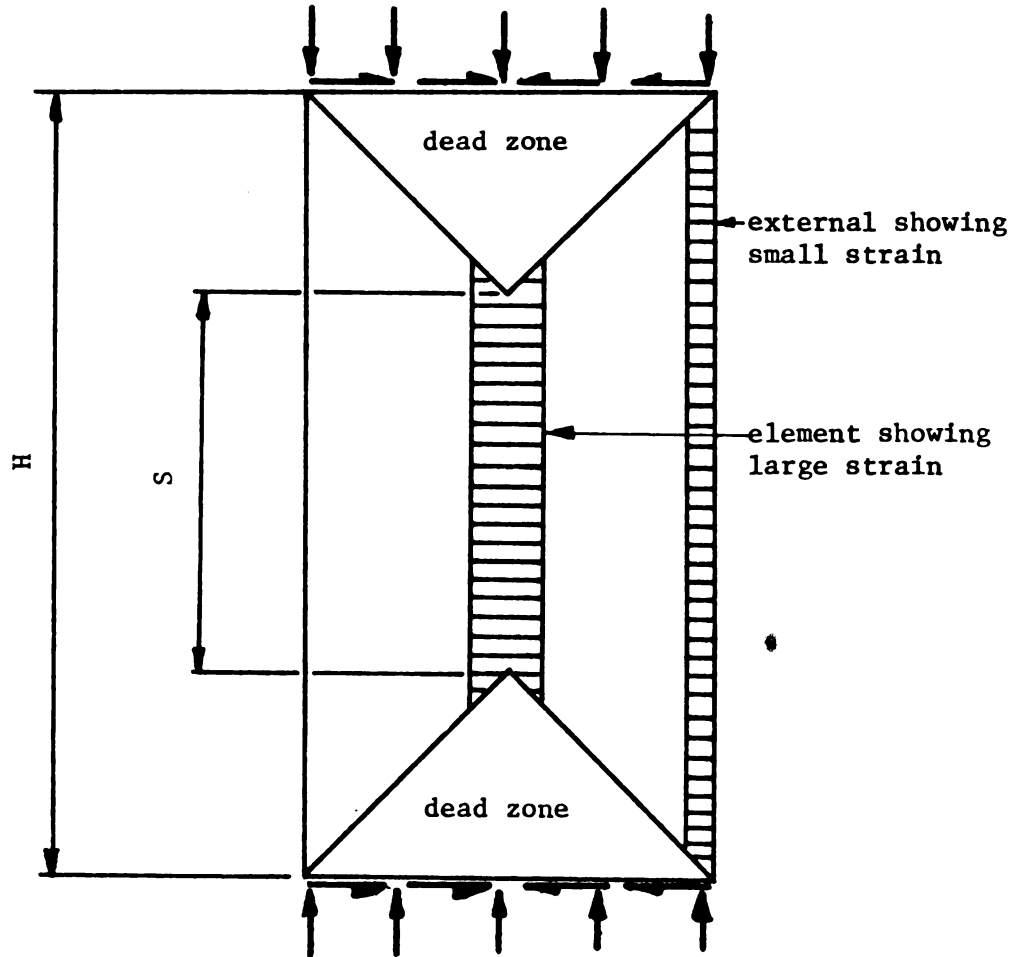


Figure 6.3. Stress and strain in a uniaxial compression test.

$\Delta h/H$. Since S is less than H , the strain is greater along the central axis of the cylinder, and, since Poisson's ratio does not change appreciably, the center pushes outward, causing bulging of the specimen. Almost all the failed samples in this project exhibited this phenomenon (see Figure 6.4).

Using the theory of elasticity and disregarding any pore pressure effects, Balla (1960) derived the solutions for stresses at a point within a loaded triaxial specimen, which shows the importance of three factors: (1) Poisson's ratio, (2) the height-diameter ratio of the test cylinders, and (3) the roughness of the loading plate. Relations arrived at for the loading condition, as shown in Figure 6.5 are:

$$\sigma_z = \sigma_1 \left[1 - \psi \frac{\nu}{1-\nu} \phi_{\sigma_z} \right] + \sigma_3 \psi \phi_{\sigma_z} \quad (6.1)$$

$$\sigma_r = \sigma_1 \psi \frac{\nu}{1-\nu} \phi_{\sigma_r} + \sigma_3 \left[1 - \psi \phi_{\sigma_r} \right] \quad (6.2)$$

$$\sigma_\theta = \sigma_1 \psi \frac{\nu}{1-\nu} \phi_{\sigma_\theta} + \sigma_3 \left[1 - \psi \phi_{\sigma_\theta} \right] \quad (6.3)$$

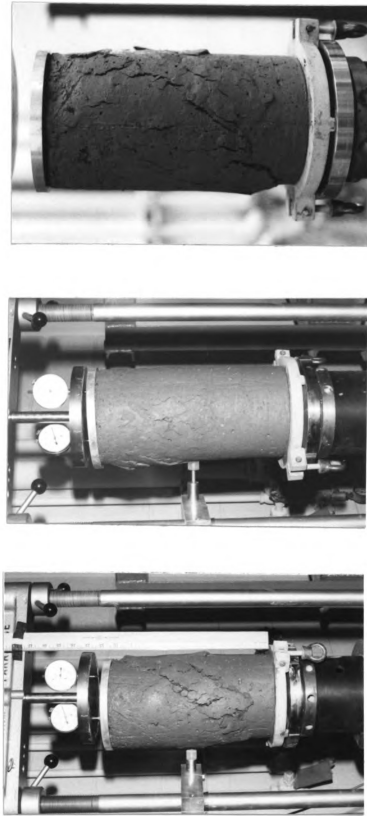
$$\tau = \sigma_1 \psi \frac{\nu}{1-\nu} \phi_\tau - \sigma_3 \psi \phi_\tau \quad (6.4)$$

where $\phi_\sigma = f(\nu, H/R, z/H, r/R)$

$\psi = f/f_{\max}$ (f = coefficient of friction).

The factor, ψ , gives the effect of roughness of the loading plate. In order for the stresses within the cylinder to be

$\sigma_z = \sigma_1$, $\sigma_r = \sigma_\theta = \sigma_3$, throughout, as is assumed in the triaxial test, ψ must equal zero. This would require an infinitely smooth



(a) shear failure

(b) tension failure

(c) combined shear and tension

Figure 6.4. Failure patterns for low slump concrete in uniaxial compression.

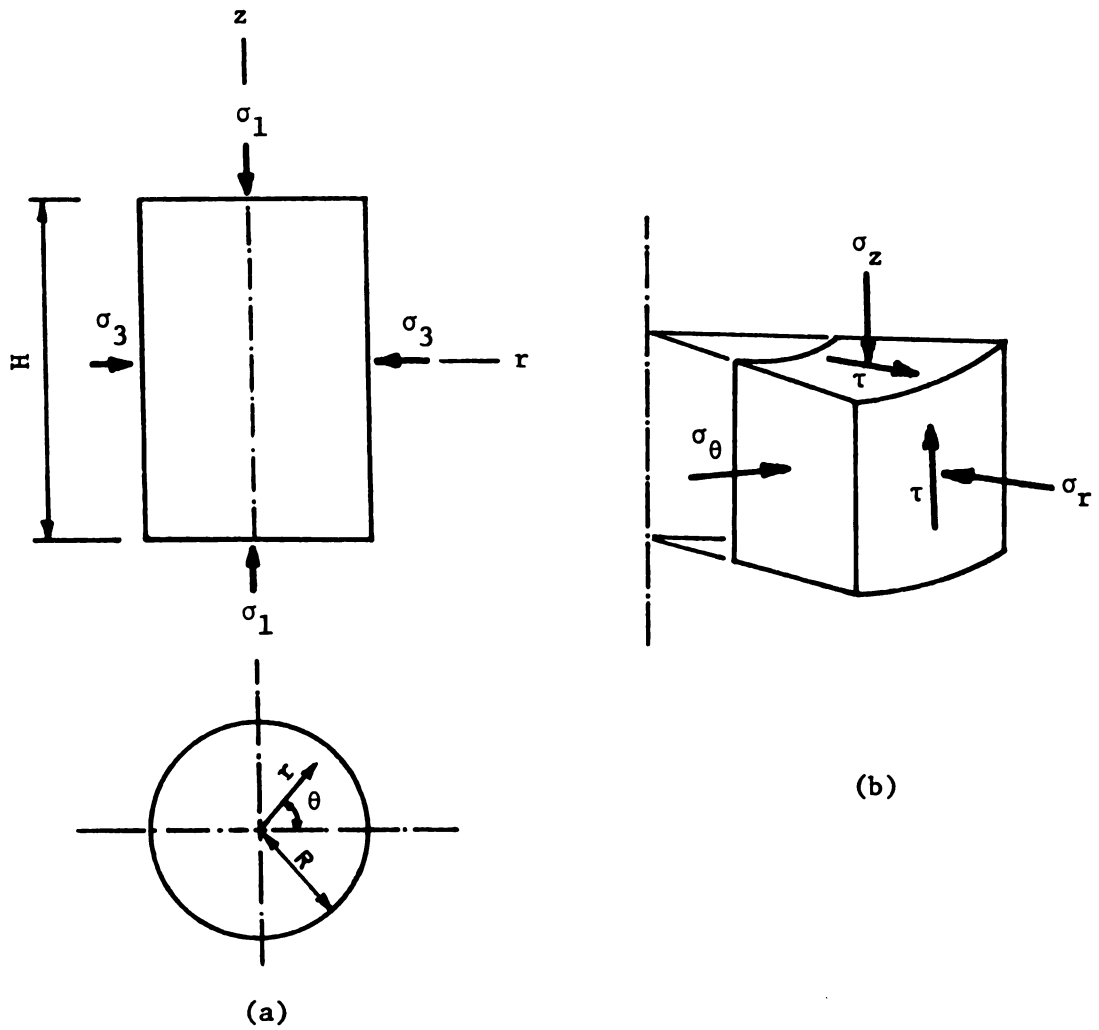


Figure 6.5. (a) Applied stresses in the triaxial test.
 (b) Stresses acting on an element of the loaded cylinder.

loading plate, which is highly impossible even with the use of paraffin or membrane as a lubricant between the sample and the plates. Fortunately, for the unconfined compression test ($\sigma_3 = 0$) the second term in the right hand side of each of the above equations drops to zero, therefore stress conditions for the smooth plate case are equivalent to a maximum roughness ($\psi = 1$) case. This is demonstrated in Table 5 of Balla's (1960) report.

The above discussion applies only to a height-diameter ratio equal to 2 as was illustrated in Balla's report. This ratio is the most commonly used for testing brittle materials under an unconfined condition. For a ratio below 1.5, the test results are seriously affected, as would be expected from a study of Figure 6.5 (Lambe, 1965). For too high a ratio, the sample under axial compression sometimes buckles elastically, exhibiting a behavior where more than one elastic state can exist, e.g., an unbuckled state and a buckled state, under the same external loads. This kind of condition actually produces an elastic stability problem that requires examination of the equilibrium equations in the deformed state (Malvern, 1969), and leads to non-linear equations. The samples used in this project were all 12 in. high and 6 in. in diameter giving a height/diameter ratio of 2.

Most of the low slump samples show a classical shear failure as illustrated in Figure 6.4(a). Fresh concrete is a mass of separate particles, hence it is compressed, the particles bear against each other and develop considerable resistance. When it fails, it flows or shears out from under the force. Since the resistance to failure

of the fresh concrete is due to both cohesion and internal friction, the angle of rupture is not 45 degrees (plane of maximum shear stress). This angle, θ , measured between the horizontal (the major principal plane) and the failure plane at the time of its formation, based on the Mohr-Coulomb theory of failure, is

$$\theta = 45^\circ + \frac{\phi}{2} . \quad (6.5)$$

The angle θ observed for the low slump concrete was between 55 and 60 degrees, which coincides very well with field observations (Goughnour, 1975). With these θ values, the angle of internal friction calculated by Equation 6.5 ranges from 20 to 30 degrees. It approaches the ϕ angle for the aggregate in the fresh concrete. This behavior suggests that a frictional mechanism determines the slope of the failure surface in fresh concrete.

Not all the samples failed in the manner of simple shear. Figure 6.4(b) shows a sample that failed by splitting, indicating failure in tension. This is not uncommon for an unconfined specimen which deforms axially under load with an increasing diameter. Assuming that ψ and σ_3 are zero, then so are σ_r and σ_θ , and $\sigma_z = \sigma_1 > 0$ according to Equations (6.1), (6.2), and (6.3). An element of the original cylinder increases in diameter as it moves outward. As a result, tensile stresses are formed which cause vertical cracks. Cylinders under a confining pressure, σ_3 , do not show this effect as much because the compressive forces, σ_r and σ_θ , offset the tensile forces.

Failure often occurs through a combination of shear and tension as indicated in Figure 6.4(c). This phenomenon may be caused by end restraint of bearing plates. Figure 6.6 shows the dead zones of two failed samples.

6.3 Strength Characteristics of the Fresh Concrete

Strength characteristics of the fresh concrete are discussed under two headings: stress-strain behavior, and mechanical properties. Factors affecting the mechanical properties will be emphasized under the second heading.

6.3.1 Stress-Strain Behavior

Typical stress-strain curves for compacted low slump fresh concrete are shown in Figure 2.7. From point 0 to A the stress and the strain are proportional, and can be expressed by Hooke's Law in terms of Young's modulus. Beyond A the deviation from Hooke's Law becomes marked; hence the stress at A is labeled the yield stress. Strain hardening starts at A and continues until the curve reaches B; the corresponding stress at B is called the ultimate strength of the material. Beyond point B, strain softening takes place rapidly and fracture occurs at a load corresponding to point D of the diagram. E_1 and E_2 are the elastic modulus and plastic modulus, respectively. Whereas the strains are linearly related to the stress by Hooke's Law in the elastic range, the relation will generally be nonlinear in the plastic range, as is evident from the unconfined compression stress-strain curve. For all the good samples, stresses in straight portions consist of 87 to 96 percent of the ultimate strength, which is shown in Table 5.6 as the σ_y/σ_u ratio.



Figure 6.6. Two examples showing the dead zone of failed samples.

Stress-strain curves are shown in Figures 5.1 through 5.8. It is seen from all these curves that strains at the yield stress range from 0.53 to 1.95 percent, whereas strains at the ultimate strength range from 0.65 to 2.23 percent. Failure was always followed by a drop in stresses after reaching the ultimate strength level for the low slump concrete. Therefore the material can be considered as a brittle material. An exception is Sample 4 with a high water-cement ratio which leads to extended plastic flow characteristics as shown by its stress-strain curve.

The ultimate strength or unconfined compressive strength ranged from 3.62 psi to 13.13 psi for all samples (Table 5.6) suitable for slipform construction. There were some samples that had an ultimate strength greater than 13.13 psi, but were difficult to work with, hence were considered unsuitable for field construction purposes. For comparison, unconfined compressive strengths in the range of 3.62 psi to 13.13 psi are equivalent to soft or very soft clays (Terzaghi and Peck, 1967).

6.3.2 Mix Properties and Mechanical Behavior

Mechanical properties were evaluated based on the factors affecting their strength and stiffness. Although 14 factors are listed in Section 2.2.4, only the first 11 were evaluated as to their effects on the unconfined compression test results. During each evaluation, only one of the factors was assigned as an independent variable while other factors were held constant. Table 5.5 summarizes the information for mix design and testing conditions, and Table 5.6 gives the corresponding mechanical properties. For discussion

purposes, these two tables have been regrouped below, according to each individual factor.

Effective Water-Cement Ratio. The influence of effective water-cement ratio, W_w/W_c , on the mechanical properties are shown in Figures 6.7 and 6.12. This is a composite drawing with abscissas as the magnitude of the influencing factor and ordinates as mechanical properties. Sample numbers are listed between the two abscissas. The same arrangements apply to Figure 6.8 through Figure 6.16.

With increasing water-cement ratio, the strength of the fresh concrete decreases. This can be seen from Figure 6.7 in which both the yield stress and the ultimate strength decrease with increasing water-cement ratio, as does the stiffness of the material, expressed as elastic modulus and plastic modulus. The reduction in strength and stiffness obviously is due to the dilution of the paste which reduces the cohesive forces in the fresh concrete. Dilution of the paste involves greater spacing of cement particles and a corresponding reduction in capillary and interparticle forces.

Coarse aggregates represented by Figure 6.7 consisted of round gravel while those represented by Figure 6.12 included crushed gravel. The same trend can be seen in these two figures. Ultimate strengths reached 12.17 psi for crushed gravel (Sample 21) and 11.69 psi for round gravel (Sample 25). Even with these high strengths, no difficulty was encountered in sample preparation. Both sample groups (round versus crushed gravel) required approximately 80 seconds of vibration time and the vibrator could be withdrawn without leaving a hole in the sample.

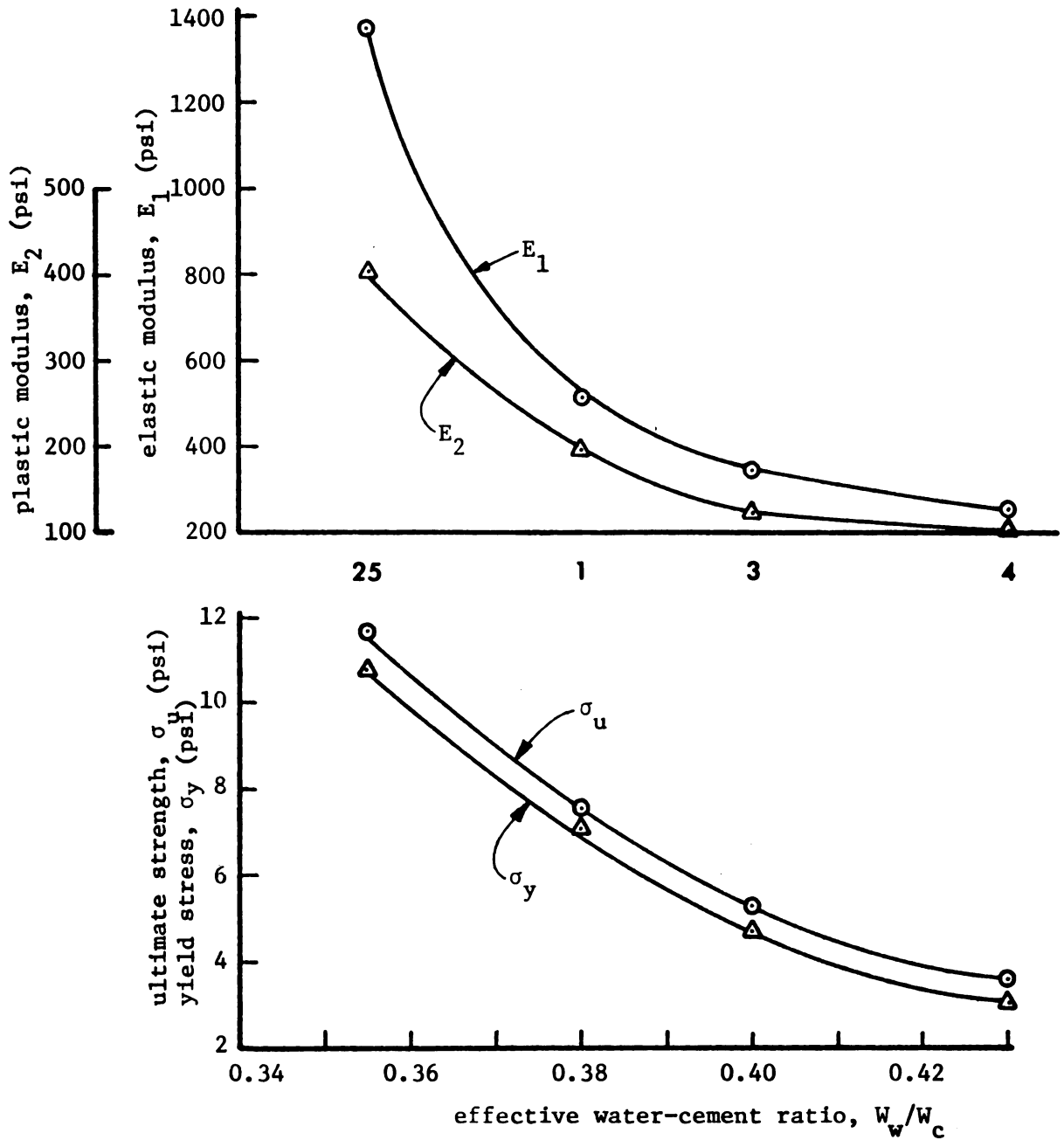


Figure 6.7. Influence of effective water-cement ratio on mechanical properties (round gravel).

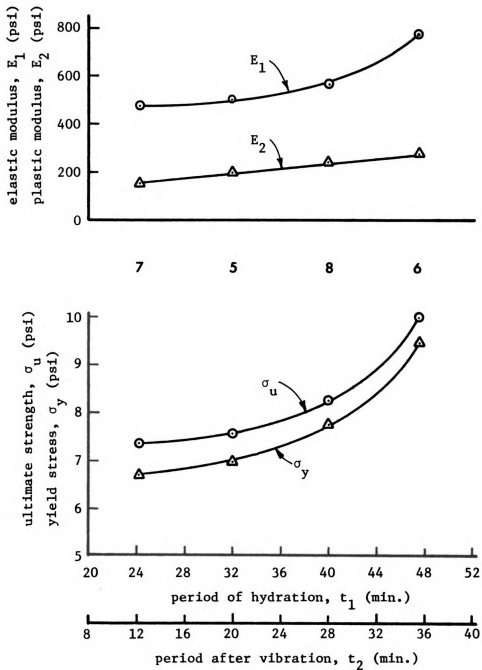


Figure 6.8. Influence of period of hydration(t_1) and period after vibration(t_2) on mechanical properties.

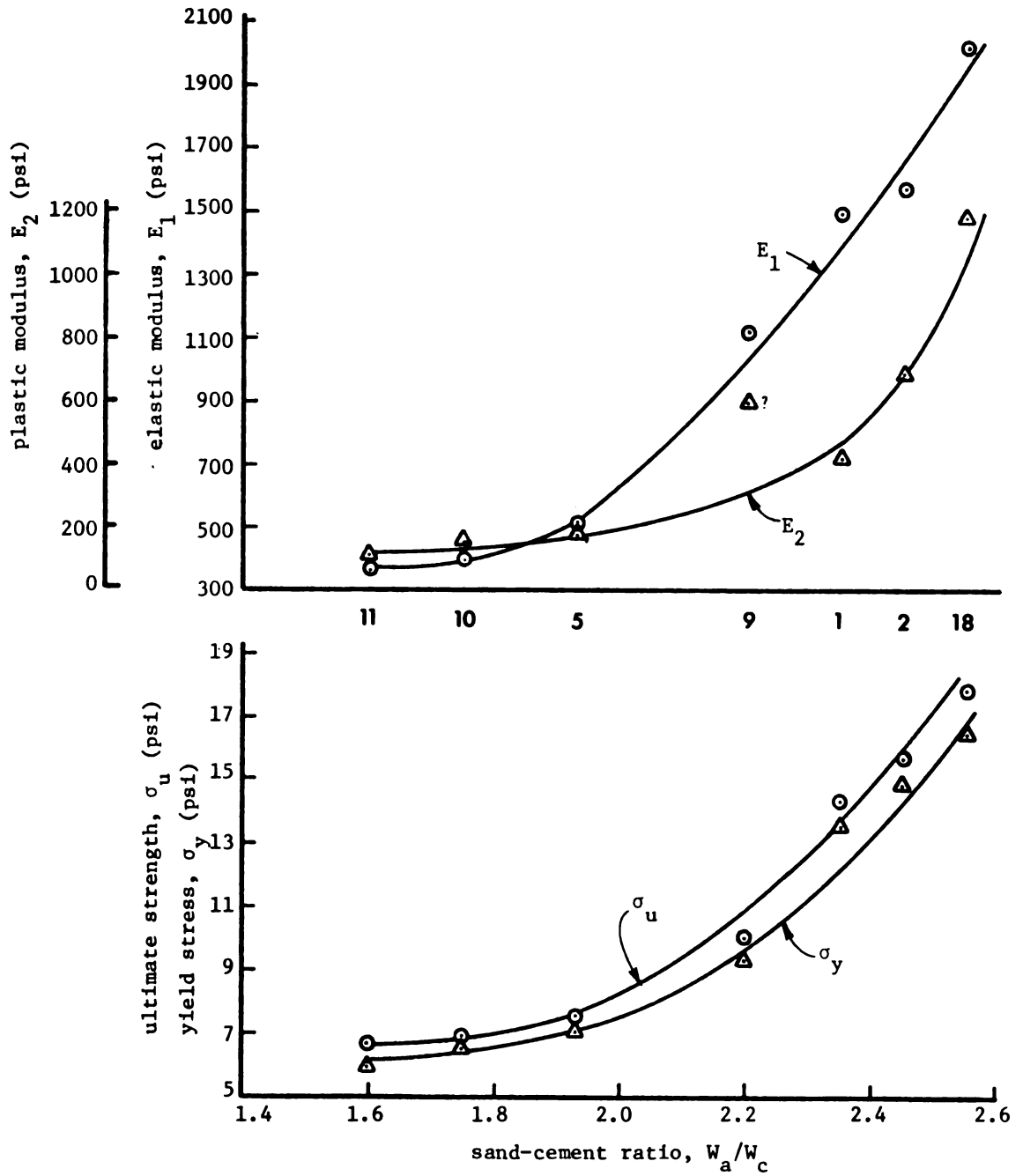


Figure 6.9. Influence of sand-cement ratio on mechanical properties.

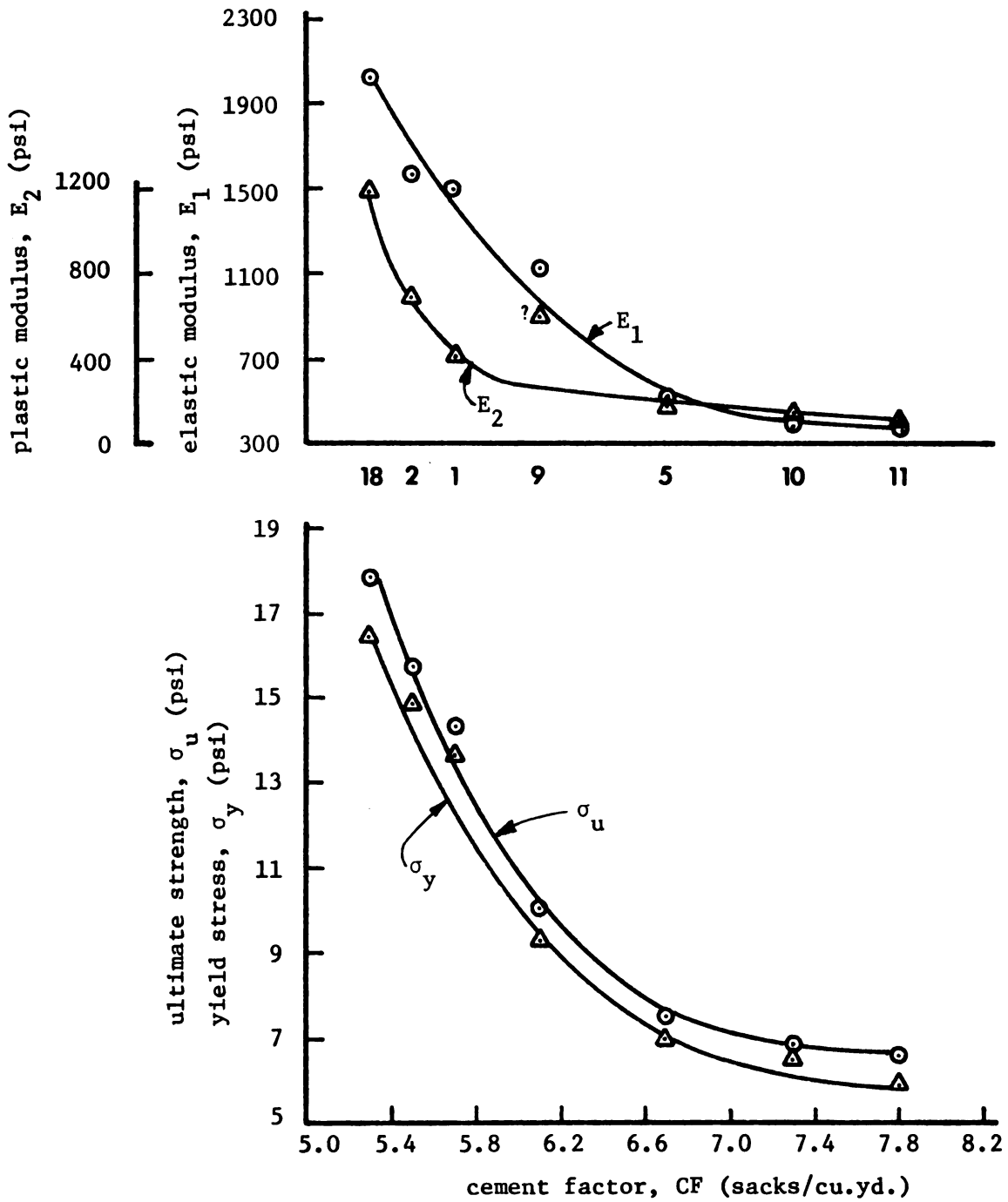


Figure 6.10. Influence of cement factor on mechanical properties.

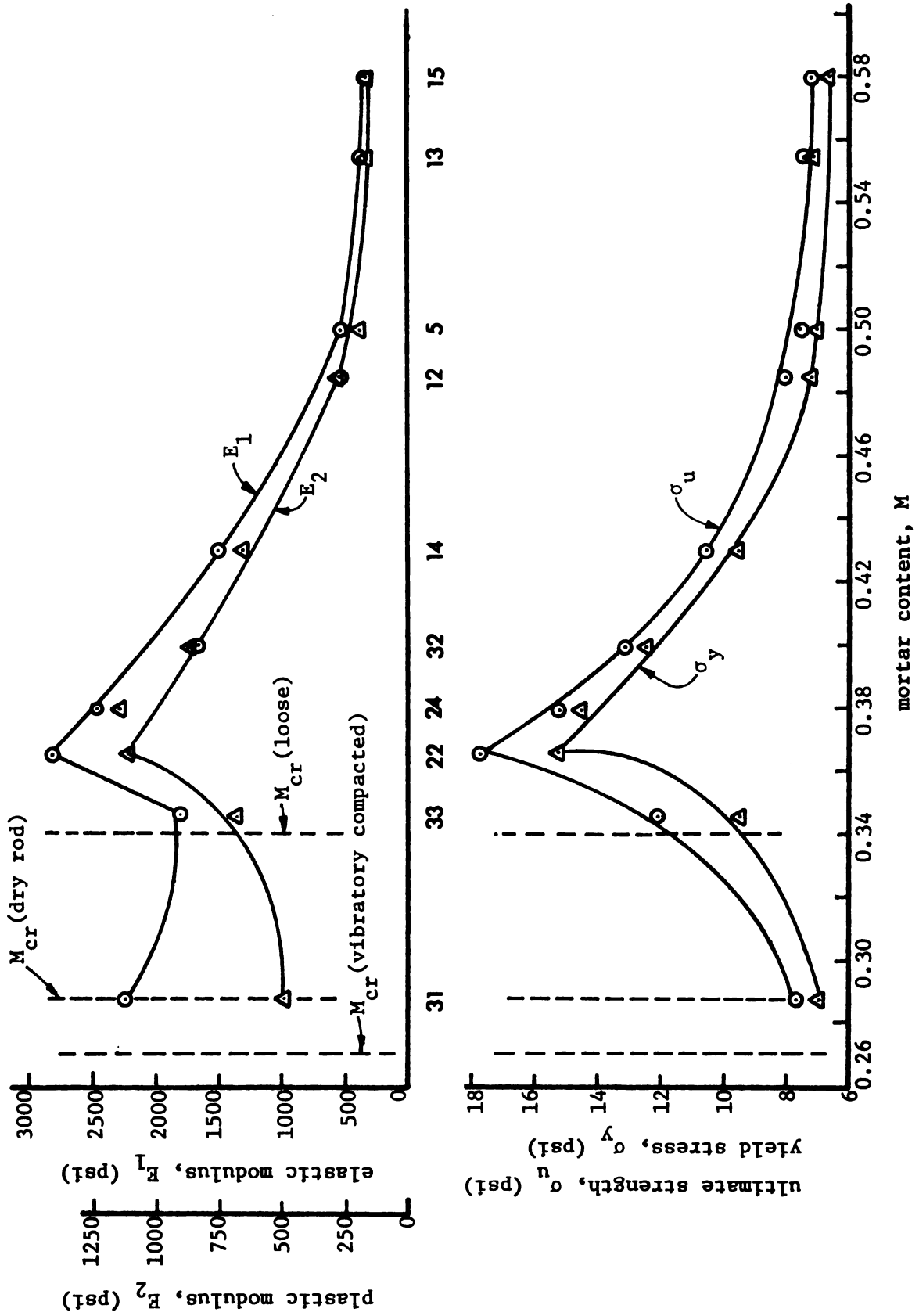


Figure 6.11. Influence of mortar content on mechanical properties.

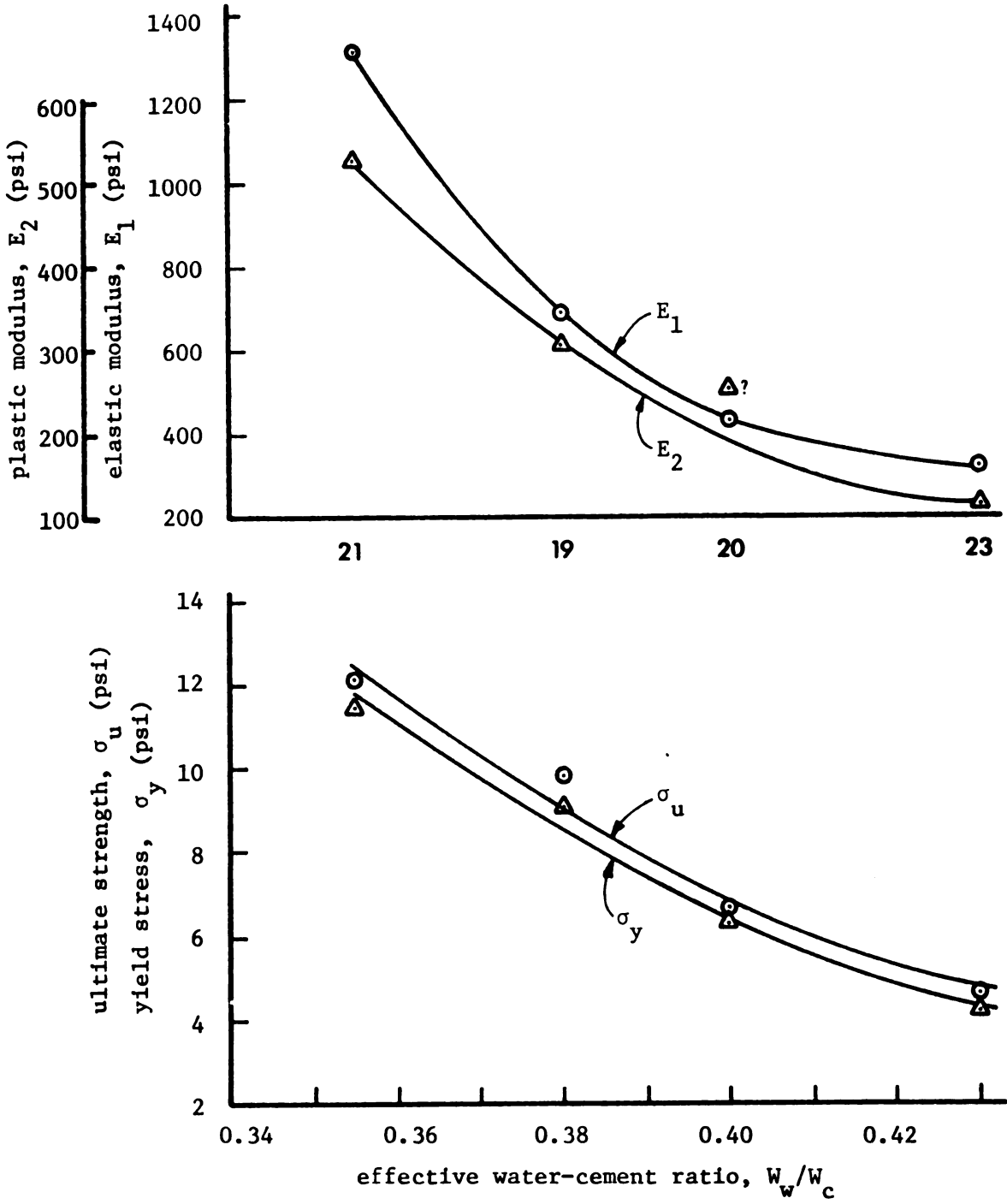


Figure 6.12. Influence of effective water-cement ratio on mechanical properties (crushed gravel).

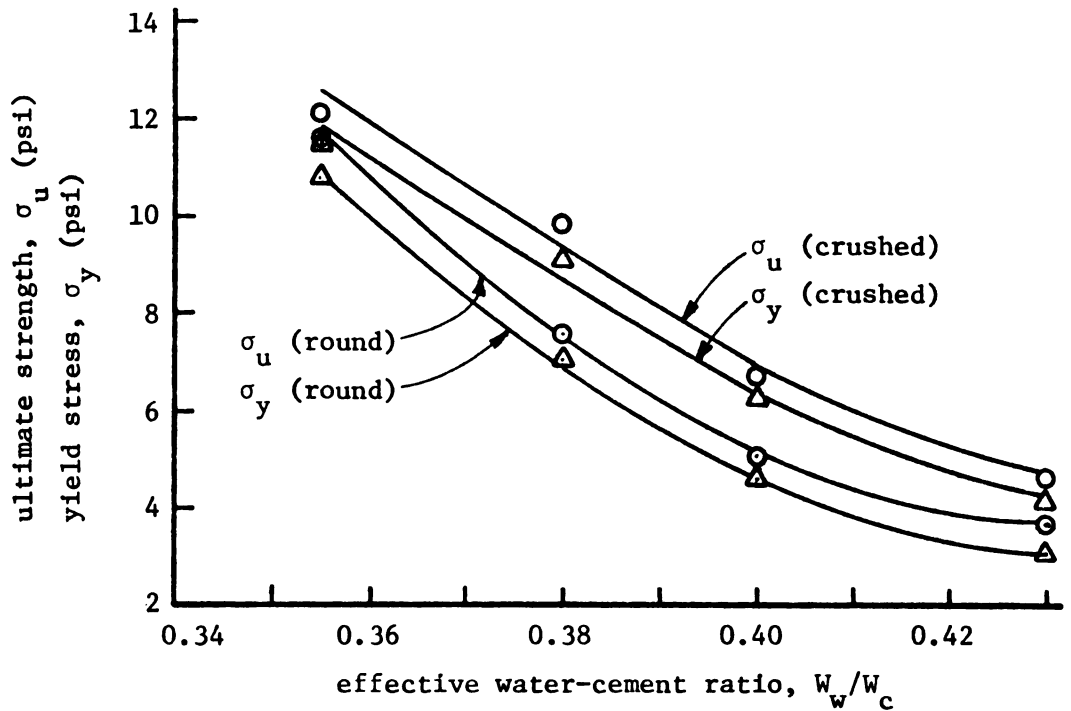
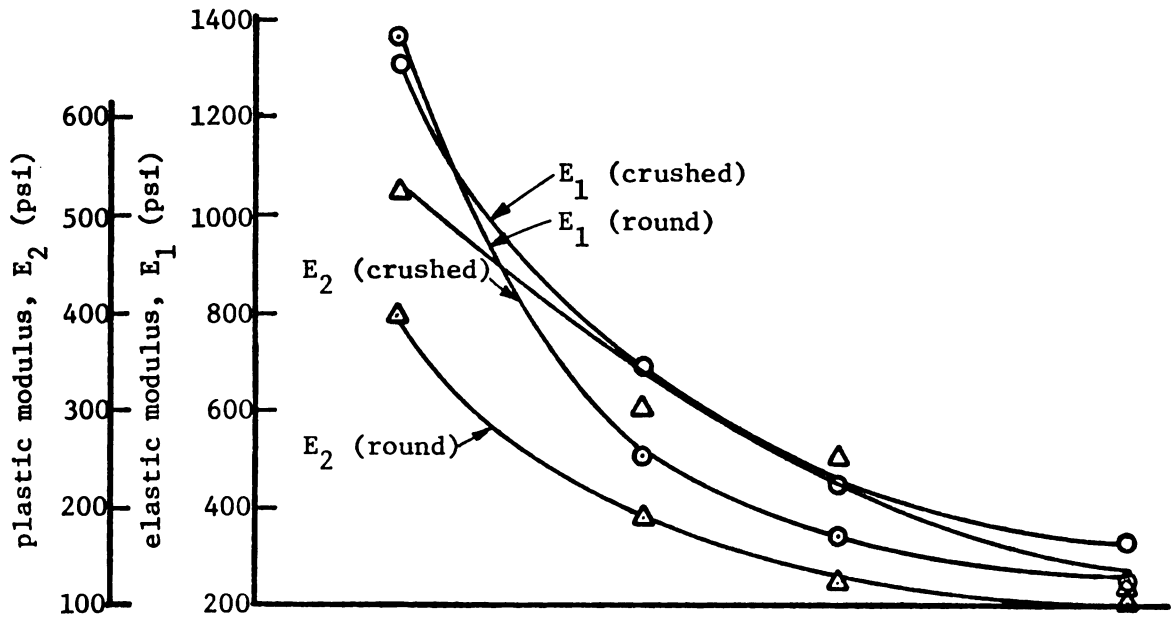


Figure 6.13. Influence of the shape of the coarse aggregate on mechanical properties.

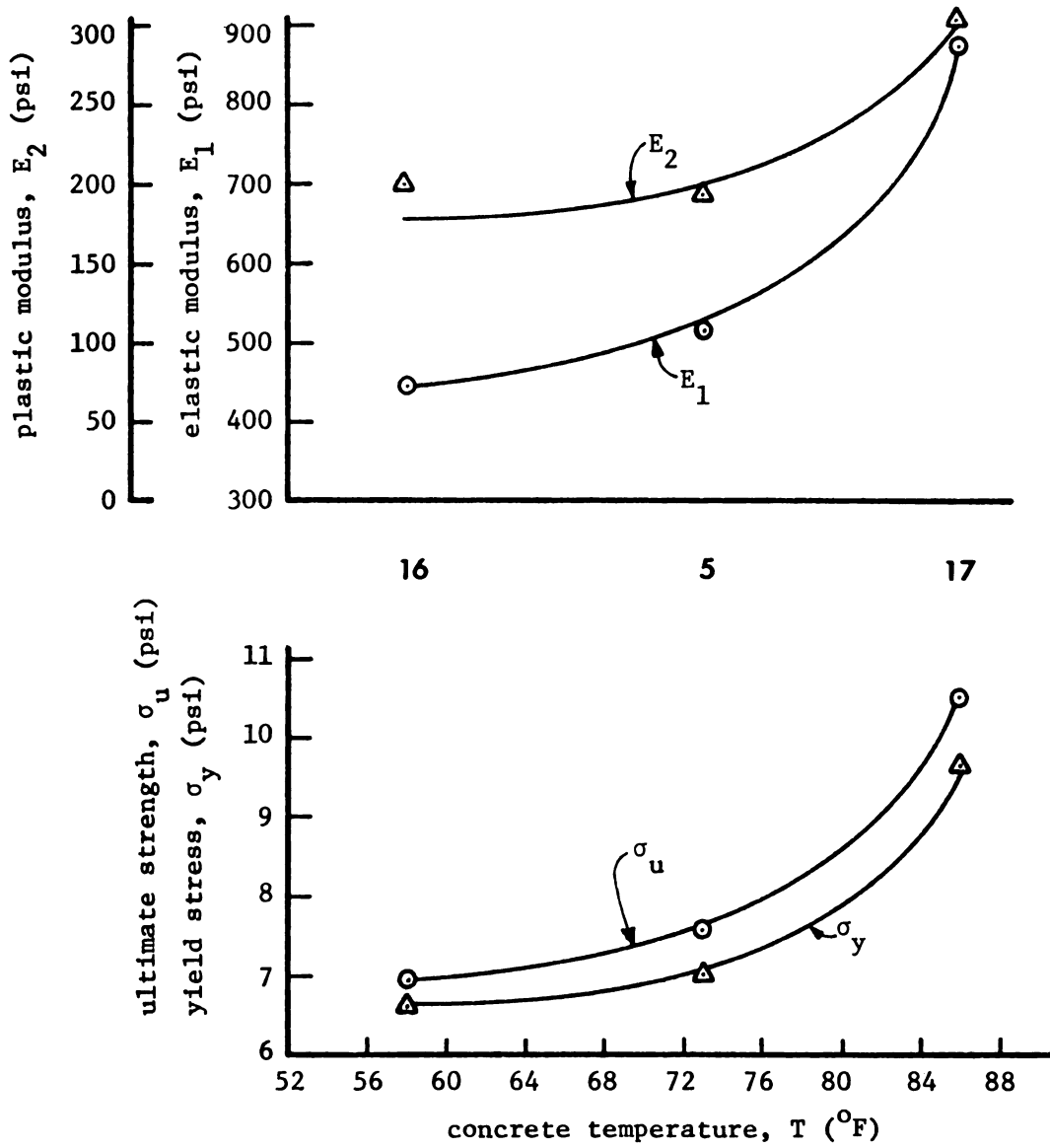


Figure 6.14. Influence of concrete temperature on mechanical properties.

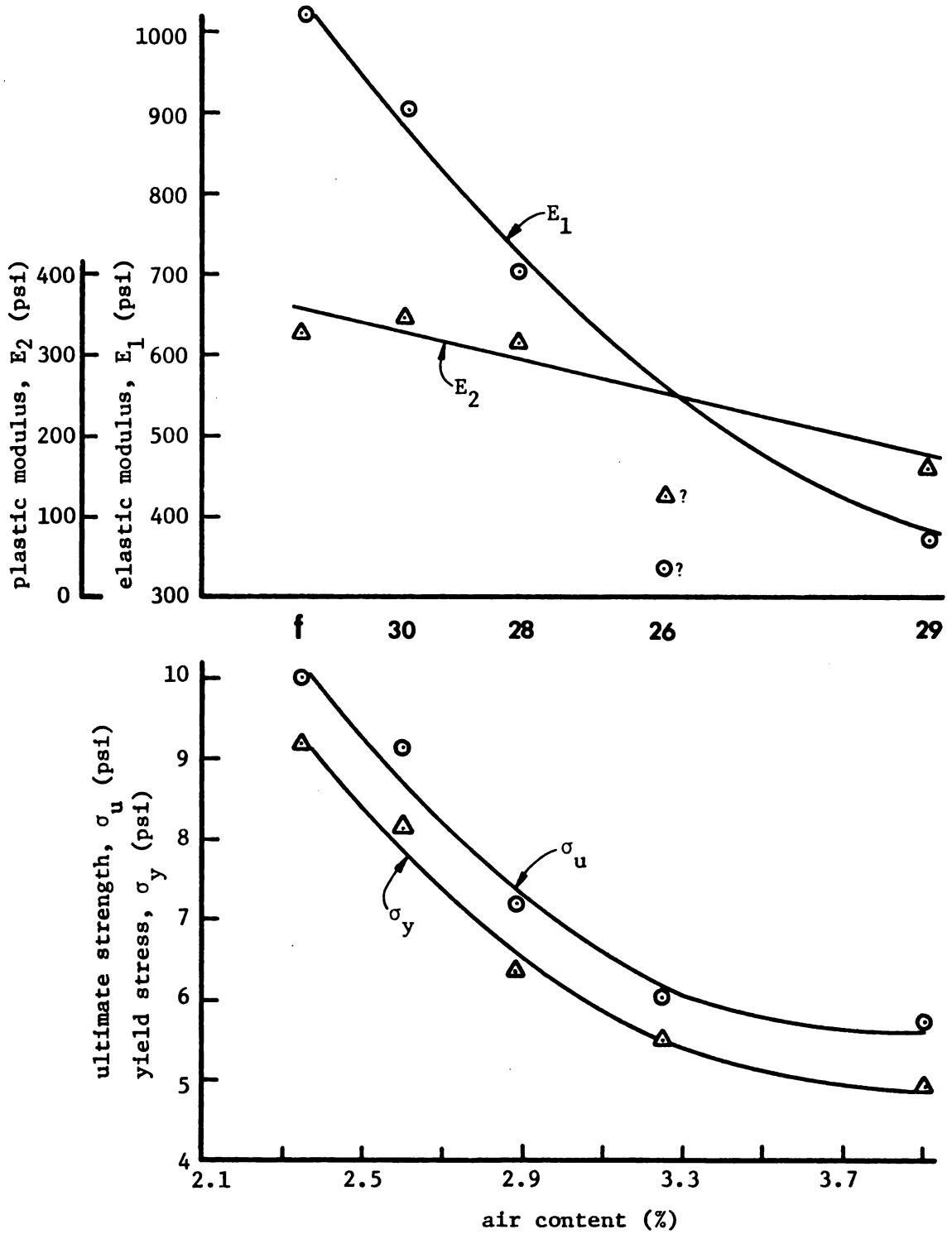


Figure 6.15. Influence of air content on mechanical properties.

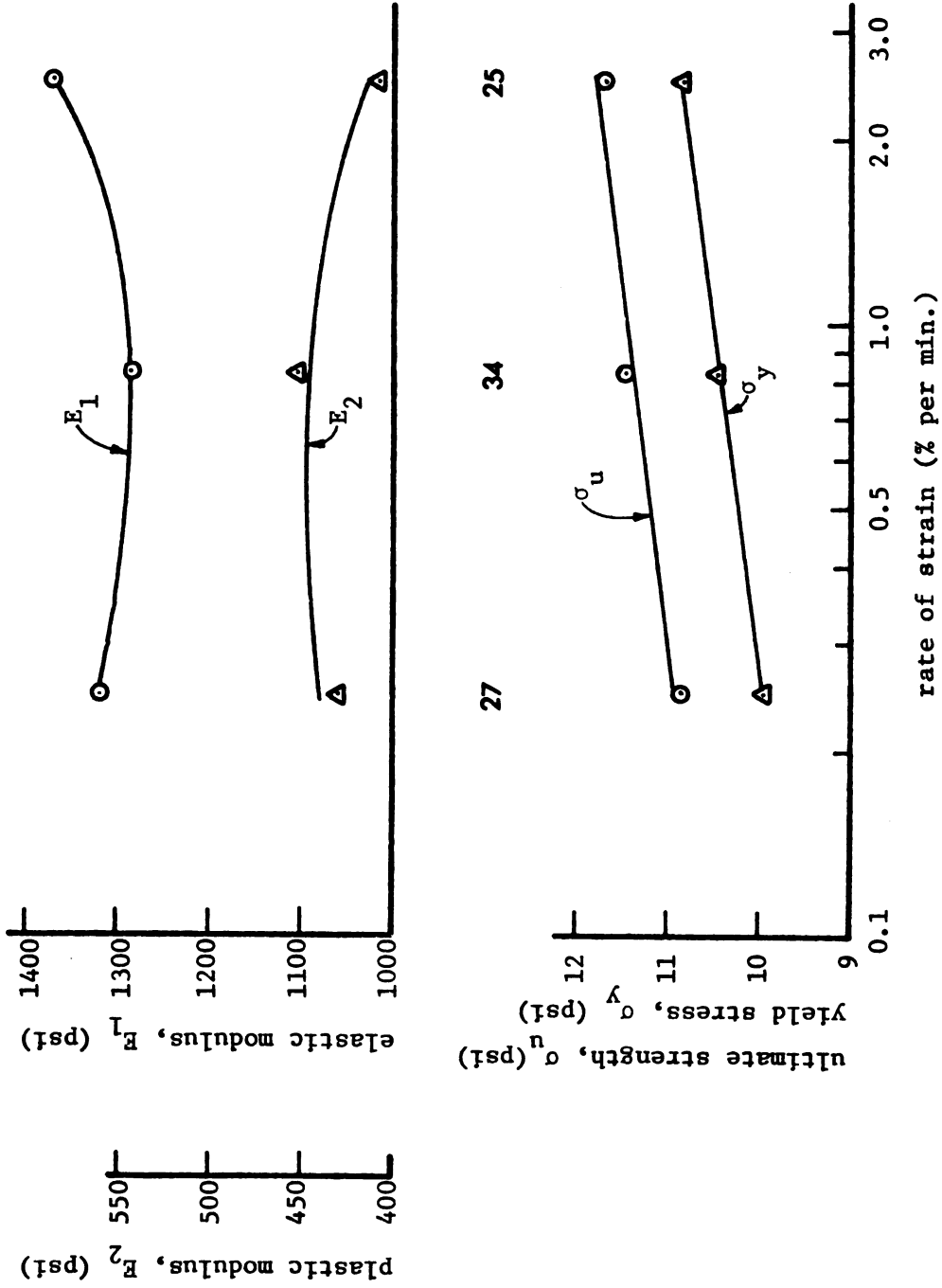


Figure 6.16. Influence of rate of strain on mechanical properties.

Period of Hydration. The period of hydration after mixing, t_1 , influences the mechanical properties as shown in Figure 6.8. In the field this period would be limited to 60 minutes according to 1976 MDSHT Specifications. In this project, t_1 ranged from 24.5 to 47.5 minutes. As predicted, the strength and stiffness increased with increased periods of hydration. Sample 7 with a period of hydration of 24.5 minutes gave an ultimate strength of 7.35 psi. The strength increased to 9.98 psi when the period of hydration was increased to 47.5 minutes for Sample 6 -- a 36 percent increase in 23 minutes. These data show that a mix design of less strength can be strengthened by prolonging the period of hydration. For slipform construction the smaller initial strength will control the size and shape of the section to be constructed.

Period After Vibration. Since the structure of fresh concrete is believed to be more stable after vibration has been completed, this factor has also been illustrated in Figure 6.8. The same data used for t_1 is used for t_2 . The data presented in this figure shows that the ultimate strength of 7.35 psi for Sample 7 increased to 9.98 for Sample 6 with an accompanying increase in t_2 from 12 minutes to 34.5 minutes. The increase in t_2 was approximately 300 percent whereas the increase in t_1 was about 200 percent (24.5 minutes to 47.5 minutes) for the same sample. This comparison demonstrates the build-up in strength due to the period of hydration. However, it is also recognized that vibration can mix the sample more thoroughly and thus accelerate the hydration.

Cement Content. With a constant water-cement ratio, strength and stiffness increased with increasing sand-cement ratios. Figure 6.9 illustrates this behavior. Samples 5, 9, 10, and 11 show an increase of ultimate strength from 6.65 psi to 10.04 psi with accompanying increases in sand-cement ratios from 1.6 to 2.2. All four samples were easy to prepare with Sample 9 having the longest vibration time of 90 seconds. Although Samples 1, 2, and 18 provide higher strength and stiffness, they also have low workability. Vibration time for these three samples were 170, 210, and 250 seconds, respectively. The higher values of sand-cement ratio resulted in a harsh concrete mix.

The sand-cement ratio can also be converted into cement factor for the concrete to evaluate its influence on mechanical properties. Equation (2.11) was used for this purpose. For the same samples used in Figure 6.9, the relationship between cement factors and the mechanical properties are shown in Figure 6.10. This figure demonstrates that, for a constant water-cement ratio by weight equal to 0.38, both the strength and the stiffness increased when the cement factor was decreased. However, if the water content was kept unchanged and only the cement factor was decreased a higher water-cement ratio results, and both the stiffness and the strength will decrease accordingly.

The importance of Figure 6.10 is that it provides information on how cement factor will affect the strength of the fresh concrete. Cement is the most costly ingredient in the concrete.

Mortar Content. The influence of mortar content M on the mechanical properties is shown in Figure 6.11. Mortar contents were calculated

by either Equation (2.12) or (2.13) with both sand-cement ratio and water-cement ratio held constant. Both strength and stiffness increased with decreasing mortar content until M approached about 0.366 for Sample 22. For smaller mortar contents the trend was reversed with strength and stiffness both decreasing.

Theoretically, the maximum strength or stiffness should develop when the volume of mortar equals the volume of voids of the coarse aggregate. The mortar content, so determined, was defined as the critical mortar content, M_{cr} , in Section 2.2.4. The calculated M_{cr} , based on void contents of dry rod state, dry loose state and dry vibrated state, are included in Appendix C for all samples shown in Figure 6.11. It is observed from Figure 6.11 that the maximum strength or stiffness develops at a mortar content higher than any of the above M_{cr} . This occurs because extra mortar, above the critical mortar content, is required to provide workability. Note that Samples 31 and 33 had unit weights of 140.4 pcf and 151.8 pcf, respectively, which indicates that even with prolonged vibration (170 seconds and 140 seconds) the samples contained a large volume of voids. Figure 6.17 shows the honeycomb structure of Sample 31.

Ultimate strength increased from 7.2 psi for Sample 15 to a maximum of 17.76 psi for Sample 22. However, both Sample 22 and Sample 24 required extra manipulation by vibration and therefore cannot be considered as a mix of suitable workability for slipform construction.

According to Equation (2.13) a low sand-gravel ratio, W_a/W_b , would result in a low mortar content. Excluding the two honeycombed

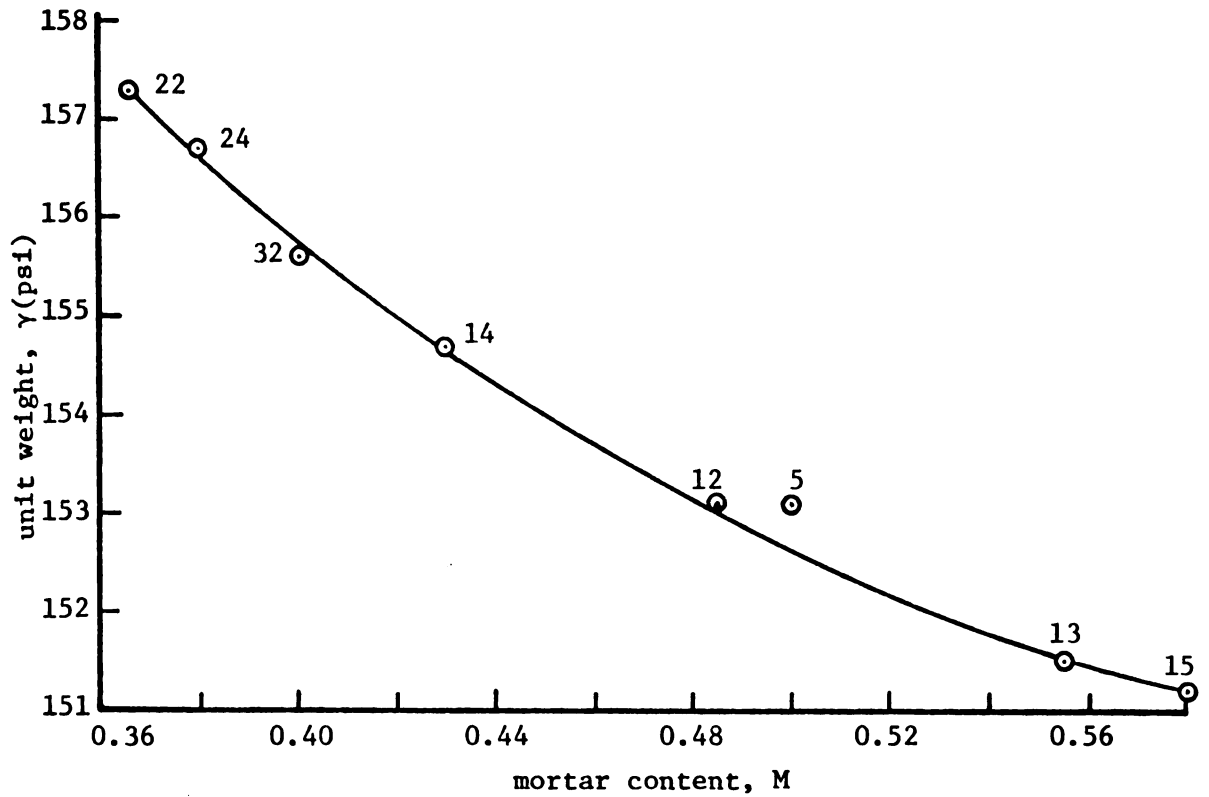


Figure 6.17. The honeycomb structure of Sample 31 for an extremely low mortar content.

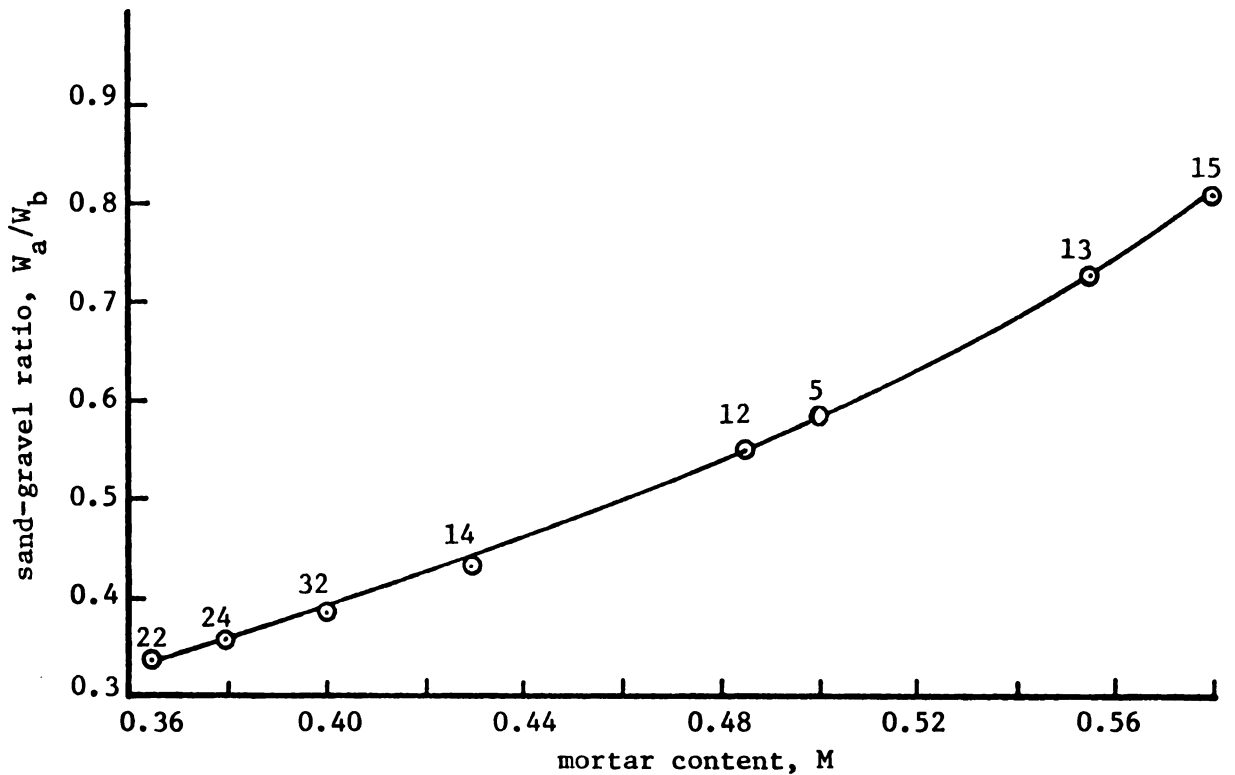
Samples 31 and 33, this relationship has been plotted in Figure 6.18. This same figure also includes the relationship between mortar content and the unit weight of the fresh concrete. It is seen that the unit weight decreases with an increase in mortar content. Since other mix design factors were held constant, this decrease in unit weight relates to the fact that mortar is lighter than the coarse aggregate used in this project. In a region where light porous volcanic rocks are used for coarse aggregate, this trend could be reversed.

Particle Shape. Crushed gravel interlocks better during shear and therefore exhibits higher strength and stiffness than round gravel. Figures 6.7 and 6.12 include the effects of round versus crushed gravel on the mechanical properties of the fresh concrete. For comparison, the two figures have been combined in Figure 6.13. It is observed that both stiffness and strength for crushed gravel samples are higher than that for round gravel samples. Only at a water-cement ratio of 0.355, does the elastic modulus of the round gravel sample exceed that of the crushed gravel sample by a small margin (1,317 psi against 1,373 psi). This deviation appears to have been caused by either a seating error or the variation in homogeneity of the material.

Concrete Temperature. Temperature alters the mechanical properties of the fresh concrete as shown in Figure 6.14. Sample temperatures were measured as described in Section 4.3. The temperature so determined was different from that computed by Equation (2.14) in that for small batch quantities changes occur during mixing due to ambient temperatures.



(a) Relationship between mortar content and unit weight of fresh concrete.



(b) Relationship between mortar content and sand-gravel ratio

Figure 6.18. Characteristics of mortar content.

Both stiffness and strength increase with increasing temperature. However, the rate of increase is far from uniform. Sample 16 with a temperature of 58°F gave E_1 equal to 446 psi and σ_u equal to 6.99 psi whereas Sample 5 with a temperature of 73°F gave E_1 equal to 516 psi and σ_u equal to 7.57 psi. The increases were 15.7 percent for E_1 and 8.3 percent for σ_u with a temperature difference of 15°F. When the temperature rose to 86°F for Sample 17, the measured E_1 and σ_u values increased to 873 psi and 10.51 psi, respectively. This is a 95.7 percent increase for E_1 and 38.8 percent increase for σ_u as compared to Sample 5 over a range of 13°F. This same phenomenon occurs in field construction where Goughnour (1975) observed that the strength of fresh concrete exhibited only a small change at lower temperature ranges but increased drastically at higher temperature ranges (85°F to 90°F). This behavior, relative to higher temperatures, raises the question as to whether advantage can be taken of the increased E_1 and σ_u values for horizontal slip-form construction. This could be an interesting area for future research.

Air Content. The air content of the mortar was measured by the concrete air indicator (Portland Cement Association, 1965). With no air-entraining agent added, the mortar contained 2.35 percent of air, slightly higher than might be expected from Type I General Portland cement. It is believed that this figure should be close to 2 percent with air entrapped during rodding compaction responsible for the slightly higher figure. If there is an error, all samples, either air-entrained or non-air-entrained, should have about the same order of error and this error appears to be small. Hence no corrections were made in measurement.

Four air-entrained samples, Samples 26, 28, 29, and 30, were used to develop Figure 6.15 showing the influence of air content on the mechanical properties. All samples have the same mix design as used in Figure 6.7 except that the water-cement ratio was fixed at 0.362. Therefore mechanical properties for a non-air-entrained sample with a $W_w/W_c = 0.362$ were read from Figure 6.7 and labeled in Figure 6.15 as Sample "f."

It is seen from Figure 6.15 that both stiffness and strength of the fresh concrete decrease with an increase in air content. The ultimate strength decreased from 10 psi for an air content of 2.35 percent to 5.73 psi for an air content of 3.9 percent. For ordinary slipform construction requirements the air content is specified between 4 and 6 percent, therefore additional strength reduction would be anticipated. Since the reduction in strength was almost 43 percent (10 psi to 5.73 psi) when comparing non-air-entrainment to 4 percent air content, a specific discussion on the air content requirements has been included in Section 6.4.

Aggregate Gradation. As shown in Equation (2.13) and Figure 6.18, the mortar content M is a function of the sand-gravel ratio W_a/W_b . A higher W_a/W_b ratio results in a higher M and hence weaker fresh concrete samples. With all other mix proportions and test conditions held constant, the W_a/W_b ratio can be plotted into gradation curves as shown in Figure 4.2. Neglecting the two honeycombed samples, 31 and 33, the lower gradation curves in Figure 4.2 give fresh concrete samples greater stiffness and higher strength as shown in Figure 6.11. The greater proportion of coarse aggregate in these stronger samples

corresponds to a lower W_a/W_b ratio. Therefore the variation in strength and stiffness is proportional to the degree of deviation of the gradation curve from the ideal diagonal line. However, the deviation cannot be quantitatively correlated to strength or stiffness since fineness modulus is not single-valued as explained in Section 2.2.4.

Rate of Strain. Three samples with rates of strain of 0.25, 0.833, and 2.5 percent per minute were used to evaluate the influence of rate of strain on mechanical properties. Figure 6.16 indicates a fairly definite relationship between the rate of strain and the strength of the fresh concrete. An increase in rate of strain is accompanied by an increase in strength approximately proportional to the logarithm of the rate of strain. The logarithmic relation appears to be incidental and not based on any fundamental law. The same relationship has also been reported for hardened concrete (Jones and Richart, 1936), in which rate of load application was logarithmically related to strength by the following equation

$$S = S_1 (1 + k \log R) \quad (6.6)$$

where S = strength at a given rate of loading R psi per second,

S_1 = strength at a loading rate of 1 psi per second,

k = a constant, about 0.08 for 28 day tests.

An equation of the same nature for fresh concrete could also be established. However, in view of the limited test results, it seems inappropriate to attempt further generalization of such an equation for this project.

Figure 6.16 also shows that the elastic moduli between the 0.25 percent and the 0.833 percent rate of strain samples were very similar, and when the rate of strain is increased to 2.5 percent for Sample 25, there appears to be a distinct increase in elastic modulus, which indicates that a part of the measured strain in the tests is due to creep or plastic deformation. The amount of creep increased with the length of time involved in the test whereas the amount of plastic deformation decreases as the rate of strain increases. The plastic modulus in Figure 6.16 cannot be correlated to the rate of strain.

Vibration Effort. Although the effect of vibration in field construction cannot be simulated in the laboratory, complete compaction appears to have been achieved for each sample. Complete compaction is achieved when the surface of the sample has become relatively smooth or when the mortar just begins to flush to the surface adjacent to the vibrator. The judgment is purely subjective.

Figure 6.19 is a best fit by eye plot of the vibration period needed to assure a complete compaction versus the ultimate strength of each sample. Numerical numbers are sample numbers. The samples are too scattered to define any kind of definite relationship, but two conclusions can be drawn from this figure.

- 1) An increase in vibration period was accompanied by an increase in ultimate strength. Similar trends can also be applied to the stiffness, which indicates that more vibration effort would be required for a stronger sample.

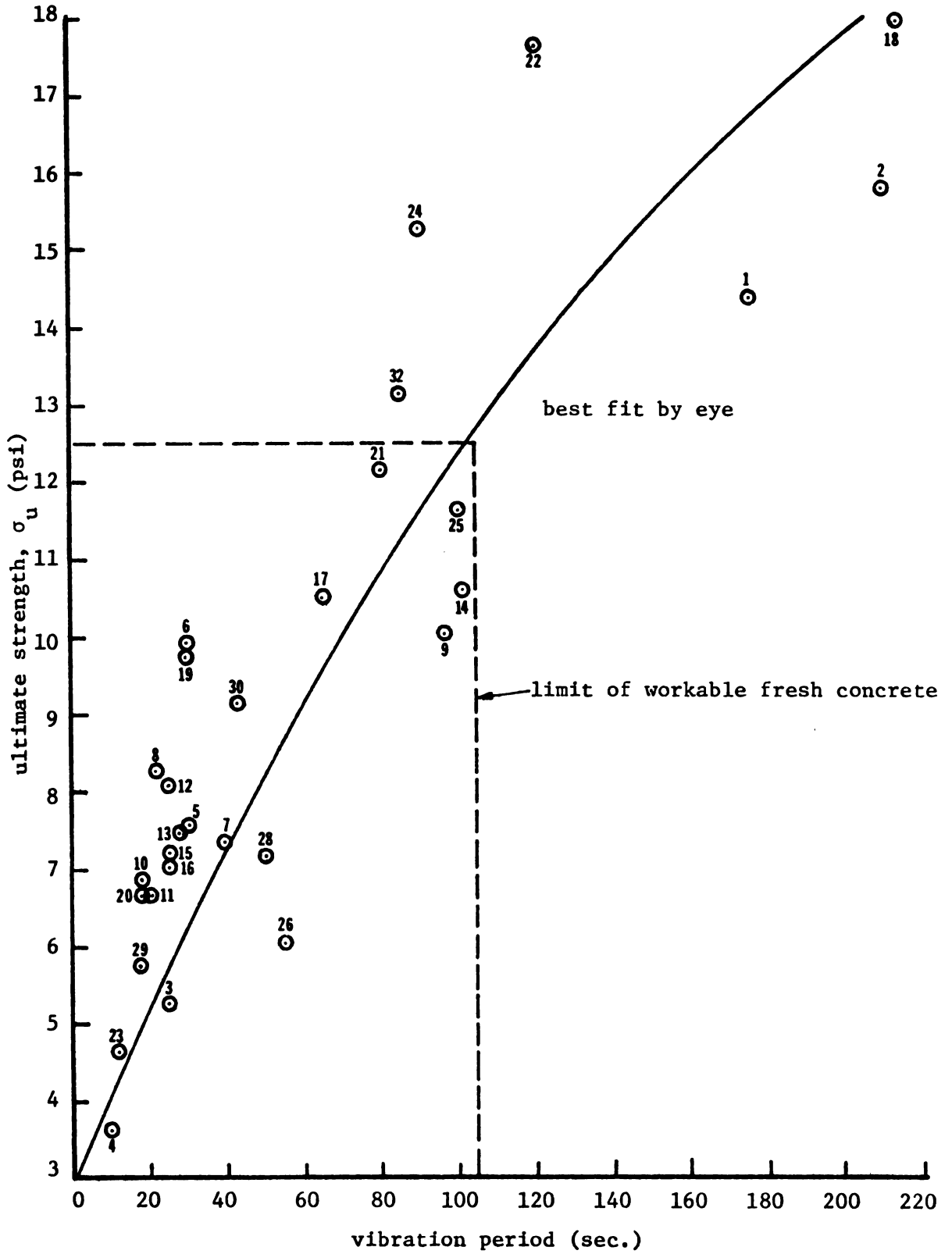


Figure 6.19. Vibration effort and ultimate strength relationship.

2) An examination of the data in Figure 6.19 indicated that samples with σ_u up to 12.5 psi or a vibration period up to 105 seconds gave a workable fresh concrete (framed in at the lower left corner). Of course, to define limits of high workability is purely subjective and may not quantitatively simulate field construction.

6.4 Air Content Requirements

Excess water, more than required for hydration, is always added to a concrete mix to obtain workability. As hydration proceeds, the absolute volume of the cement and water gradually decreases to make it impossible for a cement paste of any water-cement ratio to continue to occupy completely the space originally required by the fresh paste. Furthermore, some air is always entrapped in the mass during mixing. Consequently, the hardened paste develops some interconnected air voids or channels which absorb water either by capillary action or by seepage under pressure.

The volume of pore space in a cement paste depends on the amount of water mixed with the cement. When the paste sets, it acquires a stable volume that is approximately equal to the volume of the cement plus the volume of water. Therefore, the paste with a high water-cement ratio will have greater volume after setting. Since the amount of solid material, the hydration product, is directly proportional to the amount of cement added, it was concluded that higher water-cement ratios will produce more pores in hardened paste (Cordon, 1966).

The deterioration of concrete exposed to freezing and thawing is caused by expansion of freezing water in the void system of

the cement paste or the concrete aggregate. The deterioration may be in the form of scaling, spalling or D-line cracking (Cordon, 1966).

One method to prevent this freezing deterioration is to entrain disconnected small air bubbles into the concrete while it is in a fresh state. These bubbles, having diameters of 0.001 to 0.02 in., provide void spaces which tend to relieve any forces which are developed by the formation of the ice and thus prevent disintegration of the concrete. The air content requirement in the northern states, where severe cold weather usually is encountered, varies from 3 to 6 percent, although one study (Gonnerman, 1944) indicated that concretes containing only about 3 percent of air showed about as good resistance as those with more air.

The lower water-cement ratio has a beneficial effect upon strength and durability of the concrete in that less excess water is present to produce passageways through the cement paste, thereby reducing permeability. In general, other conditions being the same, low permeability is associated with high strength and high resistance to weathering. A study of the effect of water-cement ratio upon permeability (Ruettggers et al., 1935 and 1936) indicated that for a mix with 1-1/2 in. maximum aggregate size, the coefficient of permeability dropped to a minimum of 5×10^{-12} ft/sec at a water-cement ratio of 0.5 (see Figure 6.20). Slipform construction usually requires a water-cement ratio less than 0.5, hence adequate curing is always provided. Above that, rigorous vibratory compaction is usually required which results in uniformity of concrete and prevents leakage (Troxell et al., 1968). Experience has shown that

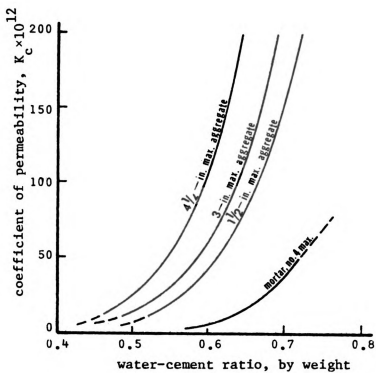


Figure 6.20 Effect of water-cement ratio upon permeability. (From Ruettgers, et al.)

low slump concrete used in slipform construction is weather-resistant and that no air-entrainment is needed.

Freezing and thawing tests were run on non-air-entrained, low water-cement ratio ($W_w/W_c = 0.4$) mortar panels by Isberner (1963). After 130 cycles of 0°F and 73°F freezing and thawing in the air, all 12 panels showed no deterioration of the concrete facing, which indicates satisfactory performance of these concretes. Subsequent freezing and thawing tests under water for another 350 cycles showed the deterioration of the concrete facing which was non-air-entrained whereas the air-entrained concrete mortar showed no deterioration. However, freezing and thawing in water is considered to be a very severe exposure condition and may be an unrealistic exposure condition for many concrete structures.

For a constant consistency, such as measured by the slump test, Cordon (1946) found that if the water-cement ratio is held constant while the air content is increased, the water content must be diminished in inverse proportion to the increase of air content. In practice concrete contractors often encounter the problem of achieving a required air content while maintaining a mix design of given workability. In addition, entrained air drastically reduces the strength and stiffness of fresh concrete (see Figure 6.15) which will limit the feasibility of the slipform construction method.

In view of the above factors, it appears that the requirement for a specified air content in slipform construction may not be needed on many projects.

6.5 Stresses in the Experimental Section

The field constructed experimental section described in Section 4.2 has been analyzed by the finite element method. In order to map the failure zones, the undrained shear strength of the concrete mix used for the construction had to be determined. It was assumed that failure zones develop in those regions where the maximum shear stress values exceed the undrained shear strength of the fresh concrete.

6.5.1 Undrained Shear Strength

According to Equation (2.19), the undrained shear strength equals one-half of the ultimate strength of the fresh concrete. The ultimate strength of the concrete used for the experimental section was obtained using field proportions and extrapolating from the curves shown in Figure 6.7 and 6.15.

Table 6.1 gives a comparison of the mix design for the test samples summarized in Figure 6.15 and the field proportions for the experimental section.

Table 6.1. Comparison of the Mix Design and the Field Proportions

| Condition | Figure 6.15 Test Samples | Field Experimental Section |
|-----------|-----------------------------|-------------------------------|
| W_w/W_c | 0.362 | 0.374 |
| W_a/W_c | 1.934 | 2.0 |
| M | 0.5 | 0.494 |
| t_1 | 32 minutes | 25 minutes |

It is noted from this table and Figures 6.7, 6.8, 6.9 and 6.11 that except for W_w/W_c , the other conditions are comparable. With reference to Figures 6.8, 6.9, and 6.11, the two sets of data should yield approximately the same strength and stiffness provided the water-cement ratio was a constant.

Extrapolation of the curves shown in Figure 6.15 provides the mechanical properties for the 4 percent air content as:

$$\sigma_u = 5.5 \text{ psi,}$$

$$\sigma_y = 4.75 \text{ psi,}$$

$$E_1 = 370 \text{ psi,}$$

$$E_2 = 163 \text{ psi .}$$

For the experimental section, these values were converted into equivalent values based on the ratios from Figure 6.7 ($W_w/W_c = 0.374$ and 0.362).

$$\sigma_u = 5.5 \text{ psi} \times \left(\frac{\sigma_u \text{ @ } W_w/W_c = 0.374}{\sigma_u \text{ @ } W_w/W_c = 0.362} \right) = 5.5 \text{ psi} \times \frac{8 \text{ psi}}{10.0 \text{ psi}} = 4.36 \text{ psi,}$$

$$\sigma_y = 4.75 \text{ psi} \times \frac{7.4 \text{ psi}}{9.2 \text{ psi}} = 3.82 \text{ psi,}$$

$$E_1 = 370 \text{ psi} \times \frac{640 \text{ psi}}{1,020 \text{ psi}} = 233 \text{ psi,}$$

$$E_2 = 163 \text{ psi} \times \frac{230 \text{ psi}}{330 \text{ psi}} = 113 \text{ psi .}$$

This approach appears reasonable since testing conditions and mix proportions were essentially the same for test specimens in Figures 6.7 and 6.15. It is noted that in one case air content was a variable and in the other case water-cement ratio was a variable,

but both variables are incorporated in the above calculations. These values were used in the finite element analysis with the undrained shear strength for the experimental section estimated as one-half of the ultimate strength ($\sigma_u/2 = 2.18$ psi).

6.5.2 Development of Failure Zones

Plane strain deformation was assumed for all cross-sections constructed by horizontal slipform construction. A finite element idealization of the experimental cross-section, illustrated in Figure 6.21, shows both the top and sides as free surfaces. The bottom, where fresh concrete contacts the ground and develops a frictional force along the interface, was represented by a fixed end condition. Field observations (Figure 6.22) on a fresh concrete median barrier section agree with the fixed end condition at the base.

The cross-section was represented by 174 rectangular elements, each 2 in. by 2 in. in size, with a total of 210 nodal points. The scheme of elements was convenient for automatic node generation within the computer. The stress-strain curve was approximated by a bilinear curve (Figure 2.7) consisting of two straight line portions representing the two moduli. Approximate material properties for the cross-section are given below:

Unit weight $\gamma = 150$ pcf (estimated)

Poisson's ratio $\nu = 0.4$ (assumed)

Ultimate strength $\sigma_u = 4.36$ psi

Yield stress $\sigma_y = 3.82$ psi

Elastic modulus $E_1 = 233$ psi

Plastic modulus $E_2 = 113$ psi

$n = E_2/E_1 = 0.484$

} By extrapolation from test data and field proportions.

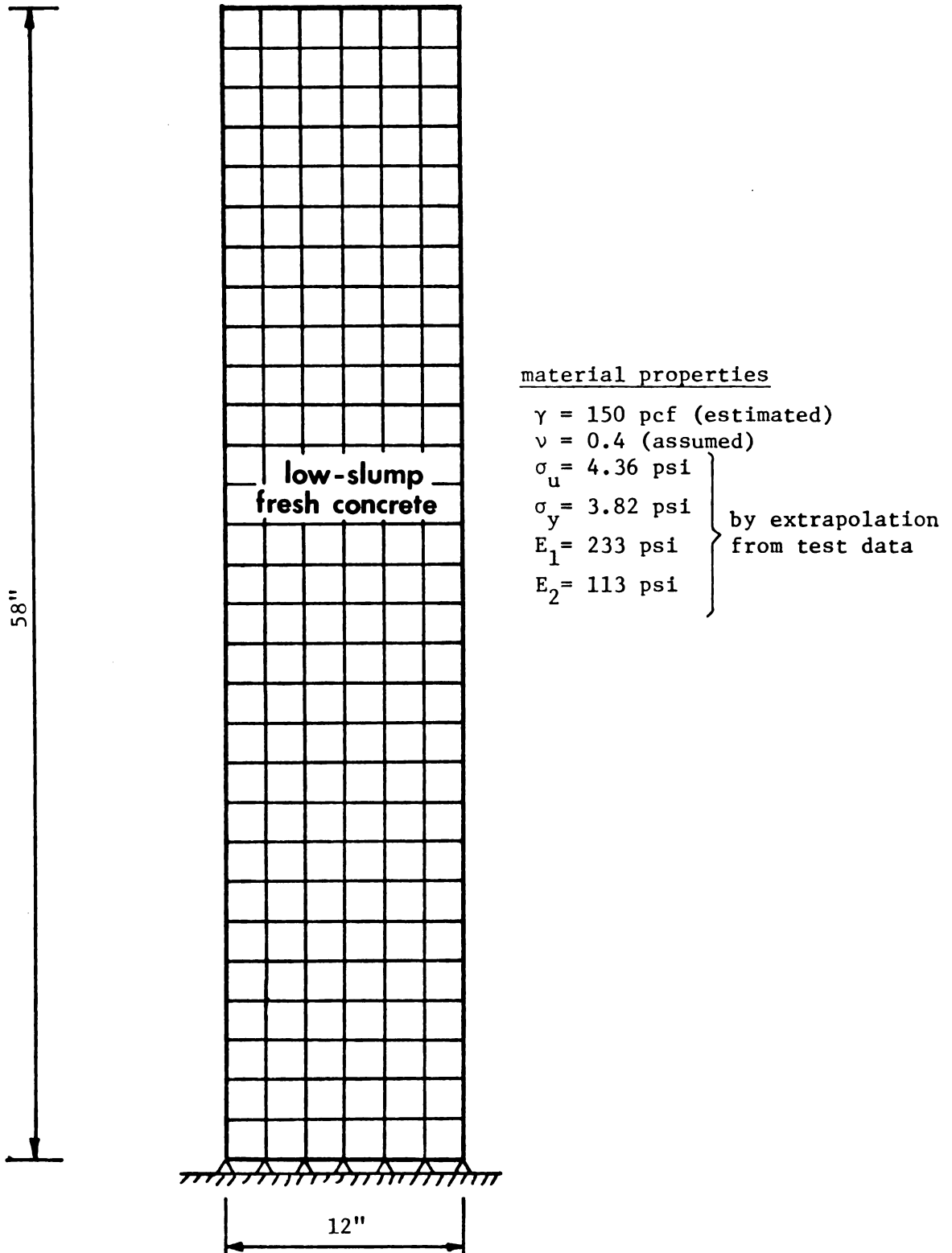


Figure 6.21. The finite element configuration of the experimental section.

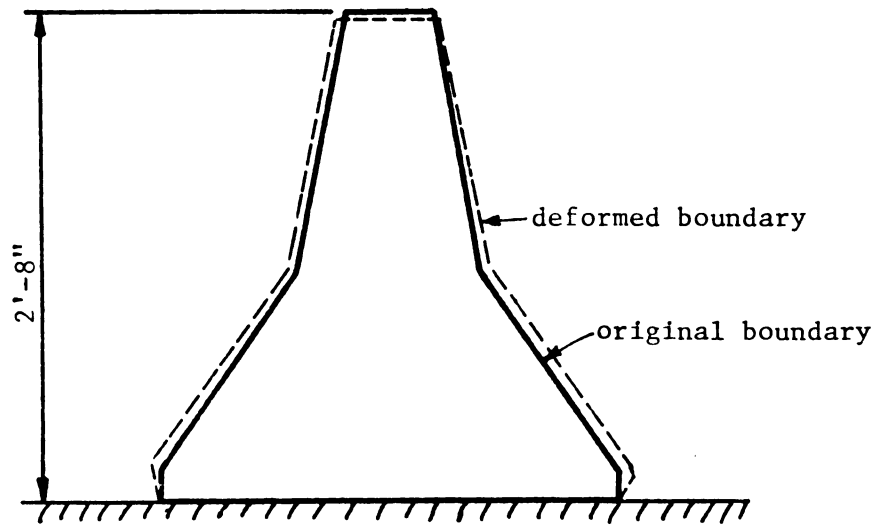


Figure 6.22. Deformation of a median barrier of wet mix.

The computer program FEAST was used to obtain the results summarized in Figure 6.23. The maximum vertical deformation predicted at the top of the wall from self-weight loading was 0.507 in. and the maximum lateral expansion of 0.063 in. occurred at about 6 in. above the base.

Although no deformations were measured in the field, it is understood from comments by Goughnour (1976) that no noticeable deformations were observed. Calculations show that for a wall of low slump mix design, deformation is definitely a secondary phenomenon and that the emphasis should be on the undrained shear strength of the material. The failure zone would be predicted to occur at about 4 to 10 in. above the base of the wall. The observed field failure Line A-A occurred slightly above the failure zone given by the finite element analysis.

The same phenomenon was observed in a 68 in. high median barrier section slipform constructed by the Aukerman Co. in Florida (Goughnour, 1976). The shear failure developed about 12 in. above the base whereas the finite element analysis predicted a maximum shear zone 2 in. below the observed failure as shown in Figure 6.24.

The discrepancy between the theoretical analysis and the observed field results is believed to be caused by either one or a combination of the following reasons:

- 1) Differences between field construction methods and laboratory sample preparation procedures.
- 2) The bottom portion of the section may develop a better consolidated condition, hence it may possess a slightly higher

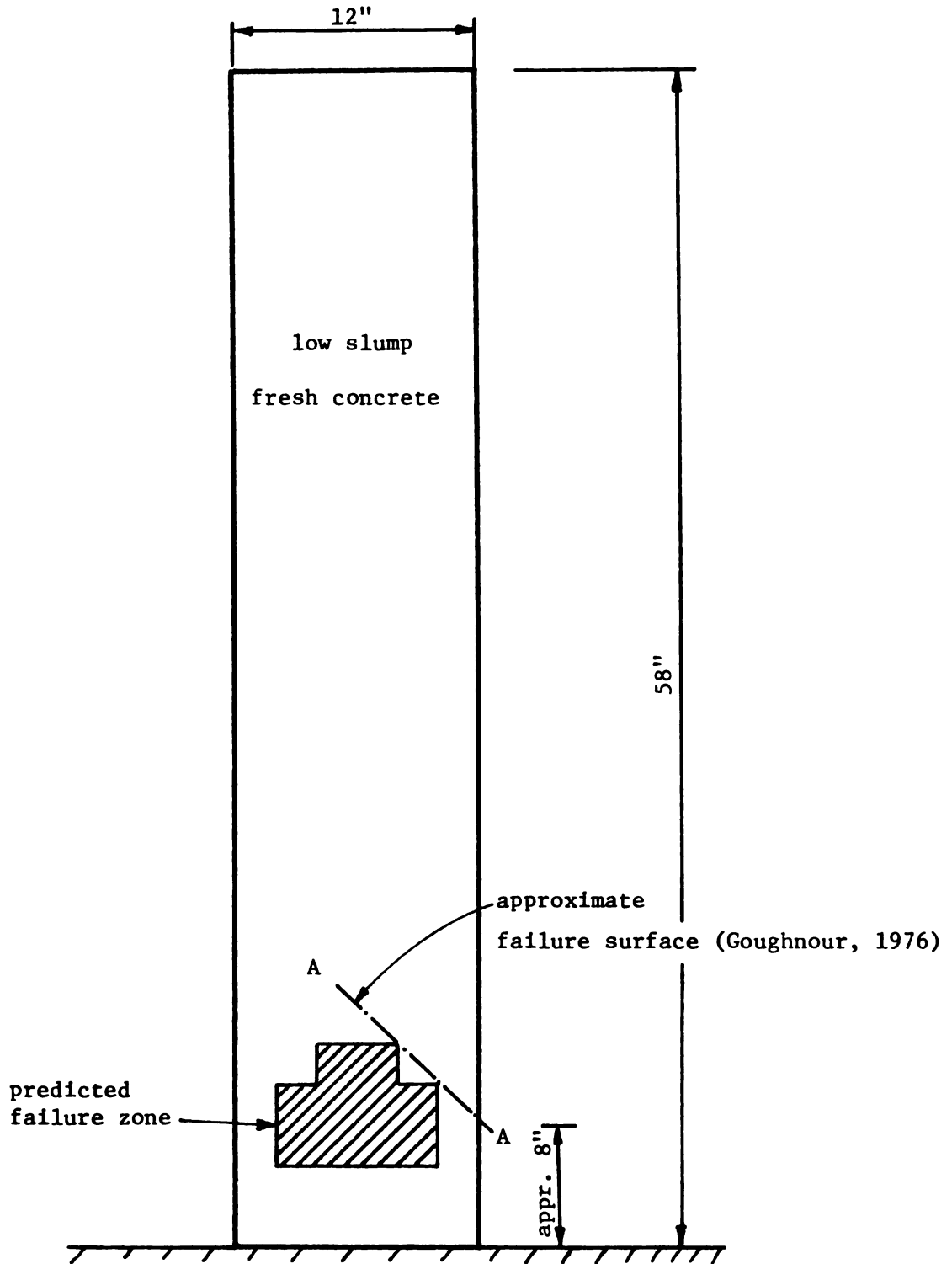


Figure 6.23. Development of a failure zone for the experimental slipformed wall section.

material properties

$\gamma = 137$ pcf
 $\nu = 0.4$ (assumed)
 $\sigma_u = \text{unknown}$

$E_1 = 350$ psi (assumed)

$E_2 = 0$ (assumed)

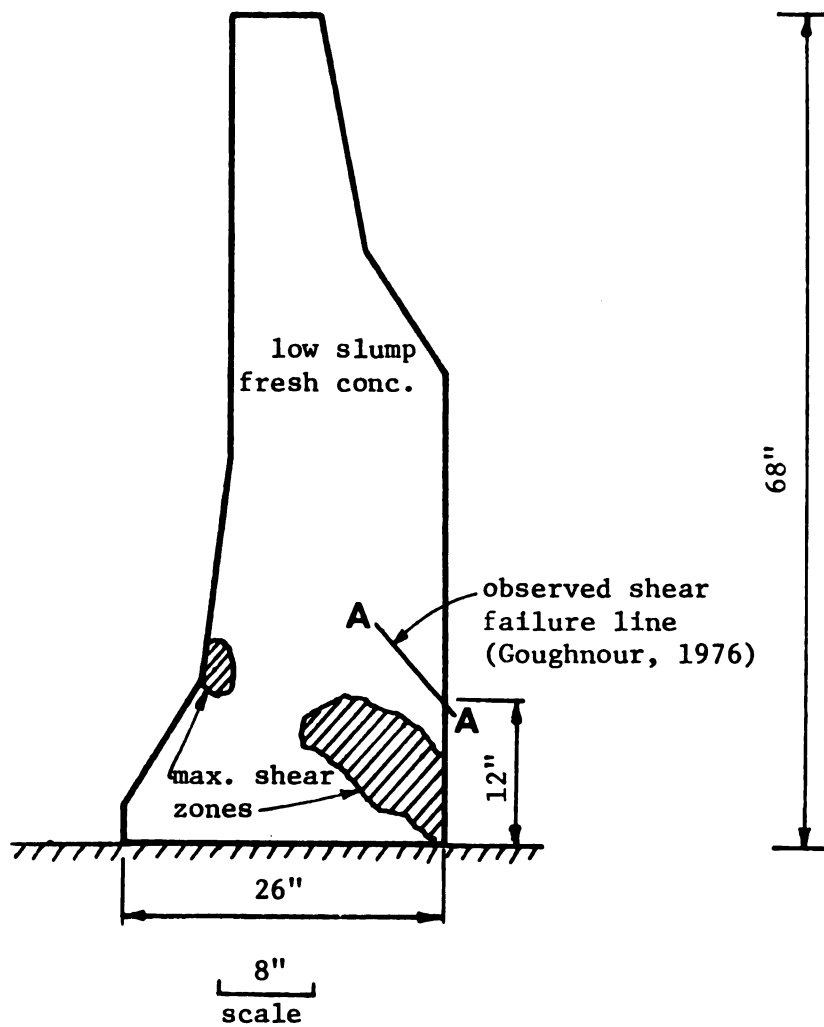


Figure 6.24. Maximum shear zones for Florida median barrier section.

strength and stiffness which would alter the location of the failure region. This phenomenon would be anticipated more for a wet mix, such as used in the Florida section with a $W_w/W_c = 0.47$. Vibration during placement would contribute to this condition.

3) Localized stresses and strains near the fixed boundary give rise to a complicated stress pattern which cannot be modeled properly in the finite element approach unless more elements are used in the analysis.

However, as shown by the experimental section, the finite element approach approximates the field performance and appears to serve as an acceptable analysis technique. Limitations on representation of the mechanical properties of the fresh concrete introduce some error in the method.

It should be noted that although the Florida section was taller than the experimental wall section, the maximum shear stress in the former was less than that in the latter as was shown by the finite element analysis results. The larger base width and smaller top width of the Florida section produces a different stress distribution, hence the Florida section developed a lower maximum shear stress near the base as compared to the experimental section. This observation is in line with comments by Goughnour (1976) that during field construction the speed of the extrusion machine needed to assure successful construction will be inversely proportional to the height-width ratio of the structure.

6.6 Simplified Analysis for Wall Stability

Although the finite element analysis is the most suitable approach for estimating stresses and strains in a fresh concrete structure of irregular shape, a simplified analysis method is desirable for those situations where an immediate engineering decision is needed or where the finite element computation facilities are inaccessible -- either due to lack of trained personnel or computational equipment.

When no external forces are acting on the structure and where no overhang section or significant amount of bending moment exists in any portion of the fresh concrete structure, the easiest way to apply a simplified analysis method is to compare the maximum vertical stress, instead of the maximum shear stress, with the undrained shear strength of the fresh concrete mix. Vertical stresses usually develop their maximum value either at or close to the bottom of the structure. If the cross-section is of rectangular shape with an adequate height to width ratio (h/d) and the interface of the bottom surface and the ground is completely frictionless, the maximum vertical stress ($\sigma_z \text{ max.}$) can be estimated as equal to the product of unit weight and the height of the structure (γh). Also, the maximum shear stress will be approximately equal to one-half of the maximum vertical stress. However, this ideal condition is limited to only a few geometrical sections. Structures with odd shapes can have γh values quite different from either the actual maximum vertical stress or twice the maximum shear stress ($2\tau_{\text{max.}} = \sigma_{\text{max.}} - \sigma_{\text{min.}}$) as computed by the finite element program.

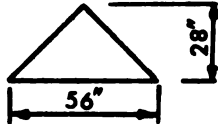
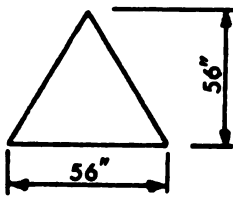
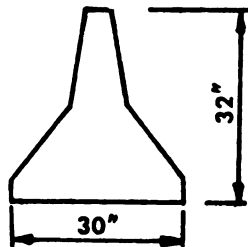
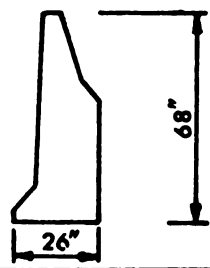
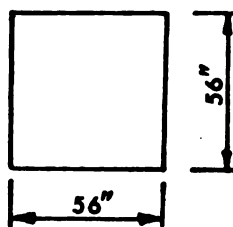
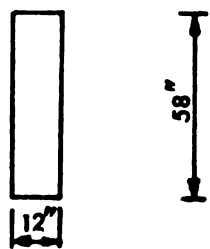
To develop a simplified analysis method for various geometrical shapes it was convenient to define a stress ratio, S , equal to twice the maximum shear stress divided by the section height times the fresh concrete unit weight, thus:

$$S = \frac{2\tau_{\max.}}{\gamma h} \quad (6.7)$$

This stress ratio served to characterize a given geometrical cross-section. When this stress ratio is close to unity ($S \approx 1.0$), it indicates that the simplified analysis method provides a fairly accurate representation of vertical stresses in the fresh concrete section. If $S < 1$, the simplified method underestimates the safe wall height. A summary of S values in Table 6.2 for a series of geometrical shapes shows that S will not exceed 1. In other words, the stress ratio can also be used as a stability indicator -- the smaller the stress ratio, the more stable the structure.

Table 6.2 gives a summary of the stress conditions and stress ratios for six different geometrical structural shapes. Among them, Shape III, IV, and VI were discussed in earlier sections and the other three shapes were selected for comparison purposes. It is seen from this table that the stress ratio is closest to unity for the Shape VI structure -- a structure which appears to be the most unstable one among the six. As the stability of the structure increases, the stress ratio decreases accordingly. It is noted that as the lateral dimension near the bottom of the structure becomes greater the stress ratio becomes smaller. Equation (6.7) can be rewritten as

$$\tau_{\max.} = \frac{S \gamma h}{2} \quad (6.8)$$

| Table 6.2. Stress conditions and stress ratios for diff. shapes. | | | | | | | |
|--|---|----------------|-----------|----------------------|-------------------------------------|-------------------|---------------------|
| shape number | shape geometry | γ (pcf) | h (in.) | $2\tau_{\max}$ (psi) | $S = \frac{2\tau_{\max}}{\gamma h}$ | $B = \frac{h}{r}$ | $\frac{\bar{y}}{h}$ |
| I |  | 148 | 28 | 0.86 | 0.36 | 2.45 | 0.333 |
| II |  | 148 | 56 | 1.92 | 0.4 | 2.45 | 0.333 |
| III (also see Fig. 2.1) |  | 150 | 32 | 1.25 | 0.45 | 2.21 | 0.361 |
| IV (also see Fig. 6.24) |  | 137 | 68 | 4.04 | 0.75 | 2.04 | 0.41 |
| V |  | 148 | 56 | 3.88 | 0.81 | 1.732 | 0.5 |
| VI |  | 148 | 58 | 4.5 | 0.9 | 1.732 | 0.5 |

The significance of Equation (6.8) is that the predicted maximum shear stress can be estimated by the simplified method and then can be compared to the undrained shear strength of the material to determine if the structure will fail. In this equation, S must be predicted according to the geometrical cross-section of the structure.

A common practice in structural engineering is to use the slenderness ratio (ℓ/r), a dimensionless factor, to characterize the strength of the structural member, where ℓ is the unsupported length and r is the least radius of gyration ($r = \sqrt{I/A}$). Since ℓ cannot be applied in this case, another dimensionless factor, the shape factor with the property $B = h/r = \frac{h}{\sqrt{I/A}}$, is introduced to express the stability of the structure. In this factor I is the moment of inertia of the structure with respect to an axis which is the base line of the structure, A is the cross-sectional area of the structure, and h is the maximum height of the structure. It appears that the larger the shape factor, the more stable the structure. If the shape factor is correlated to the stress ratio, they should be inversely proportioned. Figure 6.25 shows this relationship between the stress ratio and the shape factor B with data from Table 6.2. The relationship is almost linear.

Further simplification can be made by comparing the stress ratio and the ratio of center of gravity to maximum height (\bar{y}/h). Data summarized in Table 6.2 and Figure 6.26 show that stress ratio is almost linearly proportional to the \bar{y}/h ratio, implying that higher \bar{y}/h ratios result in less stable structures.

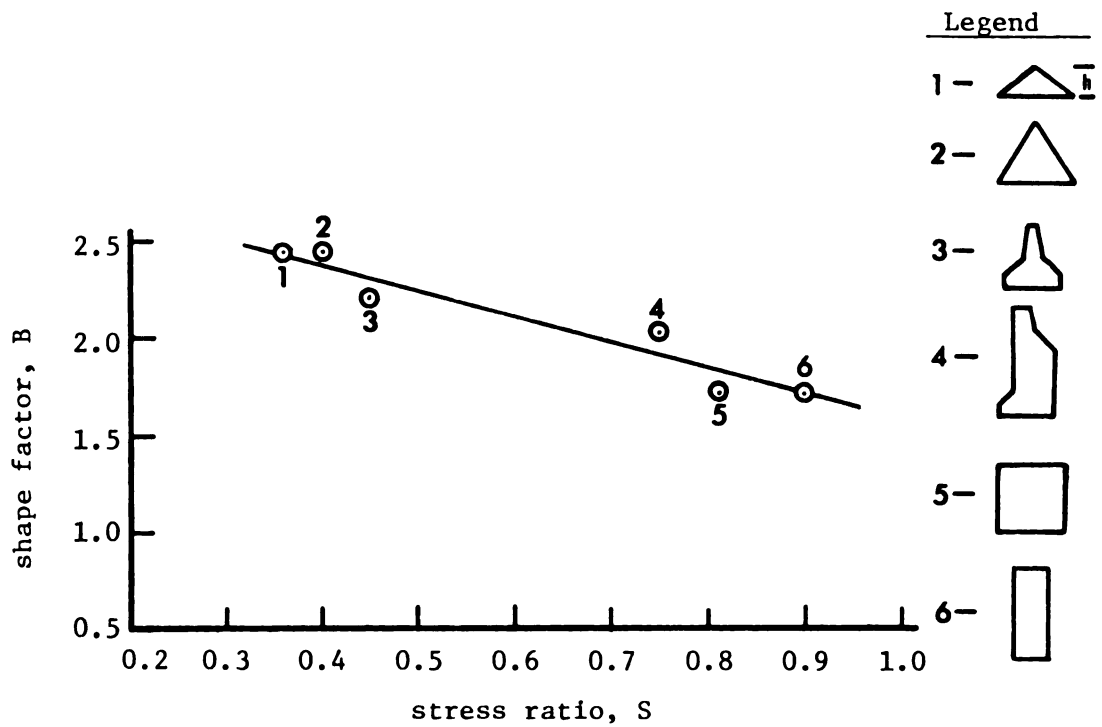


Figure 6.25. Relationship between stress ratio and shape factor.

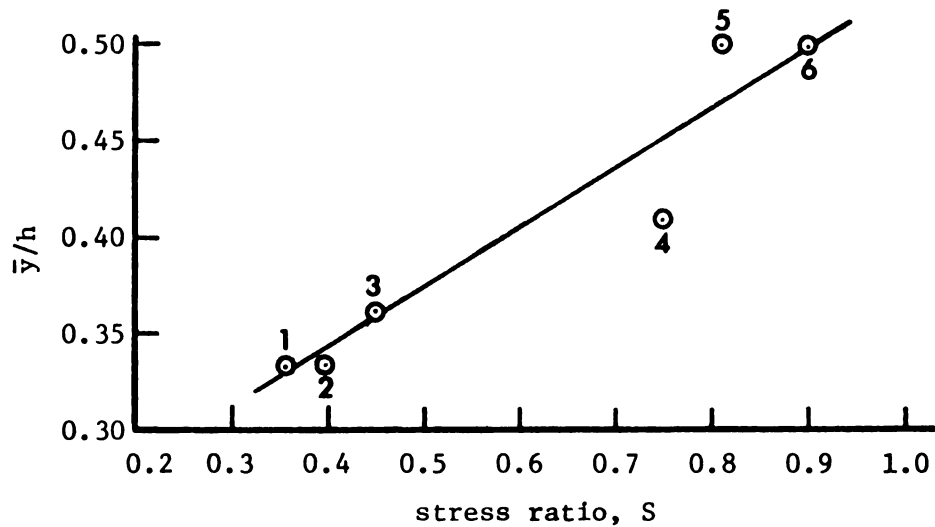


Figure 6.26. Relationship between stress ratio and \bar{y}/h ratio.

The \bar{y}/h ratio is easier to calculate than the Shape Factor B , therefore it is recommended that Figure 6.26 be employed when using the simplified method whereas Figure 6.25 provides additional information should refinement of the simplified method be needed in the future.

Once the shape factor or the \bar{y}/h ratio for a given geometrical shape is calculated, the stress ratio is then read from Figure 6.25, or Figure 6.26. Next the maximum stress of the structure can be estimated using Equation (6.8) for comparison with the undrained shear strength of material. The ratio of undrained shear strength for the fresh concrete to the maximum shear stress gives an estimate of the factor of safety for the structure.

It is imperative to emphasize the empirical nature of the simplified method and its limitations in analyzing structures with external forces acting on them other than the gravity loadings or structures in which a significant amount of bending moment may exist. Under such conditions, the simplified method does not apply. In the case where tensile stresses may exist in the structure the simplified method should not be considered but rather a complete stress analysis using material properties appropriate for the structure under consideration.

CHAPTER VII

SUMMARY AND CONCLUSIONS

The summary and conclusions are presented under three headings: 1) engineering properties of the low-slump fresh concrete; 2) behavior of a horizontal slipformed concrete structure, and 3) practical implications of the investigation.

7.1 Engineering Properties of the Low-Slump Fresh Concrete

The mix design method and variables appropriate for low slump concrete were reviewed. Both physical and mechanical properties of the low-slump fresh concrete were determined in order to evaluate the factors which influence the mechanical behavior and to provide data for the structural analysis. Physical properties are included for both the fresh concrete and individual components. Mechanical properties included stiffness and strength of the compacted fresh concrete in the unconfined compression test. The following conclusions refer to the engineering properties of the fresh concrete or its components.

1. Physical properties of both the fresh concrete and its individual components used in this project are typical as compared to the published values for ordinary concrete mixes. In addition, physical properties of the fresh concrete are dependent on mix conditions which may vary appreciably. An increase in the amount of

entrained air is accompanied by a decrease in unit weight. Basic water content of the mortar decreases with increased sand-cement ratio.

2. The stiffness (E_1 and E_2) and strength (σ_u and σ_y) of the fresh concrete for unconfined compression conditions decreases within limits for the following conditions:

- 1) an increase in effective water-cement ratio
- 2) a shorter period of hydration after the start of the mixing
- 3) a shorter period of hydration after vibration
- 4) a decrease in sand-cement ratio (in the case of constant water-cement ratio)
- 5) an increase in mortar content
- 6) a decrease in the degree of angularity of the coarse aggregate
- 7) a decrease in the temperature of the fresh concrete
- 8) an increase in air content
- 9) a deviation of the gradation curve from the ideal diagonal line on the 0.45 power grading chart
- 10) a decrease in the rate of strain

3. Concrete mixes of higher stiffness and strength required a greater vibration effort to produce a completely compacted sample.

4. The angle of internal friction of the low-slump fresh concrete, based on observed failure surfaces, was between 20 and 30 degrees. Both field and laboratory test data suggested that the direction of the failure surface is determined by a frictional mechanism.

5. The observed stress-strain behavior showed that low-slump fresh concrete can be considered as a brittle material. Stress-strain curves always showed a linear portion extending almost to the peak strength followed by an abrupt decrease in strength.

6. The air content requirement may be deleted for low-slump concrete which is used for free standing structures, provided the structure is not under severe exposure conditions. This conclusion is based on freezing and thawing test results on low-slump concrete panels (Isberner, 1963).

7. The mortar-void method is considered to be an appropriate and effective mix design method for low-slump fresh concrete.

7.2 Behavior of a Horizontal Slipformed Concrete Structure

An experimental section of rectangular shape slipform constructed by the A.C. Aukerman Company showed a shear type failure near the base of the wall. The undrained shear strength of the failed section was estimated on the basis of laboratory test results and information provided by Goughnour (1973). Also, an analysis was made to compare the available strength with shear stresses in both the experimental section and a median barrier section, slipform constructed in Florida. A simplified analysis for evaluating stability of low-slump concrete walls has been developed. The following conclusions refer to the stress conditions in the structure and method of analysis.

1. The two observed wall failures both occurred a short distance above the base of the wall. This was in agreement with the deformation-restraint condition between the ground and the low-slump concrete used in the finite element representation of the wall

section. Any natural packing or densification during placement would strengthen the fresh concrete and thereby place the actual failure surface near the top of the predicted failure zone which was in agreement with field observations.

2. Computed stresses in the field wall sections, based on measured and/or assumed strength properties of the low-slump concrete and the wall geometry, showed a failure zone close to the base of the wall. These predicted failure zones are in agreement with the two observed wall failures.

3. The simplified analysis for structural stability provides a technique for rapid evaluation of the maximum shear stress in walls of different geometrical shapes. The undrained shear strength of the low-slump concrete can then be compared with the maximum shear stress to provide a measure of wall stability. This approach appears suitable for use by contractors.

4. Lower height/width ratio of field wall sections results in lower shear stresses and a greater stability. Accordingly, this permits an increase in the speed of the extrusion machine, in agreement with field experience (Goughnour, 1976). Therefore, development of relationships between the height/width ratio of wall sections and the speed of a particular extrusion machine appears to be a reasonable goal.

7.3 Practical Implications of the Investigation

Use of undrained shear strengths from unconfined compression tests as the failure criterion and the finite element analysis method to evaluate stresses was found to be effective and fairly accurate

for low-slump fresh concrete structures horizontally slipform constructed. The procedure of testing and analysis could be extended to low-slump fresh concrete with various additives such as fly-ash, glass or steel fiber, etc.

Slipform construction saves both time and cost. If the engineer can predict the suitability of the slipform construction method prior to construction, he would be able to minimize construction costs as well as the time required for construction.

The slipform method of constructing highway or transportation facilities is particularly advantageous when they are to be built over existing roadways and traffic must be maintained during construction. The slipform method permits elimination of both setting and stripping the forms, there is much less interference to traffic, and less exposure to traffic hazards by workmen.

Earth retaining structures of low to medium height (6 ft. to 13 ft.) might be slipform constructed using a straddle type extrusion machine. Higher walls could also be slipform constructed by either changing the cross-section of the wall, by changing the material used for the paste, or by construction in a series of levels. The wall cross-section could be analyzed by the finite element method used on this project.

REFERENCES

REFERENCES

American Concrete Institute, "Proposed Standard Recommended Practice for Selecting Proportions for No-Slump Concrete," Proc. ACI, Vol. 62, January 1965.

Andreasen, A.H.M., Anderson, J., "The Relation of Grading to Interstitial Voids in Loosely Granular Products (With Some Experiments)," Kolloid-Z, 49, 1929.

Ashworth, R., "Some Investigation Into the Use of Sugar as an Admixture to Concrete," Proceedings of the Institution of Civil Engineers, Vol. 31, June 1965.

Balla, A., "Stress Conditions in Triaxial Compression," ASCE Proceedings, Vol. 86, SM6, No. 2684, December 1960.

Bauer, F.E., Plain Concrete, 3rd Edition, McGraw-Hill Book Co., Inc., 1949.

Bishop, A.W., Henkel, D.J., Measurement of Soil Properties in the Triaxial Test, Edward Arnold Ltd., 1962.

Bureau of Public Roads, Aggregate Gradation for Highways, U.S. Department of Commerce, 1962.

Casagrande, A., Wilson, S.D., "Effect of Rate of Loading on the Strength of Clays and Shales at Constant Water Content," Geotechnique, Vol. 2, 1951.

Cordon, W.A., "Entrained Air - A Factor in the Design of Concrete Mixes," Proc. ACI, 1946.

Cordon, W.A., Freezing and Thawing of Concrete-Mechanisms and Control, ACI Monograph No. 3, 1966.

Dehlen, G.L., "The Effect of Non-Linear Material Response on the Behavior of Pavements Subjected to Traffic Loads," Institute of Transportation and Traffic Eng., Univ. of California, Berkeley, graduate report, 1969.

Donnelly, W.C., "Continuous Concreting: Slipform Paving on the Move," Construction Methods and Equipment, August 1973.

FHWA, Concrete Median Barriers and Parapets, Federal Highway Administration Notice EN-20, March 19, 1971.

Gonnerman, H.F., "Tests of Concretes Containing Air-Entraining Portland Cements or Air-Entraining Materials Added to Batch at Mixer," Proc. ACI, Vol. 40, 1944.

Goughnour, R.R., President of Strahan Manufacture Co. Ltd., Florida. Formerly Executive Vice-President of A.C. Aukerman Construction Co., Jackson, Michigan, Personal Correspondence, 1975 and 1976.

Isberner, A.W., Durability Studies of Exposed Aggregate Panels, PCA Bulletin 158, 1963.

Jones, P.G. and Richart, F.E., "The Effect of Testing Speed on Strength and Elastic Properties of Concrete," Proc. ASTM, Vol. 36, pt. II, 1936.

Lambe, T.W., Soil Testing, John Wiley and Sons, Inc., 1965.

Lambe, T.W. and Whitman, R.V., Soil Mechanics, John Wiley and Sons, Inc., 1969.

Lokken, E.C., "Concrete Median Barrier Safely Redirects Impacting Cars," Civil Engineering-ASCE, October 1971.

Lokken, E.C., "Concrete Safety Barrier Design," ASCE Proceedings, Vol. 100, No. TE1, February 1974.

Majidzadeh, K., Kauffmann, E.M., Chang, C.W., "Verification of Fracture Mechanics Concepts to Predict Cracking of Flexible Pavements," Report No. FHWA-RD-73-91, Federal Highway Administration, June 1973.

Malvern, L.E., Introduction to the Mechanics of a Continuous Medium, Prentice-Hall, Inc., Englewood Cliffs, N.J., 1969.

Mendelson, A., Plasticity Theory and Application. The Macmillan Co., New York, 1968.

Michigan Department of State Highways, Standard Specifications for Highway Construction, 1976.

Nair, K. and Chang, C-Y, "Flexible Pavement Design and Management - Material Characterization," NCHRP Report 140, Highway Research Board, 1973.

Nijboer, L.W., "Plasticity as a Factor in the Design of Dense Bituminous Road Carpets," Elsevier Publishing Co., 1948.

Olson, R.M., Post, E.R., McFarland, W.F., Tentative Service Requirements for Bridge Rail Systems, NCHRP Report 86, Highway Research Board, 1970.

Popovics, S., "Relation Between the Change of Water Content and the Consistence of Fresh Concrete," Magazine of Concrete Research, 14(41), 99-108, 1962a.

Popovics, S., Comparison of Several Methods of Evaluating Aggregate Gradings, RILEM Bulletin No. 17, New Series 13-21, 1962b.

Portland Cement Association, Tips on Control Tests for Quality Concrete, PCA Publication, 1965.

Powers, T.C., The Properties of Fresh Concrete, John Wiley and Sons, Inc., 1968.

Ritchie, A.G.B., "The Triaxial Testing of Fresh Concrete," Magazine of Concrete Research, Vol. 14, No. 40, March 1962.

Ritchie, A.G.B., "The Rheology of Fresh Concrete," Journal of the Construction Division, ASCE, Vol. 94, No. CO 1, January 1968.

Roth, L., "Barriers Can Broaden Your Business Base," Michigan Contractors and Builders, February 23, 1974.

Ruetters, A., Vidal, E.N., Wing, S.P., "An Investigation of the Permeability of Mass Concrete with Particular Reference to Boulder Dam," Proc. American Concrete Institute, Vol. 31, 1935, Vol. 32, 1936.

Seki, S., Kasahara, K., Kuriyama, T., Kawasumi, M., "Relation Between Compressive Strength of Concrete and the Effective Cement-Water Ratio Calculated from the Hydration Rate of Cement," J. American Concrete Institute, March 1969.

Shehan, E.L., The Mortar Voids Method of Proportioning Concrete as Used by the Michigan Department of State Highways, MDSHT Testing Laboratory, September 1970.

Talbot, A.N., Richart, F.E., "The Strength of Concrete - Its Relation to the Cement, Aggregate, and Water," University of Illinois Eng. Expt. Sta. Bull. 137, 1922.

Terzaghi, K. and Peck, R.B., Soil Mechanics in Engineering Practice, 2nd ed., John Wiley and Sons, Inc., New York, 1967.

Timoshenko, S.P., Goodier, J.N., Theory of Elasticity, 3rd ed., McGraw-Hill Book Co., New York, 1970.

Troxell, G.E., Davis, H.E., Kelly, J.W., Composition and Properties of Concrete, McGraw-Hill Book Co., 2nd ed., 1968.

U.S. Bureau of Reclamation, Concrete Manual, 7th ed., Denver, Colorado, 1963.

Uzomaka, O.J., "Some Shear Strength Parameters of Plastic Concrete," Magazine of Concrete Research, Vol. 23, No. 75-76, June-September 1971.

Walker, S., Effect of Grading on Gravel and Sand on Voids and Weights, National Sand and Gravel Association Circular 8, Washington, 1930.

Wilson, E.L. (University of Calif., 1966), Christian, J.T. (MIT, 1967), Goughnour, R.R. (Michigan State Univ., 1971). "Program FEASTS," Michigan State University Computer Center.

Zienkiewicz, O.C., The Finite Element Method in Engineering Science, McGraw-Hill Book Co. Ltd., 1971.

APPENDICES

APPENDIX A

TABLE A-1 UNCONFINED COMPRESSION TEST DATA, SAMPLE 1

| Load, P (lb.) | Strain, ϵ_1 (%) | Stress, σ_1 (psi) | $\epsilon = \epsilon_0 + \epsilon_1$ (%) | $\sigma = \sigma_0 + \sigma_1$ (psi) |
|------------------|-----------------------------|-----------------------------|---|---|
| 0 | 0 | 0 | 0.04 | 0.54 |
| 49 | 0.21 | 1.73 | 0.25 | 2.27 |
| 135 | 0.42 | 4.76 | 0.46 | 5.30 |
| 245 | 0.63 | 8.61 | 0.67 | 9.15 |
| 353 | 0.83 | 12.40 | 0.87 | 12.94 |
| 374 | 0.88 | 13.12 | 0.92 | 13.66 |
| 395 | 1.04 | 13.83 | 1.08 | 14.37 |
| 393 | 1.13 | 13.74 | 1.17 | 14.28 |
| 374 | 1.25 | 13.07 | 1.29 | 13.61 |
| 320 | 1.46 | 11.15 | 1.50 | 11.69 |

$$\sigma_1 = P/A = \frac{P(1 - \epsilon_1)}{A_0} \quad \text{where } A_0 = 28.275 \text{ in.}^2$$

$$\epsilon_0 = \frac{\gamma l}{2E_1} = \frac{(0.08933)(12)}{(2)(1499)} \times 100\% = 0.04\%$$

$$\sigma_0 = \frac{\gamma l}{2} = \frac{(0.08933)(12)}{2} = 0.54 \text{ psi}$$

TABLE A-2 UNCONFINED COMPRESSION TEST DATA, SAMPLE 2

| Load, P (lb.) | Strain, ϵ_1 (%) | Stress, σ_1 (psi) | $\epsilon = \epsilon_0 + \epsilon_1$ (%) | $\sigma = \sigma_0 + \sigma_1$ (psi) |
|------------------|-----------------------------|-----------------------------|---|---|
| 0 | 0 | 0 | 0.03 | 0.54 |
| 70 | 0.21 | 2.47 | 0.24 | 3.01 |
| 163 | 0.42 | 5.75 | 0.45 | 6.29 |
| 268 | 0.63 | 9.43 | 0.66 | 9.97 |
| 373 | 0.83 | 13.07 | 0.87 | 13.61 |
| 410 | 0.92 | 14.37 | 0.95 | 14.91 |
| 435 | 1.04 | 15.23 | 1.08 | 15.77 |
| 385 | 1.25 | 13.45 | 1.28 | 13.99 |
| 318 | 1.46 | 11.10 | 1.49 | 11.64 |

$$\sigma_1 = P/A = \frac{P(1 - \epsilon_1)}{A_0} \quad \text{where } A_0 = 28.275 \text{ in.}^2$$

$$\epsilon_0 = \frac{\gamma l}{2E_1} = \frac{(0.08989)(12)}{(2)(1569)} \times 100\% = 0.03\%$$

$$\sigma_0 = \frac{\gamma l}{2} = \frac{(0.08989)(12)}{2} = 0.54 \text{ psi}$$

TABLE A-3 UNCONFINED COMPRESSION TEST DATA, SAMPLE 3

| Load, P (lb.) | Strain, ϵ_1 (%) | Stress, σ_1 (psi) | $\epsilon = \epsilon_0 + \epsilon_1$ (%) | $\sigma = \sigma_0 + \sigma_1$ (psi) |
|------------------|-----------------------------|-----------------------------|---|---|
| 0 | 0 | 0 | 0.16 | 0.54 |
| 19 | 0.21 | 0.67 | 0.37 | 1.21 |
| 42 | 0.42 | 1.47 | 0.58 | 2.02 |
| 63 | 0.63 | 2.27 | 0.79 | 2.81 |
| 83 | 0.83 | 2.92 | 0.99 | 3.46 |
| 103 | 1.04 | 3.61 | 1.20 | 4.15 |
| 118 | 1.21 | 4.12 | 1.37 | 4.66 |
| 130 | 1.46 | 4.53 | 1.62 | 5.07 |
| 135 | 1.67 | 4.70 | 1.83 | 5.24 |
| 127 | 1.88 | 4.41 | 2.04 | 4.95 |
| 123 | 2.08 | 4.26 | 2.24 | 4.80 |
| 115 | 2.29 | 3.97 | 2.45 | 4.51 |

$$\sigma_1 = P/A = \frac{P(1 - \epsilon_1)}{A_0} \quad \text{where } A_0 = 28.275 \text{ in.}^2$$

$$\epsilon_0 = \frac{\gamma \ell}{2E_1} = \frac{(0.08989)(12)}{(2)(341)} \times 100\% = 0.16\%$$

$$\sigma_0 = \frac{\gamma \ell}{2} = \frac{(0.08989)(12)}{2} = 0.54 \text{ psi}$$

TABLE A-4 UNCONFINED COMPRESSION TEST DATA, SAMPLE 4

| Load, P (lb.) | Strain, ϵ_1 (%) | Stress, σ_1 (psi) | $\epsilon = \epsilon_0 + \epsilon_1$ (%) | $\sigma = \sigma_0 + \sigma_1$ (psi) |
|------------------|-----------------------------|-----------------------------|---|---|
| 0 | 0 | 0 | 0.22 | 0.54 |
| 21 | 0.21 | 0.77 | 0.43 | 1.31 |
| 34 | 0.42 | 1.22 | 0.64 | 1.76 |
| 47 | 0.63 | 1.66 | 0.85 | 2.20 |
| 61 | 0.83 | 2.13 | 1.05 | 2.67 |
| 72 | 1.04 | 2.53 | 1.26 | 3.07 |
| 81 | 1.25 | 2.81 | 1.47 | 3.35 |
| 87 | 1.46 | 3.04 | 1.68 | 3.58 |
| 91 | 1.63 | 3.18 | 1.85 | 3.72 |
| 89 | 1.88 | 3.08 | 2.10 | 3.62 |
| 88 | 2.08 | 3.05 | 2.30 | 3.59 |
| 87 | 2.29 | 3.01 | 2.51 | 3.55 |
| 85 | 2.50 | 2.93 | 2.72 | 3.47 |

$$\sigma_1 = P/A = \frac{P(1 - \epsilon_1)}{A_0} \quad \text{where } A_0 = 28.275 \text{ in.}^2$$

$$\epsilon_0 = \frac{\gamma l}{2E_1} = \frac{(0.08933)(12)}{(2)(246)} \times 100\% = 0.22\%$$

$$\sigma_0 = \frac{\gamma l}{2} = \frac{(0.08933)(12)}{2} = 0.54 \text{ psi}$$

TABLE A-5 UNCONFINED COMPRESSION TEST DATA, SAMPLE 5

| Load, P (lb.) | Strain, ϵ_1 (%) | Stress, σ_1 (psi) | $\epsilon = \epsilon_0 + \epsilon_1$ (%) | $\sigma = \sigma_0 + \sigma_1$ (psi) |
|------------------|-----------------------------|-----------------------------|---|---|
| 0 | 0 | 0 | 0.10 | 0.53 |
| 36 | 0.21 | 1.26 | 0.31 | 1.79 |
| 66 | 0.42 | 2.31 | 0.52 | 2.84 |
| 96 | 0.63 | 3.36 | 0.73 | 3.89 |
| 127 | 0.83 | 4.47 | 0.93 | 5.00 |
| 159 | 1.04 | 5.57 | 1.14 | 6.10 |
| 180 | 1.25 | 6.31 | 1.35 | 6.84 |
| 195 | 1.46 | 6.82 | 1.56 | 7.35 |
| 202 | 1.54 | 7.04 | 1.64 | 7.57 |
| 189 | 1.83 | 6.56 | 1.93 | 7.09 |
| 167 | 2.04 | 5.78 | 2.14 | 6.31 |
| 135 | 2.29 | 4.66 | 2.39 | 5.19 |

$$\sigma_1 = P/A = \frac{P(1 - \epsilon_1)}{A_0} \quad \text{where } A_0 = 28.275 \text{ in.}^2$$

$$\epsilon_0 = \frac{\gamma \ell}{2E_1} = \frac{(0.08916)(12)}{(2)(516)} \times 100\% = 0.10\%$$

$$\sigma_0 = \frac{\gamma \ell}{2} = \frac{(0.08916)(12)}{2} = 0.53 \text{ psi}$$

TABLE A-6 UNCONFINED COMPRESSION TEST DATA, SAMPLE 6

| Load, P (lb.) | Strain, ϵ_1 (%) | Stress, σ_1 (psi) | $\epsilon = \epsilon_0 + \epsilon_1$ (%) | $\sigma = \sigma_0 + \sigma_1$ (psi) |
|------------------|-----------------------------|-----------------------------|---|---|
| 0 | 0 | 0 | 0.07 | 0.54 |
| 37 | 0.21 | 1.29 | 0.28 | 1.83 |
| 78 | 0.42 | 2.74 | 0.49 | 3.28 |
| 126 | 0.63 | 4.42 | 0.70 | 4.96 |
| 179 | 0.83 | 6.28 | 0.90 | 6.82 |
| 229 | 1.04 | 8.01 | 1.11 | 8.55 |
| 262 | 1.21 | 9.16 | 1.28 | 9.70 |
| 271 | 1.38 | 9.44 | 1.45 | 9.98 |
| 219 | 1.67 | 7.62 | 1.74 | 8.16 |
| 179 | 1.88 | 6.21 | 1.95 | 6.75 |

$$\sigma_1 = P/A = \frac{P(1 - \epsilon_1)}{A_0} \quad \text{where } A_0 = 28.275 \text{ in.}^2$$

$$\epsilon_0 = \frac{\gamma l}{2E_1} = \frac{(0.08922)(12)}{(2)(761)} \times 100\% = 0.07\%$$

$$\sigma_0 = \frac{\gamma l}{2} = \frac{(0.08922)(12)}{2} = 0.54 \text{ psi}$$

TABLE A-7 UNCONFINED COMPRESSION TEST DATA, SAMPLE 7

| Load, P (lb.) | Strain, ϵ_1 (%) | Stress, σ_1 (psi) | $\epsilon = \epsilon_0 + \epsilon_1$ (%) | $\sigma = \sigma_0 + \sigma_1$ (psi) |
|------------------|-----------------------------|-----------------------------|---|---|
| 0 | 0 | 0 | 0.12 | 0.54 |
| 22 | 0.21 | 0.78 | 0.33 | 1.32 |
| 46 | 0.42 | 1.61 | 0.54 | 2.15 |
| 66 | 0.63 | 2.33 | 0.76 | 2.87 |
| 106 | 0.83 | 3.71 | 0.95 | 4.25 |
| 136 | 1.04 | 4.75 | 1.16 | 5.29 |
| 169 | 1.25 | 5.90 | 1.37 | 6.44 |
| 191 | 1.46 | 6.65 | 1.58 | 7.19 |
| 196 | 1.67 | 6.81 | 1.79 | 7.35 |
| 194 | 1.88 | 6.73 | 2.00 | 7.27 |
| 186 | 2.08 | 6.43 | 2.20 | 6.97 |
| 169 | 2.29 | 5.84 | 2.41 | 6.38 |

$$\sigma_1 = P/A = \frac{P(1 - \epsilon_1)}{A_0} \quad \text{where } A_0 = 28.275 \text{ in.}^2$$

$$\epsilon_0 = \frac{\gamma \ell}{2E_1} = \frac{(0.08989)(12)}{(2)(466)} \times 100\% = 0.12\%$$

$$\sigma_0 = \frac{\gamma \ell}{2} = \frac{(0.08989)(12)}{2} = 0.54 \text{ psi}$$

TABLE A-8 UNCONFINED COMPRESSION TEST DATA, SAMPLE 8

| Load, P (lb.) | Strain, ϵ_1 (%) | Stress, σ_1 (psi) | $\epsilon = \epsilon_0 + \epsilon_1$ (%) | $\sigma = \sigma_0 + \sigma_1$ (psi) |
|------------------|-----------------------------|-----------------------------|---|---|
| 0 | 0 | 0 | 0.10 | 0.54 |
| 24 | 0.21 | 0.85 | 0.31 | 1.39 |
| 52 | 0.42 | 1.84 | 0.52 | 2.38 |
| 84 | 0.63 | 3.46 | 0.73 | 4.00 |
| 117 | 0.83 | 4.56 | 0.93 | 5.10 |
| 156 | 1.04 | 5.47 | 1.14 | 6.01 |
| 196 | 1.25 | 6.83 | 1.35 | 7.37 |
| 216 | 1.38 | 7.52 | 1.48 | 8.06 |
| 222 | 1.52 | 7.74 | 1.62 | 8.28 |
| 214 | 1.71 | 7.44 | 1.81 | 7.98 |
| 182 | 1.88 | 6.33 | 1.98 | 6.87 |
| 155 | 2.08 | 5.37 | 2.18 | 5.91 |

$$\sigma_1 = P/A = \frac{P(1 - \epsilon_1)}{A_0} \quad \text{where } A_0 = 28.275 \text{ in.}^2$$

$$\epsilon_0 = \frac{\gamma \ell}{2E_1} = \frac{(0.08989)(12)}{(2)(549)} \times 100\% = 0.10\%$$

$$\sigma_0 = \frac{\gamma \ell}{2} = \frac{(0.08989)(12)}{2} = 0.54 \text{ psi}$$

TABLE A-9 UNCONFINED COMPRESSION TEST DATA, SAMPLE 9

| Load, P (lb.) | Strain, ϵ_1 (%) | Stress, σ_1 (psi) | $\epsilon = \epsilon_0 + \epsilon_1$ (%) | $\sigma = \sigma_0 + \sigma_1$ (psi) |
|------------------|-----------------------------|-----------------------------|---|---|
| 0 | 0 | 0 | 0.05 | 0.54 |
| 70 | 0.21 | 2.47 | 0.26 | 3.01 |
| 132 | 0.42 | 4.66 | 0.47 | 5.20 |
| 204 | 0.63 | 7.18 | 0.68 | 7.72 |
| 242 | 0.75 | 8.49 | 0.80 | 9.03 |
| 271 | 0.90 | 9.50 | 0.95 | 10.04 |
| 269 | 1.04 | 9.41 | 1.09 | 9.95 |
| 246 | 1.25 | 8.58 | 1.29 | 9.12 |
| 226 | 1.46 | 7.90 | 1.51 | 8.44 |

$$\sigma_1 = P/A = \frac{P(1 - \epsilon_1)}{A_0} \quad \text{where } A_0 = 28.275 \text{ in.}^2$$

$$\epsilon_0 = \frac{\gamma l}{2E_1} = \frac{(0.08970)(12)}{(2)(1128)} \times 100\% = 0.05\%$$

$$\sigma_0 = \frac{\gamma l}{2} = \frac{(0.08970)(12)}{2} = 0.54 \text{ psi}$$

TABLE A-10 UNCONFINED COMPRESSION TEST DATA, SAMPLE 10

| Load, P (lb.) | Strain, ϵ_1 (%) | Stress, σ_1 (psi) | $\epsilon = \epsilon_0 + \epsilon_1$ (%) | $\sigma = \sigma_0 + \sigma_1$ (psi) |
|------------------|-----------------------------|-----------------------------|---|---|
| 0 | 0 | 0 | 0.14 | 0.54 |
| 19 | 0.21 | 0.67 | 0.35 | 1.21 |
| 39 | 0.42 | 1.37 | 0.56 | 1.91 |
| 66 | 0.63 | 2.31 | 0.77 | 2.85 |
| 87 | 0.83 | 3.06 | 0.97 | 3.60 |
| 113 | 1.04 | 3.97 | 1.18 | 4.51 |
| 139 | 1.25 | 4.85 | 1.39 | 5.39 |
| 165 | 1.46 | 5.75 | 1.60 | 6.29 |
| 176 | 1.58 | 6.13 | 1.72 | 6.67 |
| 182 | 1.71 | 6.34 | 1.85 | 6.88 |
| 172 | 1.88 | 5.98 | 2.02 | 6.52 |
| 155 | 2.08 | 5.26 | 2.22 | 5.90 |

$$\sigma_1 = P/A = \frac{P(1 - \epsilon_1)}{A_0} \quad \text{where } A_0 = 28.275 \text{ in.}^2$$

$$\epsilon_0 = \frac{\gamma \ell}{2E_1} = \frac{(0.08992)(12)}{(2)(400)} \times 100\% = 0.14\%$$

$$\sigma_0 = \frac{\gamma \ell}{2} = \frac{(0.08992)(12)}{2} = 0.54 \text{ psi}$$

TABLE A-11 UNCONFINED COMPRESSION TEST DATA, SAMPLE 11

| Load, P (lb.) | Strain, ϵ_1 (%) | Stress, σ_1 (psi) | $\epsilon = \epsilon_0 + \epsilon_1$ (%) | $\sigma = \sigma_0 + \sigma_1$ (psi) |
|------------------|-----------------------------|-----------------------------|---|---|
| 0 | 0 | 0 | 0.14 | 0.53 |
| 25 | 0.21 | 0.88 | 0.35 | 1.41 |
| 48 | 0.42 | 1.69 | 0.56 | 2.22 |
| 67 | 0.63 | 2.37 | 0.77 | 2.90 |
| 89 | 0.83 | 3.12 | 0.97 | 3.65 |
| 136 | 1.25 | 4.74 | 1.39 | 5.27 |
| 156 | 1.46 | 5.43 | 1.60 | 5.96 |
| 169 | 1.67 | 5.88 | 1.81 | 6.41 |
| 175 | 1.88 | 6.07 | 2.02 | 6.60 |
| 177 | 2.04 | 6.12 | 2.18 | 6.65 |
| 171 | 2.29 | 5.90 | 2.43 | 6.43 |
| 159 | 2.50 | 5.48 | 2.64 | 6.01 |
| 146 | 2.71 | 5.01 | 2.85 | 5.54 |

$$\sigma_1 = P/A = \frac{P(1 - \epsilon_1)}{A_0} \quad \text{where } A_0 = 28.275 \text{ in.}^2$$

$$\epsilon_0 = \frac{\gamma \ell}{2E_1} = \frac{(0.08898)(12)}{(2)(372)} \times 100\% = 0.14\%$$

$$\sigma_0 = \frac{\gamma \ell}{2} = \frac{(0.08898)(12)}{2} = 0.53 \text{ psi}$$

TABLE A-12 UNCONFINED COMPRESSION TEST DATA, SAMPLE 12

| Load, P (lb.) | Strain, ϵ_1 (%) | Stress, σ_1 (psi) | $\epsilon = \epsilon_0 + \epsilon_1$ (%) | $\sigma = \sigma_0 + \sigma_1$ (psi) |
|------------------|-----------------------------|-----------------------------|---|---|
| 0 | 0 | 0 | 0.10 | 0.53 |
| 32 | 0.21 | 1.14 | 0.31 | 1.67 |
| 62 | 0.42 | 2.20 | 0.52 | 2.73 |
| 94 | 0.63 | 3.30 | 0.73 | 3.83 |
| 129 | 0.83 | 4.52 | 0.93 | 5.05 |
| 164 | 1.04 | 5.73 | 1.14 | 6.26 |
| 195 | 1.25 | 6.81 | 1.35 | 7.34 |
| 203 | 1.33 | 7.10 | 1.43 | 7.63 |
| 216 | 1.50 | 7.54 | 1.60 | 8.07 |
| 204 | 1.67 | 7.09 | 1.77 | 7.62 |
| 172 | 1.88 | 5.98 | 1.98 | 6.51 |

$$\sigma_1 = P/A = \frac{P(1 - \epsilon_1)}{A_0} \quad \text{where } A_0 = 28.275 \text{ in.}^2$$

$$\epsilon_0 = \frac{\gamma \ell}{2E_1} = \frac{(0.08860)(12)}{(2)(545)} \times 100\% = 0.10\%$$

$$\sigma_0 = \frac{\gamma \ell}{2} = \frac{(0.08860)(12)}{2} = 0.53 \text{ psi}$$

TABLE A-13 UNCONFINED COMPRESSION TEST DATA, SAMPLE 13

| Load, P (lb.) | Strain, ϵ_1 (%) | Stress, σ_1 (psi) | $\epsilon = \epsilon_0 + \epsilon_1$ (%) | $\sigma = \sigma_0 + \sigma_1$ (psi) |
|------------------|-----------------------------|-----------------------------|---|---|
| 0 | 0 | 0 | 0.13 | 0.53 |
| 26 | 0.21 | 0.91 | 0.34 | 1.44 |
| 48 | 0.42 | 1.68 | 0.55 | 2.21 |
| 69 | 0.63 | 2.44 | 0.76 | 2.97 |
| 94 | 0.83 | 3.31 | 0.96 | 3.84 |
| 122 | 1.04 | 4.27 | 1.17 | 4.80 |
| 149 | 1.25 | 5.20 | 1.38 | 5.73 |
| 170 | 1.46 | 5.93 | 1.59 | 6.46 |
| 191 | 1.67 | 6.64 | 1.80 | 7.17 |
| 201 | 1.88 | 6.97 | 2.01 | 7.50 |
| 199 | 2.08 | 6.89 | 2.21 | 7.42 |
| 189 | 2.29 | 6.53 | 2.42 | 7.06 |

$$\sigma_1 = P/A = \frac{P(1 - \epsilon_1)}{A_0} \quad \text{where } A_0 = 28.275 \text{ in.}^2$$

$$\epsilon_0 = \frac{\gamma l}{2E_1} = \frac{(0.08824)(12)}{(2)(398)} \times 100\% = 0.13\%$$

$$\sigma_0 = \frac{\gamma l}{2} = \frac{(0.08824)(12)}{2} = 0.53 \text{ psi}$$

TABLE A-14 UNCONFINED COMPRESSION TEST DATA, SAMPLE 14

| Load, P (lb.) | Strain, ϵ_1 (%) | Stress, σ_1 (psi) | $\epsilon = \epsilon_0 + \epsilon_1$ (%) | $\sigma = \sigma_0 + \sigma_1$ (psi) |
|------------------|-----------------------------|-----------------------------|---|---|
| 0 | 0 | 0 | 0.04 | 0.54 |
| 96 | 0.21 | 3.37 | 0.25 | 3.91 |
| 182 | 0.42 | 6.42 | 0.46 | 6.96 |
| 256 | 0.58 | 8.99 | 0.62 | 9.53 |
| 279 | 0.68 | 9.80 | 0.72 | 10.34 |
| 287 | 0.75 | 10.08 | 0.79 | 10.62 |
| 279 | 0.83 | 9.78 | 0.87 | 10.32 |
| 248 | 1.04 | 8.68 | 1.08 | 9.22 |

$$\sigma_1 = P/A = \frac{P(1 - \epsilon_1)}{A_0} \quad \text{where } A_0 = 28.275 \text{ in.}^2$$

$$\epsilon_0 = \frac{\gamma \ell}{2E_1} = \frac{(0.08951)(12)}{(2)(1542)} \times 100\% = 0.04\%$$

$$\sigma_0 = \frac{\gamma \ell}{2} = \frac{(0.08951)(12)}{2} = 0.54 \text{ psi}$$

TABLE A-15 UNCONFINED COMPRESSION TEST DATA, SAMPLE 15

| Load, P (lb.) | Strain, ϵ_1 (%) | Stress, σ_1 (psi) | $\epsilon = \epsilon_0 + \epsilon_1$ (%) | $\sigma = \sigma_0 + \sigma_1$ (psi) |
|------------------|-----------------------------|-----------------------------|---|---|
| 0 | 0 | 0 | 0.15 | 0.53 |
| 19 | 0.21 | 0.68 | 0.36 | 1.21 |
| 59 | 0.63 | 2.09 | 0.78 | 2.62 |
| 104 | 1.04 | 3.65 | 1.19 | 4.18 |
| 129 | 1.25 | 4.52 | 1.40 | 5.05 |
| 148 | 1.46 | 5.15 | 1.61 | 5.68 |
| 166 | 1.67 | 5.77 | 1.82 | 6.30 |
| 185 | 1.88 | 6.40 | 2.03 | 6.93 |
| 193 | 2.08 | 6.67 | 2.23 | 7.20 |
| 189 | 2.29 | 6.54 | 2.44 | 7.07 |
| 183 | 2.50 | 6.30 | 2.65 | 6.83 |
| 169 | 2.71 | 5.83 | 2.86 | 6.36 |

$$\sigma_1 = P/A = \frac{P(1 - \epsilon_1)}{A_0} \quad \text{where } A_0 = 28.275 \text{ in.}^2$$

$$\epsilon_0 = \frac{\gamma l}{2E_1} = \frac{(0.08751)(12)}{(2)(344)} \times 100\% = 0.15\%$$

$$\sigma_0 = \frac{\gamma l}{2} = \frac{(0.08751)(12)}{2} = 0.53 \text{ psi}$$

TABLE A-16 UNCONFINED COMPRESSION TEST DATA, SAMPLE 16

| Load, P (lb.) | Strain, ϵ_1 (%) | Stress, σ_1 (psi) | $\epsilon = \epsilon_0 + \epsilon_1$ (%) | $\sigma = \sigma_0 + \sigma_1$ (psi) |
|------------------|-----------------------------|-----------------------------|---|---|
| 0 | 0 | 0 | 0.12 | 0.53 |
| 22.3 | 0.21 | 0.79 | 0.33 | 1.32 |
| 49 | 0.42 | 1.73 | 0.54 | 2.26 |
| 74 | 0.63 | 2.60 | 0.75 | 3.13 |
| 102 | 0.83 | 3.59 | 0.95 | 4.12 |
| 131 | 1.04 | 4.60 | 1.16 | 5.13 |
| 159 | 1.25 | 5.55 | 1.37 | 6.08 |
| 176 | 1.38 | 6.13 | 1.50 | 6.66 |
| 182 | 1.46 | 6.35 | 1.58 | 6.88 |
| 185 | 1.54 | 6.46 | 1.66 | 6.99 |
| 179 | 1.67 | 6.23 | 1.79 | 6.76 |
| 167 | 1.88 | 5.78 | 2.00 | 6.31 |
| 149 | 2.08 | 5.16 | 2.20 | 5.69 |

$$\sigma_1 = P/A = \frac{P(1 - \epsilon_1)}{A_0} \quad \text{where } A_0 = 28.275 \text{ in.}^2$$

$$\epsilon_0 = \frac{\gamma l}{2E_1} = \frac{(0.08900)(12)}{(2)(446)} \times 100\% = 0.12\%$$

$$\sigma_0 = \frac{\gamma l}{2} = \frac{(0.08900)(12)}{2} = 0.53 \text{ psi}$$

TABLE A-17 UNCONFINED COMPRESSION TEST DATA, SAMPLE 17

| Load, P (lb.) | Strain, ϵ_1 (%) | Stress, σ_1 (psi) | $\epsilon = \epsilon_0 + \epsilon_1$ (%) | $\sigma = \sigma_0 + \sigma_1$ (psi) |
|------------------|-----------------------------|-----------------------------|---|---|
| 0 | 0 | 0 | 0.06 | 0.54 |
| 50 | 0.21 | 1.75 | 0.27 | 2.29 |
| 93 | 0.42 | 3.29 | 0.48 | 3.83 |
| 147 | 0.63 | 5.16 | 0.69 | 5.70 |
| 206 | 0.83 | 7.22 | 0.89 | 7.76 |
| 260 | 1.04 | 9.10 | 1.10 | 9.64 |
| 280 | 1.21 | 9.78 | 1.27 | 10.32 |
| 285 | 1.33 | 9.97 | 1.39 | 10.51 |
| 280 | 1.50 | 9.76 | 1.56 | 10.30 |
| 259 | 1.67 | 9.02 | 1.73 | 9.56 |
| 224 | 1.88 | 7.78 | 1.94 | 8.32 |

$$\sigma_1 = P/A = \frac{P(1 - \epsilon_1)}{A_0} \quad \text{where } A_0 = 28.275 \text{ in.}^2$$

$$\epsilon_0 = \frac{\gamma l}{2E_1} = \frac{(0.08930)(12)}{(2)(873)} \times 100\% = 0.06\%$$

$$\sigma_0 = \frac{\gamma l}{2} = \frac{(0.08930)(12)}{2} = 0.54 \text{ psi}$$

TABLE A-18 UNCONFINED COMPRESSION TEST DATA, SAMPLE 18

| Load, P (lb.) | Strain, ϵ_1 (%) | Stress, σ_1 (psi) | $\epsilon = \epsilon_0 + \epsilon_1$ (%) | $\sigma = \sigma_0 + \sigma_1$ (psi) |
|------------------|-----------------------------|-----------------------------|---|---|
| 0 | 0 | 0 | 0.03 | 0.53 |
| 87 | 0.21 | 3.08 | 0.24 | 3.61 |
| 196 | 0.42 | 6.89 | 0.45 | 7.42 |
| 336 | 0.63 | 11.80 | 0.66 | 12.33 |
| 457 | 0.79 | 16.01 | 0.82 | 16.54 |
| 494 | 0.90 | 17.32 | 0.93 | 17.85 |
| 457 | 1.04 | 15.98 | 1.07 | 16.51 |
| 386 | 1.25 | 13.47 | 1.28 | 14.00 |

$$\sigma_1 = P/A = \frac{P(1 - \epsilon_1)}{A_0} \quad \text{where } A_0 = 28.275 \text{ in.}^2$$

$$\epsilon_0 = \frac{\gamma l}{2E_1} = \frac{(0.08896)(12)}{(2)(2026)} \times 100\% = 0.03\%$$

$$\sigma_0 = \frac{\gamma l}{2} = \frac{(0.08896)(12)}{2} = 0.53 \text{ psi}$$

TABLE A-19 UNCONFINED COMPRESSION TEST DATA, SAMPLE 19

| Load, P (lb.) | Strain, ϵ_1 (%) | Stress, σ_1 (psi) | $\epsilon = \epsilon_0 + \epsilon_1$ (%) | $\sigma = \sigma_0 + \sigma_1$ (psi) |
|------------------|-----------------------------|-----------------------------|---|---|
| 0 | 0 | 0 | 0.08 | 0.54 |
| 37 | 0.21 | 1.29 | 0.29 | 1.83 |
| 73 | 0.42 | 2.68 | 0.50 | 3.22 |
| 115 | 0.63 | 4.04 | 0.71 | 4.58 |
| 160 | 0.83 | 5.61 | 0.91 | 6.15 |
| 210 | 1.04 | 7.35 | 1.12 | 7.89 |
| 247 | 1.25 | 8.62 | 1.33 | 9.16 |
| 260 | 1.38 | 9.07 | 1.46 | 9.61 |
| 266 | 1.46 | 9.27 | 1.54 | 9.81 |
| 260 | 1.58 | 9.05 | 1.66 | 9.59 |
| 225 | 1.79 | 7.82 | 1.87 | 8.36 |
| 181 | 2.00 | 6.27 | 2.08 | 6.81 |

$$\sigma_1 = P/A = \frac{P(1 - \epsilon_1)}{A_0} \quad \text{where } A_0 = 28.275 \text{ in.}^2$$

$$\epsilon_0 = \frac{\gamma \ell}{2E_1} = \frac{(0.08989)(12)}{(2)(690)} \times 100\% = 0.08\%$$

$$\sigma_0 = \frac{\gamma \ell}{2} = \frac{(0.08989)(12)}{2} = 0.54 \text{ psi}$$

TABLE A-20 UNCONFINED COMPRESSION TEST DATA, SAMPLE 20

| Load, P (lb.) | Strain, ϵ_1 (%) | Stress, σ_1 (psi) | $\epsilon = \epsilon_0 + \epsilon_1$ (%) | $\sigma = \sigma_0 + \sigma_1$ (psi) |
|------------------|-----------------------------|-----------------------------|---|---|
| 0 | 0 | 0 | 0.12 | 0.54 |
| 20 | 0.21 | 0.71 | 0.33 | 1.25 |
| 41 | 0.42 | 1.43 | 0.54 | 1.97 |
| 67 | 0.63 | 2.35 | 0.75 | 2.89 |
| 94 | 0.83 | 3.30 | 0.95 | 3.84 |
| 127 | 1.04 | 4.43 | 1.16 | 4.97 |
| 156 | 1.25 | 5.45 | 1.37 | 5.99 |
| 167 | 1.33 | 5.84 | 1.45 | 6.38 |
| 177 | 1.46 | 6.16 | 1.58 | 6.70 |
| 167 | 1.58 | 5.80 | 1.70 | 6.34 |
| 147 | 1.75 | 5.12 | 1.87 | 5.66 |
| 137 | 1.88 | 4.74 | 2.00 | 5.28 |

$$\sigma_1 = P/A = \frac{P(1 - \epsilon_1)}{A_0} \quad \text{where } A_0 = 28.275 \text{ in.}^2$$

$$\epsilon_0 = \frac{\gamma \ell}{2E_1} = \frac{(0.08954)(12)}{(2)(450)} \times 100\% = 0.12\%$$

$$\sigma_0 = \frac{\gamma \ell}{2} = \frac{(0.08954)(12)}{2} = 0.54 \text{ psi}$$

TABLE A-21 UNCONFINED COMPRESSION TEST DATA, SAMPLE 21

| Load, P (lb.) | Strain, ϵ_1 (%) | Stress, σ_1 (psi) | $\epsilon = \epsilon_0 + \epsilon_1$ (%) | $\sigma = \sigma_0 + \sigma_1$ (psi) |
|------------------|-----------------------------|-----------------------------|---|---|
| 0 | 0 | 0 | 0.04 | 0.54 |
| 63 | 0.21 | 2.22 | 0.25 | 2.76 |
| 153 | 0.42 | 5.38 | 0.46 | 5.92 |
| 236 | 0.63 | 8.30 | 0.67 | 8.84 |
| 303 | 0.79 | 10.62 | 0.83 | 11.16 |
| 313 | 0.83 | 10.97 | 0.87 | 11.51 |
| 329 | 0.92 | 11.51 | 0.96 | 12.05 |
| 332 | 0.96 | 11.63 | 1.00 | 12.17 |
| 329 | 1.04 | 11.53 | 1.08 | 12.07 |
| 313 | 1.25 | 10.92 | 1.29 | 11.46 |
| 275 | 1.46 | 9.59 | 1.50 | 10.13 |

$$\sigma_1 = P/A = \frac{P(1 - \epsilon_1)}{A_0} \quad \text{where } A_0 = 28.275 \text{ in.}^2$$

$$\epsilon_0 = \frac{\gamma \ell}{2E_1} = \frac{(0.09081)(12)}{(2)(1317)} \times 100\% = 0.04\%$$

$$\sigma_0 = \frac{\gamma \ell}{2} = \frac{(0.09081)(12)}{2} = 0.54 \text{ psi}$$

TABLE A-22 UNCONFINED COMPRESSION TEST DATA, SAMPLE 22

| Load, P (lb.) | Strain, ϵ_1 (%) | Stress, σ_1 (psi) | $\epsilon = \epsilon_0 + \epsilon_1$ (%) | $\sigma = \sigma_0 + \sigma_1$ (psi) |
|------------------|-----------------------------|-----------------------------|---|---|
| 0 | 0 | 0 | 0.02 | 0.55 |
| 181 | 0.21 | 6.39 | 0.23 | 6.94 |
| 328 | 0.42 | 11.54 | 0.44 | 12.09 |
| 452 | 0.63 | 15.91 | 0.65 | 16.46 |
| 475 | 0.67 | 16.68 | 0.69 | 17.23 |
| 490 | 0.73 | 17.21 | 0.75 | 17.76 |
| 461 | 0.79 | 16.81 | 0.81 | 16.73 |
| 432 | 0.83 | 15.15 | 0.85 | 15.70 |

$$\sigma_1 = P/A = \frac{P(1 - \epsilon_1)}{A_0} \quad \text{where } A_0 = 28.275 \text{ in.}^2$$

$$\epsilon_0 = \frac{\gamma \ell}{2E_1} = \frac{(0.09101)(12)}{(2)(2827)} \times 100\% = 0.02\%$$

$$\sigma_0 = \frac{\gamma \ell}{2} = \frac{(0.09101)(12)}{2} = 0.55 \text{ psi}$$

TABLE A-23 UNCONFINED COMPRESSION TEST DATA, SAMPLE 23

| Load, P (lb.) | Strain, ϵ_1 (%) | Stress, σ_1 (psi) | $\epsilon = \epsilon_0 + \epsilon_1$ (%) | $\sigma = \sigma_0 + \sigma_1$ (psi) |
|------------------|-----------------------------|-----------------------------|---|---|
| 0 | 0 | 0 | 0.16 | 0.54 |
| 26 | 0.21 | 0.92 | 0.37 | 1.46 |
| 48 | 0.42 | 1.70 | 0.58 | 2.24 |
| 65 | 0.63 | 2.30 | 0.79 | 2.84 |
| 83 | 0.83 | 2.90 | 0.99 | 3.44 |
| 106 | 1.13 | 3.71 | 1.29 | 4.25 |
| 111 | 1.25 | 3.88 | 1.41 | 4.42 |
| 116 | 1.38 | 4.05 | 1.54 | 4.59 |
| 118 | 1.46 | 4.11 | 1.62 | 4.65 |
| 116 | 1.67 | 4.02 | 1.83 | 4.56 |
| 113 | 1.88 | 3.91 | 2.04 | 4.45 |
| 108 | 2.08 | 3.75 | 2.24 | 4.29 |
| 102 | 2.29 | 3.52 | 2.45 | 4.06 |

$$\sigma_1 = P/A = \frac{P(1 - \epsilon_1)}{A_0} \quad \text{where } A_0 = 28.275 \text{ in.}^2$$

$$\epsilon_0 = \frac{\gamma \ell}{2E_1} = \frac{(0.08933)(12)}{(2)(329)} \times 100\% = 0.16\%$$

$$\sigma_0 = \frac{\gamma \ell}{2} = \frac{(0.08933)(12)}{2} = 0.54 \text{ psi}$$

TABLE A-24 UNCONFINED COMPRESSION TEST DATA, SAMPLE 24

| Load, P (lb.) | Strain, ϵ_1 (%) | Stress, σ_1 (psi) | $\epsilon = \epsilon_0 + \epsilon_1$ (%) | $\sigma = \sigma_0 + \sigma_1$ (psi) |
|------------------|-----------------------------|-----------------------------|---|---|
| 0 | 0 | 0 | 0.02 | 0.54 |
| 156 | 0.21 | 5.49 | 0.23 | 6.03 |
| 297 | 0.42 | 10.41 | 0.44 | 10.95 |
| 354 | 0.50 | 12.46 | 0.52 | 13.00 |
| 396 | 0.58 | 13.91 | 0.60 | 14.45 |
| 419 | 0.68 | 14.73 | 0.65 | 15.27 |
| 421 | 0.69 | 14.78 | 0.71 | 15.32 |
| 379 | 0.79 | 13.30 | 0.81 | 13.84 |
| 362 | 0.88 | 12.70 | 0.90 | 13.24 |

$$\sigma_1 = P/A = \frac{P(1 - \epsilon_1)}{A_0} \quad \text{where } A_0 = 28.275 \text{ in.}^2$$

$$\epsilon_0 = \frac{\gamma \ell}{2E_1} = \frac{(0.09066)(12)}{(2)(2473)} \times 100\% = 0.02\%$$

$$\sigma_0 = \frac{\gamma \ell}{2} = \frac{(0.09066)(12)}{2} = 0.54 \text{ psi}$$

TABLE A-25 UNCONFINED COMPRESSION TEST DATA, SAMPLE 25

| Load, P (lb.) | Strain, ϵ_1 (%) | Stress, σ_1 (psi) | $\epsilon = \epsilon_0 + \epsilon_1$ (%) | $\sigma = \sigma_0 + \sigma_1$ (psi) |
|------------------|-----------------------------|-----------------------------|---|---|
| 0 | 0 | 0 | 0.04 | 0.54 |
| 90 | 0.21 | 3.17 | 0.25 | 3.71 |
| 167 | 0.42 | 5.87 | 0.46 | 6.41 |
| 253 | 0.63 | 8.90 | 0.67 | 9.44 |
| 293 | 0.75 | 10.30 | 0.79 | 10.84 |
| 310 | 0.83 | 10.87 | 0.87 | 11.41 |
| 318 | 0.96 | 11.15 | 1.00 | 11.69 |
| 314 | 1.04 | 11.00 | 1.08 | 11.54 |
| 277 | 1.25 | 9.66 | 1.29 | 10.20 |
| 227 | 1.46 | 7.90 | 1.50 | 8.44 |

$$\sigma_1 = P/A = \frac{P(1 - \epsilon_1)}{A_0} \quad \text{where } A_0 = 28.275 \text{ in.}^2$$

$$\epsilon_0 = \frac{\gamma \ell}{2E_1} = \frac{(0.09054)(12)}{(2)(1373)} \times 100\% = 0.04\%$$

$$\sigma_0 = \frac{\gamma \ell}{2} = \frac{(0.09054)(12)}{2} = 0.54 \text{ psi}$$

TABLE A- 26 UNCONFINED COMPRESSION TEST DATA, SAMPLE 26

| Load, P (lb.) | Strain, ϵ_1 (%) | Stress, σ_1 (psi) | $\epsilon = \epsilon_0 + \epsilon_1$ (%) | $\sigma = \sigma_0 + \sigma_1$ (psi) |
|------------------|-----------------------------|-----------------------------|---|---|
| 0 | 0 | 0 | 0.15 | 0.53 |
| 19 | 0.21 | 0.68 | 0.36 | 1.21 |
| 38 | 0.42 | 1.33 | 0.57 | 1.86 |
| 56 | 0.63 | 1.97 | 0.78 | 2.50 |
| 79 | 0.83 | 2.78 | 0.98 | 3.31 |
| 100 | 1.04 | 3.51 | 1.19 | 4.04 |
| 123 | 1.25 | 4.28 | 1.40 | 4.81 |
| 142 | 1.42 | 4.94 | 1.57 | 5.47 |
| 150 | 1.54 | 5.23 | 1.69 | 5.76 |
| 156 | 1.67 | 5.43 | 1.82 | 5.96 |
| 159 | 1.88 | 5.53 | 2.03 | 6.06 |
| 153 | 2.08 | 5.28 | 2.23 | 5.81 |
| 144 | 2.29 | 4.99 | 2.44 | 5.52 |

$$\sigma_1 = P/A = \frac{P(1 - \epsilon_1)}{A_0} \quad \text{where } A_0 = 28.275 \text{ in.}^2$$

$$\epsilon_0 = \frac{\gamma \ell}{2E_1} = \frac{(0.08751)(12)}{(2)(340)} \times 100\% = 0.15\%$$

$$\sigma_0 = \frac{\gamma \ell}{2} = \frac{(0.08751)(12)}{2} = 0.53 \text{ psi}$$

TABLE A-27 UNCONFINED COMPRESSION TEST DATA, SAMPLE 27

| Load, P (lb.) | Strain, ϵ_1 (%) | Stress, σ_1 (psi) | $\epsilon = \epsilon_0 + \epsilon_1$ (%) | $\sigma = \sigma_0 + \sigma_1$ (psi) |
|------------------|-----------------------------|-----------------------------|---|---|
| 0 | 0 | 0 | 0.05 | 0.54 |
| 33 | 0.21 | 1.18 | 0.26 | 1.72 |
| 83 | 0.42 | 2.94 | 0.47 | 3.48 |
| 150 | 0.63 | 5.27 | 0.68 | 5.81 |
| 232 | 0.83 | 8.13 | 0.88 | 8.67 |
| 268 | 0.94 | 9.40 | 0.99 | 9.94 |
| 278 | 1.00 | 9.75 | 1.05 | 10.29 |
| 293 | 1.10 | 10.26 | 1.15 | 10.80 |
| 285 | 1.17 | 9.96 | 1.22 | 10.50 |
| 272 | 1.29 | 9.51 | 1.34 | 10.05 |
| 243 | 1.58 | 8.47 | 1.63 | 9.01 |

$$\sigma_1 = P/A = \frac{P(1 - \epsilon_1)}{A_0} \quad \text{where } A_0 = 28.275 \text{ in.}^2$$

$$\epsilon_0 = \frac{\gamma \ell}{2E_1} = \frac{(0.08972)(12)}{(2)(1002)} \times 100\% = 0.05\%$$

$$\sigma_0 = \frac{\gamma \ell}{2} = \frac{(0.08972)(12)}{2} = 0.54 \text{ psi}$$

TABLE A-28 UNCONFINED COMPRESSION TEST DATA, SAMPLE 28

| Load, P (lb.) | Strain, ϵ_1 (%) | Stress, σ_1 (psi) | $\epsilon = \epsilon_0 + \epsilon_1$ (%) | $\sigma = \sigma_0 + \sigma_1$ (psi) |
|------------------|-----------------------------|-----------------------------|---|---|
| 0 | 0 | 0 | 0.08 | 0.53 |
| 47 | 0.21 | 1.65 | 0.29 | 2.18 |
| 87 | 0.42 | 3.05 | 0.50 | 3.58 |
| 130 | 0.63 | 4.57 | 0.71 | 5.10 |
| 150 | 0.75 | 5.27 | 0.83 | 5.80 |
| 167 | 0.83 | 5.85 | 0.91 | 6.38 |
| 178 | 0.92 | 6.25 | 1.00 | 6.78 |
| 187 | 1.00 | 6.54 | 1.08 | 7.07 |
| 190 | 1.08 | 6.65 | 1.16 | 7.18 |
| 183 | 1.25 | 6.40 | 1.33 | 6.93 |
| 170 | 1.46 | 5.93 | 1.54 | 6.46 |
| 157 | 1.67 | 5.45 | 1.75 | 5.98 |

$$\sigma_1 = P/A = \frac{P(1 - \epsilon_1)}{A_0} \quad \text{where } A_0 = 28.275 \text{ in.}^2$$

$$\epsilon_0 = \frac{\gamma \ell}{2E_1} = \frac{(0.08854)(12)}{(2)(702)} \times 100\% = 0.08\%$$

$$\sigma_0 = \frac{\gamma \ell}{2} = \frac{(0.08854)(12)}{2} = 0.53 \text{ psi}$$

TABLE A-29 UNCONFINED COMPRESSION TEST DATA, SAMPLE 29

| Load, P (lb.) | Strain, ϵ_1 (%) | Stress, σ_1 (psi) | $\epsilon = \epsilon_0 + \epsilon_1$ (%) | $\sigma = \sigma_0 + \sigma_1$ (psi) |
|------------------|-----------------------------|-----------------------------|---|---|
| 0 | 0 | 0 | 0.14 | 0.51 |
| 27 | 0.21 | 0.94 | 0.35 | 1.45 |
| 48 | 0.42 | 1.70 | 0.56 | 2.21 |
| 73 | 0.63 | 2.58 | 0.77 | 3.09 |
| 93 | 0.83 | 3.27 | 0.97 | 3.78 |
| 112 | 1.04 | 3.91 | 1.18 | 4.42 |
| 130 | 1.25 | 4.54 | 1.39 | 5.05 |
| 142 | 1.46 | 4.94 | 1.60 | 5.45 |
| 150 | 1.67 | 5.22 | 1.81 | 5.73 |
| 147 | 1.88 | 5.09 | 2.02 | 5.60 |
| 137 | 2.08 | 4.73 | 2.22 | 5.24 |

$$\sigma_1 = P/A = \frac{P(1 - \epsilon_1)}{A_0} \quad \text{where } A_0 = 28.275 \text{ in.}^2$$

$$\epsilon_0 = \frac{\gamma l}{2E_1} = \frac{(0.08583)(12)}{(2)(371)} \times 100\% = 0.14\%$$

$$\sigma_0 = \frac{\gamma l}{2} = \frac{(0.08583)(12)}{2} = 0.51 \text{ psi}$$

TABLE A-30 UNCONFINED COMPRESSION TEST DATA, SAMPLE 30

| Load, P (lb.) | Strain, ϵ_1 (%) | Stress, σ_1 (psi) | $\epsilon = \epsilon_0 + \epsilon_1$ (%) | $\sigma = \sigma_0 + \sigma_1$ (psi) |
|------------------|-----------------------------|-----------------------------|---|---|
| 0 | 0 | 0 | 0.06 | 0.53 |
| 57 | 0.21 | 2.00 | 0.27 | 2.53 |
| 117 | 0.42 | 4.11 | 0.48 | 4.64 |
| 173 | 0.63 | 6.09 | 0.69 | 6.62 |
| 217 | 0.83 | 7.60 | 0.89 | 8.13 |
| 228 | 0.92 | 8.00 | 0.98 | 8.53 |
| 240 | 1.04 | 8.40 | 1.10 | 8.93 |
| 247 | 1.13 | 8.62 | 1.19 | 9.15 |
| 240 | 1.25 | 8.38 | 1.31 | 8.91 |
| 217 | 1.46 | 7.55 | 1.52 | 8.08 |
| 197 | 1.67 | 6.84 | 1.73 | 7.37 |

$$\sigma_1 = P/A = \frac{P(1 - \epsilon_1)}{A_0} \quad \text{where } A_0 = 28.275 \text{ in.}^2$$

$$\epsilon_0 = \frac{\gamma \ell}{2E_1} = \frac{(0.08842)(12)}{(2)(912)} \times 100\% = 0.06\%$$

$$\sigma_0 = \frac{\gamma \ell}{2} = \frac{(0.08842)(12)}{2} = 0.53 \text{ psi}$$

TABLE A-31 UNCONFINED COMPRESSION TEST DATA, SAMPLE 31

| Load, P (lb.) | Strain, ϵ_1 (%) | Stress, σ_1 (psi) | $\epsilon = \epsilon_0 + \epsilon_1$ (%) | $\sigma = \sigma_0 + \sigma_1$ (psi) |
|------------------|-----------------------------|-----------------------------|---|---|
| 0 | 0 | 0 | 0.02 | 0.49 |
| 88 | 0.13 | 3.11 | 0.15 | 3.60 |
| 143 | 0.21 | 5.05 | 0.23 | 5.54 |
| 166 | 0.25 | 5.87 | 0.27 | 6.36 |
| 186 | 0.29 | 6.57 | 0.31 | 7.06 |
| 196 | 0.33 | 6.92 | 0.35 | 7.41 |
| 204 | 0.42 | 7.19 | 0.44 | 7.68 |
| 193 | 0.50 | 6.79 | 0.52 | 7.28 |
| 173 | 0.63 | 6.08 | 0.65 | 6.57 |

$$\sigma_1 = P/A = \frac{P(1 - \epsilon_1)}{A_0} \quad \text{where } A_0 = 28.275 \text{ in.}^2$$

$$\epsilon_0 = \frac{\gamma \ell}{2E_1} = \frac{(0.08123)(12)}{(2)(2250)} \times 100\% = 0.02\%$$

$$\sigma_0 = \frac{\gamma \ell}{2} = \frac{(0.08123)(12)}{2} = 0.49 \text{ psi}$$

TABLE A-32 UNCONFINED COMPRESSION TEST DATA, SAMPLE 32

| Load, P (lb.) | Strain, ϵ_1 (%) | Stress, σ_1 (psi) | $\epsilon = \epsilon_0 + \epsilon_1$ (%) | $\sigma = \sigma_0 + \sigma_1$ (psi) |
|------------------|-----------------------------|-----------------------------|---|---|
| 0 | 0 | 0 | 0.03 | 0.55 |
| 82 | 0.21 | 2.88 | 0.24 | 3.43 |
| 183 | 0.42 | 6.43 | 0.45 | 6.98 |
| 296 | 0.63 | 10.40 | 0.66 | 10.95 |
| 338 | 0.71 | 11.86 | 0.74 | 12.41 |
| 359 | 0.79 | 12.58 | 0.83 | 13.13 |
| 350 | 0.88 | 12.28 | 0.91 | 12.83 |
| 328 | 1.00 | 11.47 | 1.03 | 12.02 |

$$\sigma_1 = P/A = \frac{P(1 - \epsilon_1)}{A_0} \quad \text{where } A_0 = 28.275 \text{ in.}^2$$

$$\epsilon_0 = \frac{\gamma \ell}{2E_1} = \frac{(0.09120)(12)}{(2)(1675)} \times 100\% = 0.03\%$$

$$\sigma_0 = \frac{\gamma \ell}{2} = \frac{(0.09120)(12)}{2} = 0.55 \text{ psi}$$

TABLE A-33 UNCONFINED COMPRESSION TEST DATA, SAMPLE 33

| Load, P (lb.) | Strain, ϵ_1 (%) | Stress, σ_1 (psi) | $\epsilon = \epsilon_0 + \epsilon_1$ (%) | $\sigma = \sigma_0 + \sigma_1$ (psi) |
|------------------|-----------------------------|-----------------------------|---|---|
| 0 | 0 | 0 | 0.03 | 0.53 |
| 99 | 0.21 | 3.51 | 0.24 | 4.04 |
| 203 | 0.38 | 7.14 | 0.41 | 7.67 |
| 223 | 0.42 | 7.84 | 0.45 | 8.37 |
| 256 | 0.50 | 9.01 | 0.54 | 9.54 |
| 292 | 0.63 | 10.26 | 0.66 | 10.79 |
| 300 | 0.71 | 10.54 | 0.74 | 11.07 |
| 296 | 0.75 | 10.39 | 0.78 | 10.92 |
| 329 | 0.88 | 11.55 | 0.91 | 12.08 |
| 314 | 0.96 | 11.01 | 0.99 | 11.54 |
| 321 | 1.04 | 11.24 | 1.07 | 11.77 |
| 311 | 1.25 | 10.86 | 1.28 | 11.39 |
| 279 | 1.46 | 9.74 | 1.49 | 10.27 |

$$\sigma_1 = P/A = \frac{P(1 - \epsilon_1)}{A_0} \quad \text{where } A_0 = 28.275 \text{ in.}^2$$

$$\epsilon_0 = \frac{\gamma \ell}{2E_1} = \frac{(0.08786)(12)}{(2)(1802)} \times 100\% = 0.03\%$$

$$\sigma_0 = \frac{\gamma \ell}{2} = \frac{(0.08786)(12)}{2} = 0.53 \text{ psi}$$

TABLE A-34 UNCONFINED COMPRESSION TEST DATA, SAMPLE 34

| Load, P (lb.) | Strain, ϵ_1 (%) | Stress, σ_1 (psi) | $\epsilon = \epsilon_0 + \epsilon_1$ (%) | $\sigma = \sigma_0 + \sigma_1$ (psi) |
|------------------|-----------------------------|-----------------------------|---|---|
| 0 | 0 | 0 | 0.05 | 0.54 |
| 28 | 0.14 | 1.00 | 0.19 | 1.54 |
| 62 | 0.28 | 2.18 | 0.33 | 2.72 |
| 102 | 0.42 | 3.58 | 0.47 | 4.12 |
| 148 | 0.56 | 5.22 | 0.61 | 5.76 |
| 198 | 0.69 | 6.97 | 0.74 | 7.51 |
| 245 | 0.83 | 8.59 | 0.88 | 9.13 |
| 283 | 0.97 | 9.91 | 1.03 | 10.45 |
| 303 | 1.04 | 10.62 | 1.09 | 11.16 |
| 311 | 1.11 | 10.87 | 1.16 | 11.41 |
| 312 | 1.18 | 10.89 | 1.23 | 11.43 |
| 303 | 1.25 | 10.60 | 1.30 | 11.14 |
| 287 | 1.32 | 10.00 | 1.37 | 10.54 |

$$\sigma_1 = P/A = \frac{P(1 - \epsilon_1)}{A_0} \quad \text{where } A_0 = 28.275 \text{ in.}^2$$

$$\epsilon_0 = \frac{\gamma \ell}{2E_1} = \frac{(0.08980)(12)}{(2)(1019)} \times 100\% = 0.05\%$$

$$\sigma_0 = \frac{\gamma \ell}{2} = \frac{(0.08980)(12)}{2} = 0.54 \text{ psi}$$

APPENDIX B

Table B-1. Basic Water Content Test Data

| G_a (surface dry) = 2.68 | | Absorption = 1.28% | | Fineness Modulus = 2.95 | | $G_c = 3.12$ | | Volume of Mold = 404 c.c. | | | | | | | |
|----------------------------|-------------|--------------------|--------------|-------------------------|--------------|--------------------|------|---------------------------|-----------------------------|------------------------|-------------|-------|-------|-------|-------|
| a_m/c_m | $a_m + c_m$ | Sand weight (gm.) | a_m (c.c.) | Cement weight (gm.) | c_m (c.c.) | Water weight (gm.) | % | Total Wt. of Mat'l. (gm.) | Wt. of Mortar in Mold (gm.) | Volume of Batch (c.c.) | % of Solids | V_m | W_m | | |
| 2 | 336 | 600 | 224 | 349 | 112 | 0 | 0 | 949 | 767 | 545 | 0.617 | 0.383 | 0.156 | | |
| | | | | | | 85 | 9 | 1034 | 798 | 529 | 0.635 | 0.365 | 0.180 | | |
| | | | | | | 104 | 10 | 1044 | 903 | 471 | 0.713 | 0.287 | 0.221 | | |
| | | | | | | 114 | 11 | 1053 | 924 | 465 | 0.723 | 0.277 | 0.245 | | |
| | | | | | | 123 | 12 | 1063 | 932 | 464 | 0.724 | 0.276 | 0.265 | | |
| | | | | | | 133 | 13 | 1072 | 921 | 475 | 0.707 | 0.293 | 0.280 | | |
| | | | | | | 123 | 14 | 1082 | 931 | 464 | 0.724 | 0.276 | 0.265 | | |
| | | | | | | 142 | 15 | 1091 | 918 | 480 | 0.700 | 0.300 | 0.296 | | |
| | | | | | | 171 | 18 | 1120 | 910 | 497 | 0.676 | 0.324 | 0.344 | | |
| | | | | 681 | 254 | 264 | 84.7 | 0 | 0 | 945 | 924 | 459 | 0.738 | 0.262 | 0.277 |
| | | | | | | | | 104 | 11 | 1049 | 933 | 458 | 0.739 | 0.261 | 0.247 |
| | | | | | | | | 113 | 12 | 1058 | 928 | 465 | 0.728 | 0.272 | 0.265 |
| | | | | | | | | 123 | 13 | 1068 | 933 | 458 | 0.739 | 0.261 | 0.247 |
| | | | | | | | | 113 | 12 | 1058 | 919 | 473 | 0.715 | 0.284 | 0.279 |
| | | | | | | 132 | 14 | 1077 | 909 | 492 | 0.688 | 0.312 | 0.327 | | |
| | | | | | | 161 | 17 | 1106 | 955 | 459 | 0.751 | 0.249 | 0.209 | | |
| | | 740 | 276 | 215 | 69 | 0 | 0 | 955 | 927 | 459 | 0.751 | 0.249 | 0.209 | | |
| | | | | | | 96 | 10 | 1051 | 932 | 459 | 0.752 | 0.248 | 0.229 | | |
| | | | | | | 105 | 11 | 1060 | 922 | 469 | 0.736 | 0.264 | 0.245 | | |
| | | | | | | 115 | 12 | 1070 | 932 | 459 | 0.752 | 0.248 | 0.229 | | |
| | | | | | | 105 | 11 | 1060 | 919 | 474 | 0.727 | 0.273 | 0.262 | | |
| | | | | | | 124 | 13 | 1079 | 910 | 492 | 0.701 | 0.299 | 0.311 | | |
| | | | | | | 153 | 16 | 1108 | | | | | | | |

note: Volume of Batch = (Total Wt. of Mat'l/Wt. of Mortar in Mold) x Volume of Mold; % of Solids = $(a_m + c_m)/\text{Volume of Batch}$;
 $V_m = 1 - \% \text{ of Solids}$; $W_m = \text{Weight of Water/Volume of Batch}$

APPENDIX C

APPENDIX C

CRITICAL MORTAR CONTENT CALCULATION

From Tables 51, 5.2 and 5.3 it is known that

$$\left\{ \begin{array}{l} \text{Voids content @ } \gamma_b, e = 32.3\% - \text{ dry rod} \\ \text{Voids content @ } \gamma_{dl}, e = 37.7\% - \text{ dry loose} \\ \text{Voids content @ } \gamma_{dv}, e = 30.4\% - \text{ dry vibrated} \\ G_a = 2.68, G_b = 2.64 \\ G_c = 3.12 \\ \gamma_w = 62.4 \text{ pcf} \end{array} \right.$$

It is also known from Table 5.5 that all samples using mortar content as a variable, such as Sample 5, has the following mix proportions:

$$\left\{ \begin{array}{l} W_a/W_c = 1.934 \\ W_w/W_c = 0.38 \end{array} \right.$$

The volume of mortar, V_m , is the combination of volume of cement, fine aggregate and water provided the volume of voids is excluded. Therefore:

$$\begin{aligned} V_m &= V_c + V_a + V_w \\ &= \frac{W_c}{G_c \gamma_w} + \frac{W_a}{G_a \gamma_w} + \frac{W_w}{\gamma_w} \\ &= \left[\frac{W_c/W_a}{G_c \gamma_w} + \frac{1}{G_a \gamma_w} + \frac{(W_w/W_c)(W_c/W_a)}{\gamma_w} \right] W_a \end{aligned}$$

Substitution of all the known values gives:

$$V_m = 0.0117843 W_a \quad (C-1)$$

Assuming the air content is 2.3 percent and also that 2 percent of the mortar is lost in the mixing bowl, then a unit volume of concrete, V , will contain a volume of mortar as:

$$V_m = \frac{(e - 2.3\%)}{(1 - 2\%)} V \quad (C-2)$$

In the case of a critical mortar content there is no excess mortar except that which fills the voids between the coarse aggregate particles. The two equations, (C-1) and (C-2), when equated give the weight of fine aggregates in a unit volume of concrete.

Then:

$$W_a = 86.6 (e - 2.3\%)V \quad (C-3)$$

The weight of coarse aggregate in a unit volume of concrete is determined by:

$$\begin{aligned} W_b &= G_b \gamma_w V_b = G_b \gamma_w (V - V_v) = G_b \gamma_w V (1 - e) \\ &= 164.7 V (1 - e) \end{aligned} \quad (C-4)$$

Weights of cement and water in a unit volume of concrete are determined by the W_a/W_c and W_w/W_c ratios.

1. For the dry rod case $e = 32.3\%$. Using Equation (C-3):

$$W_a = 86.6(0.323 - 0.023)V = 25.98V$$

$$W_c = W_a/1.934 = 13.433V$$

$$W_w = 0.38 W_c = 5.105V$$

Using Equation (C-4):

$$W_b = 164.7(1 - 0.323) V = 111.502 V$$

The critical mortar content is then given by the expression

$$M_{cr} = \frac{W_a + W_c + W_w}{W} = \frac{(25.98 + 13.433 + 5.105)}{(25.98 + 13.433 + 5.105 + 111.502)} \frac{V}{V}$$

$$= 0.285$$

2. For the dry loose case $e = 37.7\%$. Using Equation (C-3):

$$W_a = 86.6(0.377 - 0.023)V = 30.656V$$

$$W_c = W_a/1.934 = 15.851V$$

$$W_w = 0.38 W_c = 6.024 V$$

Using Equation (C-4):

$$W_b = 164.7(1 - 0.377)V = 102.608 V$$

Critical mortar content is then

$$M_{cr} = \frac{W_a + W_c + W_w}{W} = \frac{(30.656 + 15.851 + 6.024)}{(30.656 + 15.851 + 6.024 + 102.608)} \frac{V}{V}$$

$$= 0.339$$

3. For the dry vibrated case $e = 30.4\%$. Using Equation (C-3):

$$W_a = 86.6 (0.304 - 0.023)V = 24.335 V$$

$$W_c = W_a/1.934 = 12.583V$$

$$W_w = 0.38 W_c = 4.781 V$$

Using Equation (C-4):

$$W_b = 164.7(1 - 0.304)V = 114.631 V$$



Critical mortar content is then

$$M_{cr} = \frac{W_a + W_c + W_w}{W} = \frac{(24.335 + 12.583 + 4.781)}{(24.335 + 12.583 + 4.781 + 114.631)} \frac{V}{V}$$
$$= 0.267$$

APPENDIX D

TYPICAL WORK SHEET FOR MIX PROPORTION

SAMPLE NO. 2

Proportioning

$$W_w/W_c = 0.38 \quad W_a/W_c = 1.934 \quad W_a/W_b = 0.588 \quad M = 0.498$$

$$\text{Sand} = W_a = \quad \quad \quad = 10.29 \text{ lb}$$

$$\text{Gravel} = W_b = 10.29 \text{ lb}/0.588 = 17.50 \text{ lb}$$

$$\text{Cement} = W_c = 10.29 \text{ lb}/1.934 = 5.32 \text{ lb}$$

$$\text{Water} = W_w = 5.32 \text{ lb} \times 0.38 = 2.02 \text{ lb}$$

$$\text{Total Weight of Mix} = \quad \quad \quad W = 35.13 \text{ lb}$$

Gradation

$$\underline{W_b = 17.5 \text{ lb (6A round gravel):}}$$

$$1\text{-in.} - 3/4\text{-in.} \quad 17.5 \text{ lb} \times 23\% = 4.02 \text{ lb}$$

$$3/4\text{-in.} - 1/2\text{-in.} \quad 17.5 \text{ lb} \times 28\% = 4.90 \text{ lb}$$

$$1/2\text{-in.} - 3/8\text{-in.} \quad 17.5 \text{ lb} \times 17\% = 2.98 \text{ lb}$$

$$3/8\text{-in.} - \text{No. 4} \quad \underline{17.5 \text{ lb} \times 32\% = 5.60 \text{ lb}}$$

$$17.5 \text{ lb} \times 100\% = 17.5 \text{ lb}$$

$$\underline{W_a = 10.29 \text{ lb (2NS sand):}}$$

$$\text{No. 4} - \text{No. 8} \quad 10.29 \text{ lb} \times 18\% = 1.85 \text{ lb}$$

$$\text{No. 8} - \text{No. 16} \quad 10.29 \text{ lb} \times 18\% = 1.85 \text{ lb}$$

$$\text{No. 16} - \text{No. 30} \quad 10.29 \text{ lb} \times 24\% = 2.47 \text{ lb}$$

$$\text{No. 30} - \text{No. 100} \quad 10.29 \text{ lb} \times 39\% = 4.01 \text{ lb}$$

$$\text{Passing No. 100} \quad \underline{10.29 \text{ lb} \times 1\% = 0.11 \text{ lb}}$$

$$10.29 \text{ lb} \times 100\% = 10.29 \text{ lb}$$

APPENDIX E

APPENDIX E.1

Unconfined Compression Test on Low Slump Concrete

1. Mix requirements -- mix sample according to ASTM designation C 192-69. Total ingredient weight should be at least 10 percent but no more than 17 percent over what is required to prepare a sample.
2. Sample size -- 6 in. by 12 in. cylindrical sample.
3. Sample preparation -- no more than two layers in a split cylinder mold with appropriate linings. The lining serves to prevent adhesion to the mold and it may consist of polyethylene plastic next to the sample with paper towel next to the mold. The sample should be compacted by internal vibration until sufficient water comes to the surface to give it a shiny appearance.
4. Time limitations -- from the start of the mixing to the end of the unconfined compression test should be no more than 60 min.
5. Unconfined compression test -- recommended accuracy of load measurement of ± 0.5 lb.
6. Rate of loading -- strain rate of 2.5 percent per min.

APPENDIX E.2

Use of the Simplified Method for Estimate of Section Stability

1. Computations relative to section: calculate γh where γ is the unit weight of the fresh concrete and h is the maximum vertical height of the fresh concrete section.
2. Use of \bar{y}/h to find stress ratio, S : calculate \bar{y}/h where \bar{y} is the center of gravity of the section. Stress ratio is found by reading the S vs. \bar{y}/h graph as shown in Figure 6.26.
3. Calculate maximum shear stress, τ_{\max} : maximum shear stress is calculated by Equation (6.8).

$$\tau_{\max} = \frac{S\gamma h}{2}$$

4. Measure the undrained shear strength, τ , of the fresh concrete: undrained shear strength of the fresh concrete is equal to one-half of the ultimate strength as obtained from the unconfined compression test.
5. Calculate factor of safety of the section: the ratio of the undrained shear strength to the maximum shear stress gives an estimate of the factor of safety. Recommended factor of safety is between 1.2-1.5 or as adjusted by field observation.
6. Limitations of the simplified method: no tensile stress should be allowed in any portion of the structure. Observation and

judgement by an experienced structural engineer is recommended when questions arise concerning the validity of the simplified method.